

Design of a photovoltaic solar installation for the irrigation of the Vallada cultivation area (Valencia)

Víctor Felip Plaza

Thesis to obtain the Master of Science Degree in
Mechanical Engineering

Supervisors: Prof. Paulo José da Costa Branco
Prof. Modesto Pérez Sánchez

Examination Committee

Chairperson: Prof. Carlos Frederico Neves Bettencourt da Silva

Supervisor: Prof. Paulo José da Costa Branco

Member(s) of the Committee: Prof. João Carlos de Campos Henriques

July of 2021

Acknowledgments

This master thesis is the culmination of a 6-year academic study period (4 years of degree and 2 years of master). It aims to apply the knowledge acquired in the specialty of Power Generation of the MUII. Therefore, it constitutes the opportunity to demonstrate the learning of these concepts to a real case, giving rise to a document which content is similar to what can be found in a project prepared by a company or an individual who is already an engineer.

Naturally, its elaboration has not been brief, nor simple, having in addition that it has been elaborated in a non-mother language and a foreign and demanding university such as the IST, even more so with the difficulties in its development due to the limitations caused by the pandemic that started more than 1 year ago.

Therefore, I would like to thank, first of all and in a particularly effusive way, the time, patience, help and encouragement to my tutors, Mr. Paulo Jose da Costa Branco, professor at the Department of Electrotechnical and Computer Engineering at IST Lisbon and main tutor, and João Carlos de Campos Henriques, professor in the Department of Engenharia Mecânica del IST, who was my first contact at the IST when I started looking for a tutor for the thesis, for his patience, understanding, encouragement and interest in being aware of the result of the development of this work throughout my stay in Lisbon. I would also like to dedicate a heartfelt and appreciation message to Mr. Modesto Pérez Sánchez, professor of the Department of Hydraulic Engineering and the Environment of the UPV who also helped me in the development and supervision of this work from my home university. They have facilitated my work as much as they could, trying to explain the fundamental concepts necessary for its development and being available as much as they have been able to.

Secondly, I would also like to thank Mr. Fernando Ibáñez Escobar, who without being my tutor has helped me on some specific occasions to resolve doubts related to the project's approach.

Last, but not least, there is the support received from people outside of my academic life. I am naturally referring to my closest family and friends. My parents, my sister, my maternal uncle, my grandparents, as well as my friends from Castellón, Valencia, Madrid, Tenerife, Bolonia and much more. They have always shown interest in knowing how the development of my thesis was evolving, and in those moments in which my strength and confidence in my own abilities were wavering, they have been there to cheer me up and motivate me to improve myself and to continue with this work.

Therefore, this document is not only a way of showing myself my ability to make an effort and to address challenges, but also a dedication to all those people who, to a greater or lesser extent, have been there to support me, both academically and in other aspects of my life.

Resumen

Las energías renovables tienen un futuro prometedor, puesto que en las próximas décadas desplazarán a las fuentes de energía no renovables en la generación de energía a nivel mundial. Este tipo de tecnologías permiten obtener energía de forma limpia y, pese a que el ciclo de vida de este tipo de instalaciones naturalmente tiene un cierto impacto ambiental, este resulta ser mucho menor que el generado en la obtención de energía por medio de otras fuentes de energía tradicionales, como son el petróleo y el carbón.

De entre las múltiples aplicaciones que este tipo de energías tienen, la que atañe el presente TFM se conoce como bombeo solar fotovoltaico, que consiste en el empleo de una instalación fotovoltaica para la obtención de la energía requerida en el funcionamiento de un sistema de bombeo en este caso empleado para el abastecimiento de un terreno de cultivo en la zona de Vallada (Valencia).

En este sentido, este TFM tiene como objetivo emplear los resultados de un TFM anterior, en el que se analizó la viabilidad y la optimización de la recuperación energética por medio de la instalación de bombas funcionando como turbinas (PATs) como sustitución de las válvulas reguladoras de presión (PRV) previamente empleadas en la instalación hidráulica presente en la zona de cultivo anteriormente mencionada, con el fin de diseñar, calcular y proyectar la instalación fotovoltaica requerida para el abastecimiento energético de los sistemas de bombeo.

De esta forma, se desarrollarán diferentes alternativas (si resulta más rentable no utilizar las PATs, si se escoge finalmente instalarlas y alcanzar el autoabastecimiento mediante baterías, si se decide emplear la red eléctrica para alimentar parte de la demanda a lo largo de los meses del año en lugar del empleo de bancos de baterías, etc.) y, de entre ellas, se escogerá y justificará la óptima desde el punto de vista técnico-económico.

Palabras clave: Energías renovables; energía fotovoltaica; sistemas solares fotovoltaicos; grupos de bombeo; Coeficiente de Rendimiento; emisiones.

Resum

Les energies renovables tenen un futur prometedor, ja que en les pròximes dècades desplaçaran a les fonts d'energia no renovables en la generació d'energia a nivell mundial. Este tipus de tecnologies permeten obtenir energia de forma neta i, a pesar que el cicle de vida d'este tipus d'instal·lacions naturalment té un cert impacte ambiental, este resulta ser molt menor que el generat en l'obtenció d'energia per mitjà d'altres fonts d'energia tradicionals, com són el petroli i el carbó.

D'entre les múltiples aplicacions que este tipus d'energies tenen, la que afecta el present TFM es coneix com a bombament solar fotovoltaic, que consistix en l'ocupació d'una instal·lació fotovoltaica per a l'obtenció de l'energia requerida en el funcionament d'un sistema de bombament en aquest cas empleat per a l'abastiment d'un terreny de cultiu en la zona de Vallada (València) .

En aquest sentit, aquest TFM té com a objectiu emprar els resultats d'un TFM anterior, en el que es va analitzar la viabilitat i l'optimització de la recuperació energètica per mitjà de la instal·lació de bombes funcionant com a turbines (PATs) com a substitució de les vàlvules reguladores de pressió (PRV) prèviament empleades en la instal·lació hidràulica present en la zona de cultiu anteriorment mencionada, a fi de dissenyar, calcular i projectar la instal·lació fotovoltaica requerida per a l'autoabastiment energètic dels sistemes de bombament.

D'aquesta forma, es desenvoluparan diferents alternatives (si resulta més rendible no utilitzar les PATs, si es tria finalment instal·lar-les i aconseguir l'autoabastiment per mitjà de bateries, si es decidix emprar la xarxa elèctrica per a alimentar part de la demanda al llarg dels mesos de l'any en lloc de l'ocupació de bancs de bateries, etc) i, d'entre elles, es triarà i justificarà l'òptima des del punt de vista tecnicoeconòmic.

Paraules clau: Energies renovables; energia fotovoltaica; sistemes solars fotovoltaics; grups de bombament; Coeficient de Rendiment; emissions.

Abstract

Renewable energies have a promising future, since in the coming decades they will displace non-renewable energy sources in power generation worldwide. This type of technology allows obtaining energy in a clean way and, despite the fact that the life cycle of this type of facilities naturally has a certain environmental impact, it turns out to be much less than that generated in obtaining energy through other sources of energy. traditional energy, such as oil and coal.

Among the many applications that this type of energy has, the one that concerns the present TFM is known as photovoltaic solar pumping, which consists of the use of a photovoltaic installation to obtain the energy required in the operation of a pumping system in this case used to supply a farmland in the Vallada area (Valencia).

In this sense, this TFM aims to use the results of a previous TFM, in which the feasibility and optimization of energy recovery was analysed through the installation of pumps operating as turbines (PATs) as a replacement for regulating valves. pressure (PRV) previously used in the hydraulic installation present in the aforementioned cultivation area, in order to design, calculate and project the photovoltaic installation required for the energy self-sufficiency of the pumping systems.

In this way, different alternatives will be developed (if it is more profitable not to use the PATs, if it is finally chosen to install them and achieve self-sufficiency by means of batteries, if it is decided to use the electricity grid to supply part of the demand throughout the months of the year instead of using battery banks, etc.) and, from among them, the optimal one from the technical-economic point of view will be chosen and justified.

Keywords: Renewable energies; photovoltaic energy; solar photovoltaic systems; pumping groups; Performance Ratio; emissions.

INDEX OF CONTENTS

- Acknowledgments i
- Resumen..... ii
- Resum..... iii
- Abstract iv
- INDEX OF CONTENTS v
- List of tables vii
- List of figures x
- Chapter 1..... 1
 - 1.1 Importance of RR.EE. Evolution and current situation 1
 - 1.2 Origins and development of pv energy 4
 - 1.3 Evolution in implantation, current situation and perspectives of PVE 6
 - 1.4 Applications of PV energy 9
 - 1.5 Description of the location area of the facilities 10
 - 1.6 Available data and existing facilities..... 11
 - 1.7 Results of the previous study 12
 - 1.8 Technical conditions. Regulations in force applied to the project 13
- Chapter 2..... 15
 - 2.1 Determination of the water needs of the sectors..... 15
 - 2.2 Determination of the required pumping parameters. Commercial pump selection..... 16
 - 2.3 Approach to possible alternatives..... 20
 - 2.4 Calculation of the power required at the input of the pump motor 21
 - 2.5 Determination of the optimal position of the photovoltaic modules 23
 - 2.5.1 Obtention of the incident solar irradiance..... 23
 - 2.5.2 Criteria for the selection of the optimal inclination angle..... 24
 - 2.6 Calculation of the power to install in the photovoltaic generator 26
 - 2.7 Photovoltaic generator sizing..... 27
 - 2.7.1 Commercial PV panels compared 27
 - 2.7.2 Minimum distance between rows of modules..... 28
 - 2.7.3 Comparison of the commercial modules and selection of the best option 30
 - 2.8 Inverter calculations 33
 - 2.9 Evaluation of alternatives in the sizing of the photovoltaic system 36
 - 2.10 Number of panels and inverters finally installed, total power and cost..... 38
 - 2.11 Panel structure..... 39
 - 2.12 Calculation of cabling 40

2.12.1 DC Cabling.....	40
2.12.1.1DC cabling of the strings	40
2.12.1.2DC cabling between the junction boxes and the inverters.....	48
2.12.2 AC Cabling.....	52
2.13 Protection tubes	55
2.13.1 Protection tubes for DC cabling	55
2.13.2 Protection tubes for AC cabling	56
2.14 Protection devices specifications.....	56
2.14.1 DC Protection devices	56
2.14.1.1Protection against overcurrents and short circuits	56
2.14.1.2Protection against overvoltages. Surge arresters	60
2.14.1.3Protection against direct and indirect contacts. DC side grounding	60
2.14.2 AC Protection devices	63
2.14.2.1Protection against overcurrents and short circuits	63
2.14.2.2Protection against direct and indirect contacts	66
2.14.2.3AC side grounding	66
2.15 Maintenance of the hydraulic-photovoltaic installation	67
Chapter 3.....	68
3.1 Introduction	68
3.2 Economic feasibility analysis	69
Chapter 4.....	80
Annex I.....	82
Plans.....	82
Annex II. Environmental analysis of the project	89
II.1 Introduction	90
II.2 Project peculiarities	90
II.3 Actions carried out in the natural environment.....	91
II.4 Impacts on the environment.....	91
II.5 Environmental benefits.....	91
Annex III. Planning of the temporal evolution of the execution of the works.....	95
III.1 Introduction	96
III.2 Gantt Chart	97
Annex IV. Bibliographic references.....	98

List of tables

- 1.1 Several applications of PV energy 9
- 1.2 Results of the feasibility analysis according to scenario 12
- 1.3 Energy recovery and turbinate volume in lines 2004 and 2070 13
- 1.4 Real case feasibility analysis 13

- 2.1 Total monthly consumption of the intakes of each sector in an average year 15
- 2.2 Characteristics of pumping at Sector 1 18
- 2.3 Characteristics of pumping at Sector 2 18
- 2.4 Operating point, performances and powers of the pumping groups of Sector 1 23
- 2.5 Operating point, performances and powers of the pumping groups of Sector 2 23
- 2.6 Coordinates of the limits of the pv installation 23
- 2.7 Annual mean value of daily radiation for each inclination 25
- 2.8 Optimal inclination of the photovoltaic panel depending on the design period 25
- 2.9 Performances and powers required at the photovoltaic system of Sector 1 27
- 2.10 Performances and powers required at the photovoltaic system of Sector 2 27
- 2.11 Mechanical data of the comercial pv panels compared 28
- 2.12 Characteristics of the comercial pv panels compared 28
- 2.13 Geometric parameters related to the arrangement of photovoltaic panels 30
- 2.14 Maximum deliverable power and number of modules required each hour depending on the conditions of irradiance and temperature, cost and occupied surface. January 1st. Sector 1 31
- 2.15 Maximum deliverable power and number of modules required each hour depending on the conditions of irradiance and temperature, cost and occupied surface. July 15th. Sector 1 31
- 2.16 Maximum deliverable power and number of modules required each hour depending on the conditions of irradiance and temperature, cost and occupied surface. January 1st. Sector 2 31
- 2.17 Maximum deliverable power and number of modules required each hour depending on the conditions of irradiance and temperature, cost and occupied surface. July 15th. Sector 2 32
- 2.18 Maximum number of required panels, cost and occupied area in Sector 1 32
- 2.19 Maximum number of required panels, cost and occupied area in Sector 2 32
- 2.20 Total maximum number of required panels, cost and occupied area 32
- 2.21 Characteristics of the comercial inverters compared 35
- 2.22 Values for the configuration of the string connections to the compared inverter commercial models 36
- 2.23 Surface finally occupied by the panels and number of panels installed in total 39
- 2.24 Nominal cross section of unipolar conductors. Source: Ingemecánica 41

2.25 Calculation of the section of the wiring of the strings of the PV installation corresponding to Sector 1. Criterion of the maximum allowable voltage drop	42
2.26 Calculation of the section of the wiring of the strings of the PV installation corresponding to Sector 2. Criterion of the maximum allowable voltage drop	43
2.27 Table B.52-1 of the UNE-HD 60364-5-52 (2014). Reference installation methods	45
2.28 Table A.52-2 bis of the UNE 20460-5-523 (2004). Admissible currents for buried cables for a temperature of 25 °C in the ground (A)	45
2.29 Table B.52.17 of the UNE-HD 60364-5-52 (2014). Correction factors according to the number of bundled cables	46
2.30 Table A.4 of the UNE-EN 50618 (2015) standard. Correction factors for an operating temperature different to 60°C	46
2.31 Calculation of the section of the wiring between the junction boxes and the inverters of the PV installation corresponding to Sector 1. Criterion of the maximum allowable voltage drop	48
2.32 Calculation of the section of the wiring between the junction boxes and the inverters of the PV installation corresponding to Sector 2. Criterion of the maximum allowable voltage drop	48
2.33 Table C.52-1 bis of the UNE-HD 60364-5-52 (2014). Admissible currents (A)	50
2.34 Calculation of the section of the wiring between the inverters and the AC measurement and protection panel of the PV installation corresponding to Sector 1. Criterion of the maximum allowable voltage drop	53
2.35 Calculation of the section of the wiring between the inverters and the AC measurement and protection panel of the PV installation corresponding to Sector 2. Criterion of the maximum allowable voltage drop	53
2.36 Table 1 of the ITC-BT-07. Section of the neutral conductor as a function of the section of the phase conductors (mm ²)	54
2.37 Table 9 of the ITC-BT-21. Minimum external diameters for buried cable protection tubes (mm)	55
2.38 Approximate average values of resistivity as a function of the terrain	61
2.39 Relationship between the sections of the protective conductors and the phase conductors	62
3.1 Monthly and annual consumptions (kWh) of the pumping systems of Sector 1, 2 and total	70
3.2 Considerations for the cash flows and economic indicators (NPV, IRR and PP)	71
3.3 Results of the financial indicators of the economic analysis	72
3.4 Evolution of the last 5 years of the EAR interest rates for new operations. Loans and credits to households and NPISHs and non-financial corporations. Credit institutions and EFC	72
3.5 Financial parameters considered (Case 1)	77
3.6 Annual payment of the loan amortization and the interests generated (Case 1)	77
3.7 Results of the financial indicators of the economic analysis (Case 1)	77
3.8 Results of income, expenses and evolution of annual updated accumulated cash flows (Case 1)	78
3.9 Financial parameters considered (Case 2)	79
3.10 Annual payment of the loan amortization and the interest generated (Case 2)	79

3.11 Results of the financial indicators of the economic analysis (Case 2)	79
3.12 Results of income, expenses and evolution of annual updated accumulated cash flows (Case 2)	80
II.1 Environmental impact of the electricity consumption	91

List of figures

- 1.1 Chronogram of some of the most important milestones towards sustainable development 2
- 1.2 Renewables consumption by region (in Exajoules) 3
- 1.3 Global power generation capacity (by source) between 2008 and 2018 3
- 1.4 Annual additions of renewable power capacity, by technology and total, between 2013-2019) 4
- 1.5 Global renewable energy employment by technology (2012-2019) 4
- 1.6 Advertising of the silicon photovoltaic cell manufactured by Bell Laboratories 5
- 1.7 Relation between the absorption coefficient (α) and the wavelength of radiation. Source: PV Education
..... 6
- 1.8 Efficiency records in different solar cell technologies 6
- 1.9 Solar PV global capacity by country and region (2009-2019) 7
- 1.10 European total solar PV installed capacity (2000-2019) 7
- 1.11 Installed and accumulated photovoltaic solar power in Spain (2003-2019) 8
- 1.12 World electricity generation by power station type (in PWh/year) 8
- 1.13 Example of a photovoltaic solar pumping system 9
- 1.14 Geographical location of Vallada 10
- 1.15 Total monthly consumption of an average year, monthly consumptions in amount per one and theoretical
consumption of the orange trees and olive trees 11
- 1.16 Configuration of PATs in parallel 12

- 2.1 Aerial view of the well and the water reservoir in Sector 1 17
- 2.2 Aerial view of the well and the water reservoir in Sector 2 18
- 2.3 Characteristic parameters of the position of the photovoltaic module 24
- 2.4 Portrait vs Landscape disposition of the solar panels 28
- 2.5 Distance between rows of panels 29
- 2.6 Available surface for the installation of the pv panels that feed the pumping systems of Sectors 1 and 2
..... 39

- 3.1 Energy flows of both sectors 73
- 3.2 Expected savings and benefits of both sectors in the first year 74
- 3.3 Cash flows and updated accumulated cash flows 75

- II.1 Estimated annual emissions of different pollutants, without and with the pv installation 92

II.2 Estimated emissions of different pollutants during the next 25 years, without and with the pv installation 93

III.1 Gantt diagram 96

Chapter 1.

Introduction and description of the case study

1.1 Importance of RR.EE. Evolution and current situation

The exploitation of mineral resources to obtain materials and energy (mechanical, thermal, electrical) on a large scale since the first industrial revolution and especially since the beginning of the 20th century has allowed, together with advances in medicine and social rights, the intense development of technology and population growth and quality of life worldwide.

As is known, this growth and development have been based on the use of resources of mineral origin (burning coal, oil, natural gas) almost exclusively for decades, as well as on the use of production methods and products that are not very respectful with the environment, such as aerosols. This has caused the appearance and aggravation of multiple problems on the planet, such as acid rain, photochemical smog, eutrophication, the destruction of the ozone layer and the disappearance of animal species, as a consequence of polluting emissions originating in the combustion of these resources and the excessive exploitation of their deposits.

Consequently, at the end of the 19th century and the beginning of the 20th century, the first wave of environmentalism or movement for the conservation of the earth and its resources took place, which sought to highlight the importance of respect for the environment and the responsible and sustainable exploitation of the resources of the planet, but it was in the 1960s and 70s that a more widespread ecological awareness emerged in society and institutions, and since then it has gained a strong momentum, especially in recent years [1]. This has led to a greater involvement of the population in caring for the environment, for example in the increasingly widespread use of public means of transport and in contributing to the recycling of household waste. The following Figure 1.1 is intended to schematically illustrate the chronology of some of the main milestones towards sustainable development:

1958	First carbon dioxide measurements by Charles Keeling. (Hawaii)
1972	Club of Rome's Report: <i>Limits to Growth</i>
1972	United Nations Conference on the Human Environment (Stockholm)
1979	First World Conference about Climate Change (Stockholm)
1980	World Conservation Strategy (IUCN, UNEP and WWF)
1985	Vienna Convention for the Protection of the Ozone Layer
1987	Montreal Protocol on Substances that Deplete the Ozone Layer
1987	Brundtland Report: <i>Our Common Future</i>
1988	Creation of the Intergovernmental Panel on Climate Change (IPCC)
1990	Creation of the World Business Council on Sustainable Development
1992	United Nations Framework Convention on Climate Change (New York)
1992	UNCED. <i>Rio Declaration. Agenda 21</i> . (Rio de Janeiro)
1997	III Conference of the U.U.NN about Climate Change. (Kyoto). Kyoto Protocol
1998	European Community signs the Kyoto Protocol on 29 th April
2002	U.U.NN World Summit on Sustainable Development. (Johannesburg)
2005	Entry into force of the Kyoto Protocol without USA on 16 th February
2007	IPCC Synthesis Report (Valencia); Nobel Peace Prize for IPCC and Al Gore
2015	US announces the Clean Energy Plan to reduce CO ₂ emissions by 32% (2030)
2015	XXI Conference of the U.U.NN. 195 countries sign Paris Agreement. (Paris)
2018	XXIV Conference of the U.U.NN. Paris Agreement implementation guidelines

Figure 1.1- Chronogram of some of the most important milestones towards sustainable development.
Source: Own, based on Castilla-La Mancha media [2]:

Together with the policies promoted by governments and multiple international organizations aimed at reducing dependence on conventional energy sources and the emissions of polluting substances for the environment, the development and implementation of renewable energies constitutes the other fundamental pillar in the ecological transition at a global level aimed at achieving a more responsible and respectful use of the planet and its resources by human beings.

There are several technologies that have emerged as an alternative to the use of fossil fuels (hydraulic, wind, solar photovoltaic, geothermal, tidal, solar thermal) and which have allowed a notable reduction in polluting emissions in the countries where they represent a relevant percentage of global electricity production. These countries are currently mainly European, as well as the USA (where renewable energies contributed 17.1% of electricity generation in 2017), Australia (which managed to reach 21% of energy production from renewable sources in 2018), China (where renewable energies reached 38.3% of energy capacity in 2018) or Brazil (in 2018, hydroelectric energy represented 62.7% of the country's total installed capacity). The following graph (Figure 1.2) represents the consumption of renewable energies of the main earth regions from 1999 to 2019:

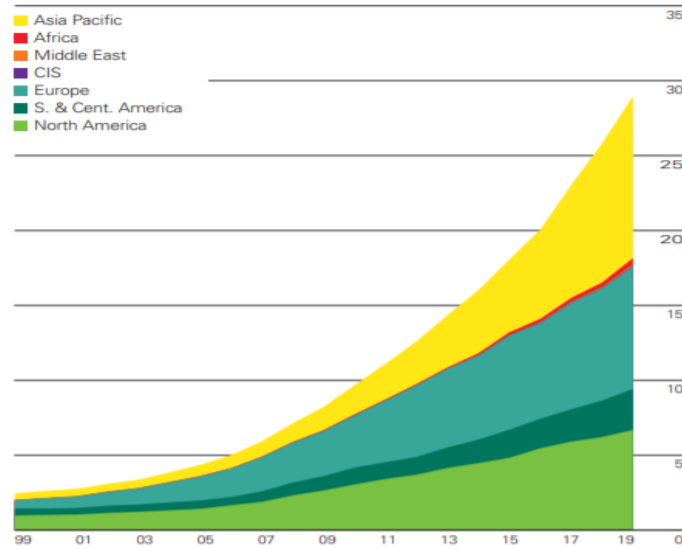


Figure 1.2- Renewables consumption by region (in Exajoules). Source: BP [3]

Moreover, the Figure 1.3 shown below illustrates the growth, both in absolute and relative terms, of the global power generation capacity of the different renewable energies in recent years (data available until 2018):

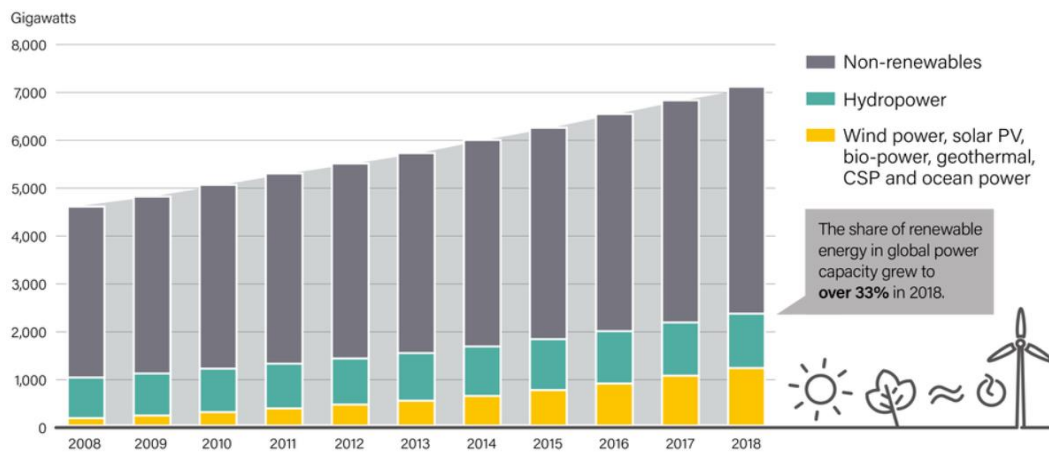


Figure 1.3- Global power generation capacity (by source) between 2008 and 2018. Source: Ren21 [4]

At the same time, the following figure indicates that, despite the fact that hydraulic continues to be the main source in terms of installed (accumulated) power among the different renewables, in recent years, specifically since 2016, the photovoltaic energy in first place, and wind power in second place, are the sources that accumulate the highest installed power generation capacity. Specifically, in 2018, of the approximately 185 gigawatts added, 105 correspond to solar photovoltaic; similarly, around 115 of the 205 gigawatts of installed power from renewable sources in 2019 come from photovoltaics (Figure 1.4):

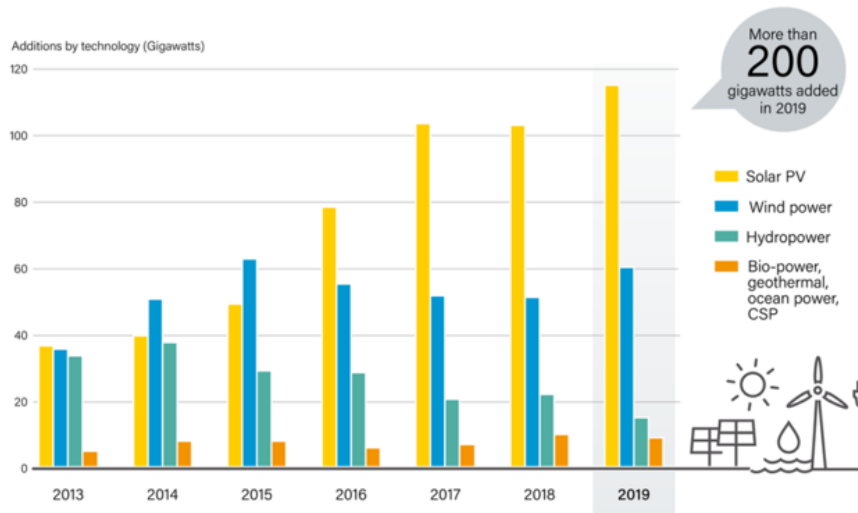


Figure 1.4- Annual additions of renewable power capacity, by technology and total, between 2013-2019. Source: Ren21 [5]

This highlights the importance that renewable sources have acquired in energy generation for years, as well as the dependence that will be on them in the near future. For this reason, it is necessary to continue investing and researching in mathematical forecasting models for the generation of wind and solar photovoltaic energies, as well as in energy storage systems that allow an adequate and efficient use of these variable renewable energy sources.

To conclude, it is equally relevant to illustrate the importance that renewable energies have acquired not only in contributing to energy generation but also in their penetration into the labour market, by employing an increasing number of employees. Precisely, the following graph (Figure 1.5) reflects the employability figures that the main renewable energy sources have achieved in recent years:

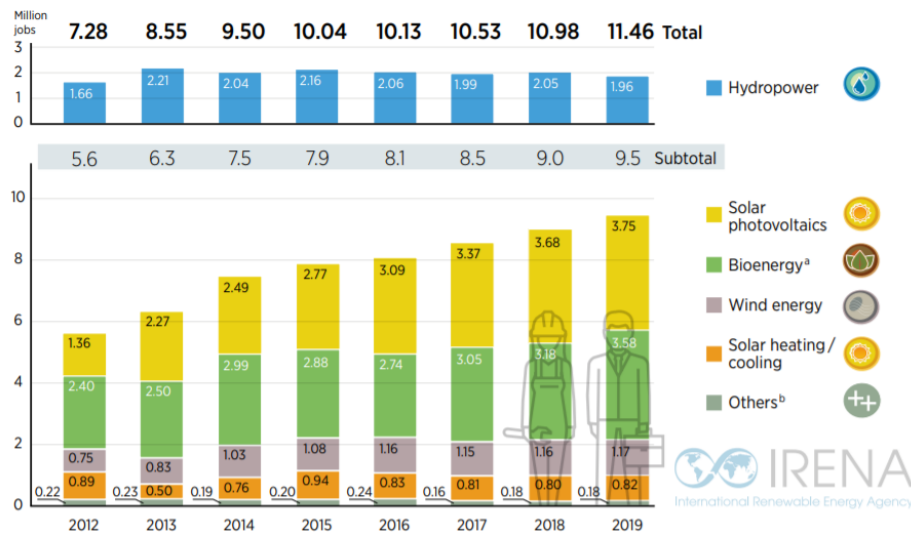


Figure 1.5- Global renewable energy employment by technology (2012-2019). Source: IRENA [6]

1.2 Origins and development of pv energy

The beginnings of photovoltaic solar energy [7] go back to the year 1839, when the French physicist Alexandre Edmond Becquerel, who was only 19 years old, verified that the current rose in one of the platinum electrodes of the electrolytic cell he was experiencing with when said electrode was exposed to the sun.

The next milestone in the development of photovoltaic use of solar energy occurred in 1873 when the English electrical engineer Willoughby Smith discovered the photovoltaic effect in solids, specifically in selenium.

Just 4 years later, in 1877, William Grylls, professor of natural philosophy at King College (London) and his student Richard Evans developed the first selenium photovoltaic cell.

Although the efficiency that could be obtained was tremendously low, thus ruling out any practical application, it did make it clear that it was possible to generate an electric current through a solid if solar radiation impinged on it. This concept was the germ that gave rise to the subsequent development of photovoltaic panels and the large-scale use of photovoltaic solar energy some decades later.

The first time that a photovoltaic cell was achieved to a minimally acceptable efficiency was in 1883, when Charles Fritts created a solar cell based on selenium and a thin layer of gold as a cover. Specifically, the efficiency achieved was 1%, still too low to be used in electricity generation, also taking into account its high cost.

Although the origin of the silicon photovoltaic cell dates back to 1940, when Russell Ohl developed the first cell of this type (and which he attempted in 1946), its true impetus, which gave rise to modern silicon cells and the possibility of a practical application of the photovoltaic effect in the generation of electricity, occurred in 1954, when Gerald Pearson of Bell Laboratories, while experimenting with semiconductors, found by chance that silicon increased its sensitivity to light by carrying certain impurities, manufacturing in this way a first silicon cell with greater efficiency than any of the previous selenium-based cells. Subsequently, Daryl Chapin and Calvin Fuller, physicists who also worked in the Bell Labs, perfected this invention and produced silicon solar cells capable of providing enough electrical energy to achieve practical applications for them.



Figure 1.6- Advertising of the silicon photovoltaic cell manufactured by Bell Laboratories. Source: IB Solar

And why did silicon-based cells turn out to be so much more efficient than selenium-based ones? The answer to this is found in the Figure 1.7, which shows the relationship between the absorption coefficient of the material and the wavelength of the incident radiation. It shows how, for practically the entire spectrum of light, the absorption coefficient is higher in the case of silicon compared to selenium (and it is always so in the case of amorphous silicon). On the other hand, it is interesting to comment that, despite the fact that germanium has the best absorption coefficient for all wavelengths, photovoltaic cells are not manufactured with this material because they turn out to have a much higher cost.

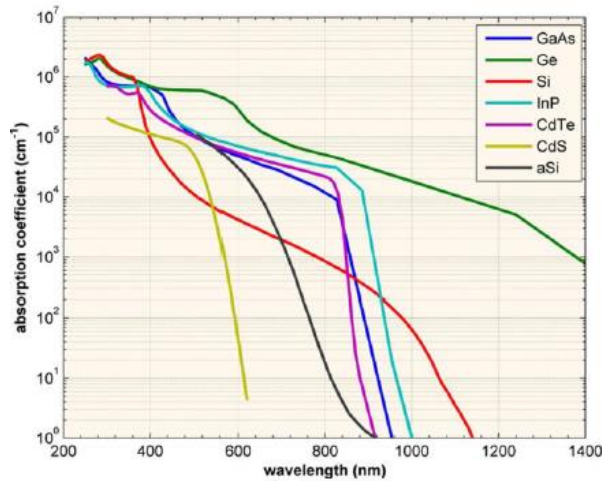


Figure 1.7- Relation between the absorption coefficient (α) and the wavelength of radiation. Source: PV Education [8]

All this development has led to the availability of a wide range of photovoltaic cell typologies today, with already notable efficiencies (an average of around 15%), while research continues on new and better configurations that allow to increase these efficiencies, extend their useful life and have a lower impact on the environment.

It is also interesting to analyse the evolution in the performance of different photovoltaic technologies in the last 45 years. The graph below (Figure 1.8) illustrates this progress, although it should be noted that these percentages of efficiency refer to the cells (not to the panels, which always have somewhat less efficiency) and under laboratory test conditions.

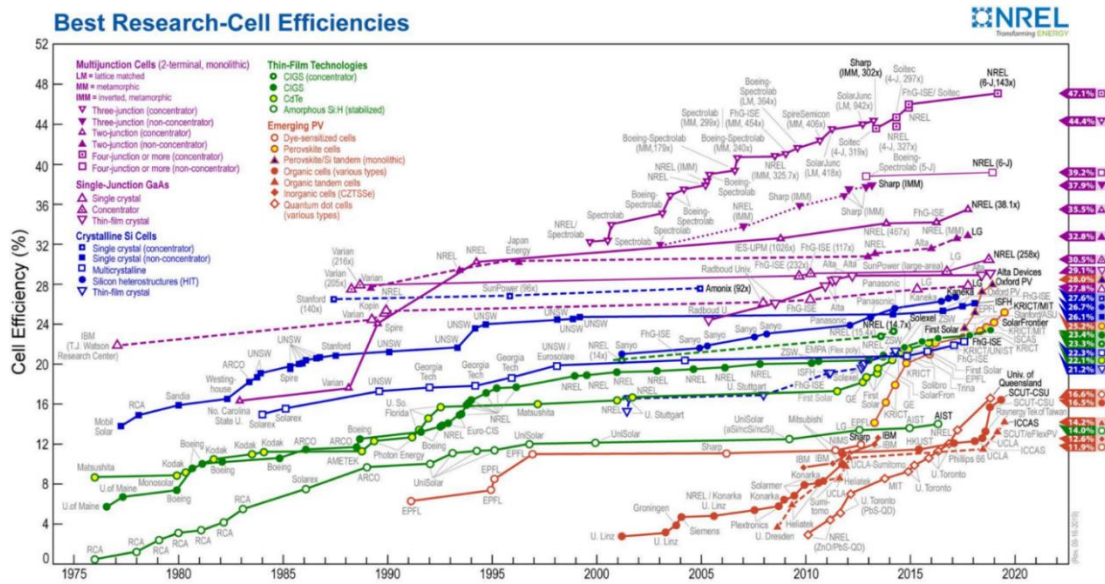


Figure 1.8- Efficiency records in different solar cell technologies. Source: NREL [9]

1.3 Evolution in implantation, current situation and perspectives of PVE

It is possible to visualize in a simple and direct way the growth that this energy source has experienced in the world in the last decade by observing the graph shown below (Figure 1.9):

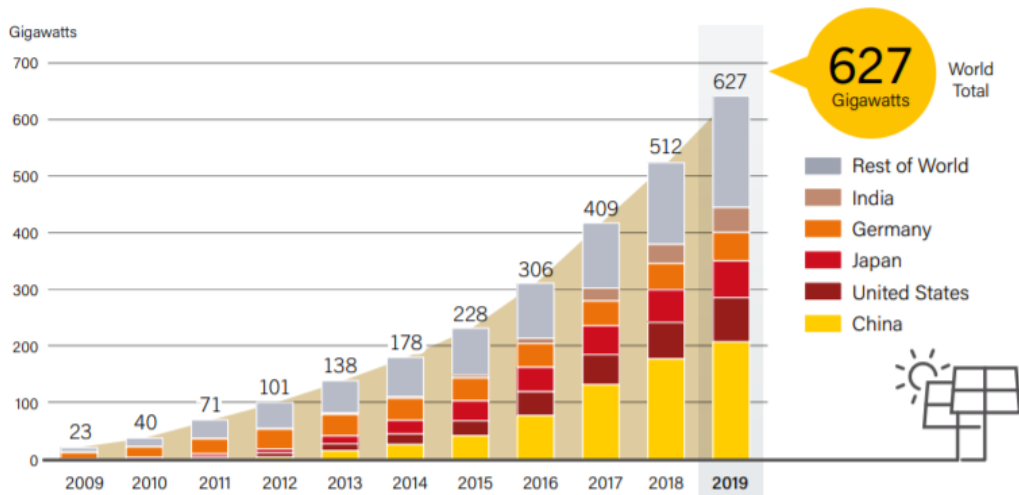


Figure 1.9- Solar PV global capacity by country and region (2009-2019). Source: Ren21 [5]

On it, the clear upward trend in the development and implementation of photovoltaic energy worldwide can be seen, since it has been growing for several years, especially in the last five.

Obviously, not all countries increase their photovoltaic potential in the same proportions. Those countries with greater economic capacity, greater extension and with more areas of high solar irradiance have a much greater capacity to increase their photovoltaic park.

In this way, the graph shown above also reflects the participation of the main countries in the growth of photovoltaic energy.

On it, the clear dominance of China over the rest of the countries is observed, with the USA and Japan in second and third place, respectively. These are the countries where the biggest PV fields projects are being developed, together with India, which will soon overtake Germany if its capacity continues to increase at the rate of last years.

On the other hand, it is interesting to comment how, from the perspective of the installed system capacities per inhabitant, Australia, Germany, Japan and Belgium are the countries that lead this ranking.

In the European case, Germany is the leading country in electricity generation from photovoltaic installations, followed by Italy and UK. This is reflected in the Figure 1.10:

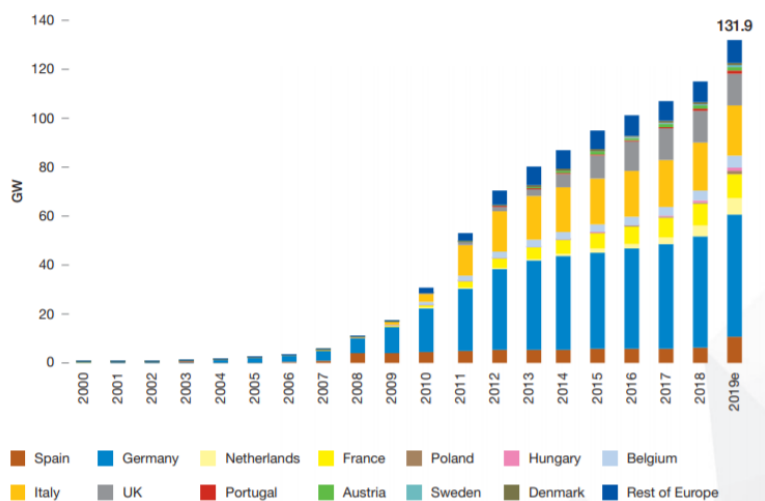


Figure 1.10- European total solar PV installed capacity (2000-2019). Source: SolarPower Europe [10]

Lastly, in the case of Spain, the birth of photovoltaic energy dates back to 1984, when Iberdrola installed the first grid-connected photovoltaic plant in San Agustín de Guadalix. This 100 kWp connection was the only one the peninsula had for almost 10 years. From this moment on, in successive years photovoltaic energy grew timidly and slowly in Spain until 2007, and especially in the following year 2008, there was a very notable growth in installed photovoltaic power [11]. However, and despite a rebound in 2010, from 2009 to 2018 the growth of this energy source was again almost non-existent, mainly due to the change in the incentive system and the arrival of the economic crisis. Then, last year 2019, Spain once again provided a great boost to photovoltaics by carrying out a large-scale photovoltaic power installation. All this can be seen in the Figure 1.11 shown below:

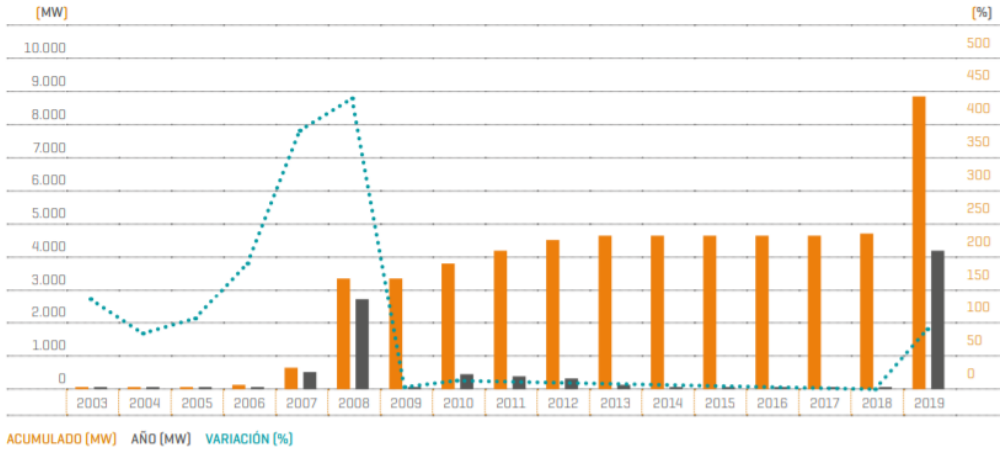


Figure 1.11- Installed and accumulated photovoltaic solar power in Spain (2003-2019). Source: REE [12]

On the other hand, the future of renewable energies is promising: renewables are expected to generate 50% of electricity worldwide by 2050. Thanks to the progressive reduction in the price of photovoltaic panels, the increase in the performance achieved by the different photovoltaic technologies and other factors mentioned above, such as the ecological awareness of society and the policies aimed at promoting the development and implementation of renewable energies to the detriment of the most polluting sources, the weight of photovoltaic energy has experienced notable growth in recent years (as can be seen in figure 4 of this document), making it one of the main renewable sources currently and one of the sources with the best future prospects (if not the most).

This predicted growth in the weight of photovoltaic energy in the energy mix in the coming years can be seen in the following graph (Figure 1.12), which shows the expected participation in electricity generation of the different technologies (renewable and non-renewable) until said year 2050:

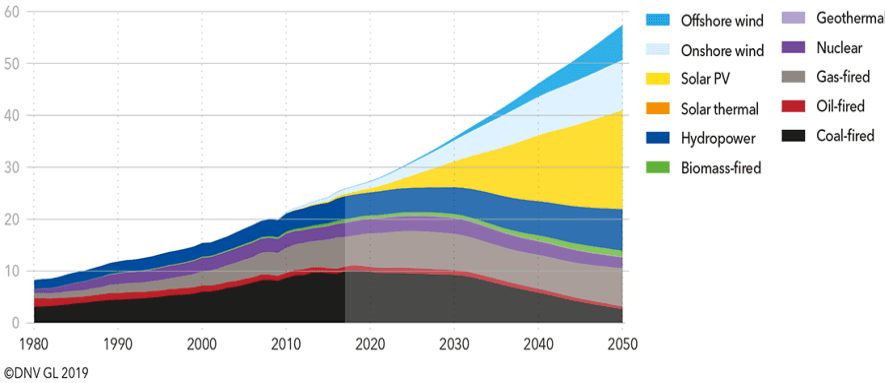


Figure 1.12- World electricity generation by power station type (in PWh/year). Source: DNV-GL [13]

1.4 Applications of PV energy

There are many ways in which photovoltaic solar energy is used for electricity production, such as photovoltaic parks, the installation of panels on building roofs, the operation of electric vehicles (cars, small boats, etc.), charging of batteries for phones or calculators or powering satellites.

Table 1.1- Several applications of PV energy. Source: Own



Among all of them, in this document, it is intended to develop a project based on an application known as “photovoltaic solar pumping”, which, as its name indicates, consists of the use of photovoltaic panels to generate the necessary current for a pumping system to carry out the irrigation of a certain growing area or allow the supply of water for human consumption, livestock or industrial facilities. Figure 1.13 reflects its general scheme:

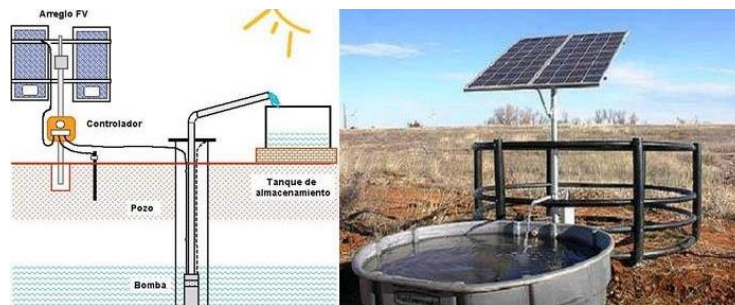


Figure 1.13- Example of a photovoltaic solar pumping system. Source: AutoSolar [14]

This electrical supply system is especially necessary for those growing areas that, due to their geographical location, cannot have access to the electricity grid or that access is too precarious. However, its use is becoming more and more common also among those users who are not in the circumstances outlined above, since although it requires a large initial investment, it offers numerous advantages compared to other energy supply options. In this sense, the reduction in the cost of photovoltaic panels, at the same time as the progressive increase in their performance and the rise in the price of fossil fuels, are promoting and making their implementation more attractive and profitable. Moreover, the combination of micro-hydropower systems (with the use of PATs, what will be discussed later) and solar/wind systems provides an energy improvement in these water systems from a more sustainable point of view.

This type of irrigation system continues to be perfected and extended today, which is fundamental in a country like Spain that needs to use its water resources in a particularly responsible and sustainable way, since it has an important agricultural sector, which consumes a relevant part of these resources, at the same time that due to its geographical location, it does not have abundant rainfall in most of its territory. A very attractive aspect of these systems in countries like Spain is that those months in which the irradiation is greater and, therefore, it is possible to obtain photovoltaic energy on a larger scale, are in turn those in which the temperatures are higher and therefore the demand for water increases, both for human consumption and for crops. In this way, in those

critical months these systems are especially useful, since their characteristics are used to the maximum. In addition, they are durable, reliable and versatile systems.

1.5 Description of the location area of the facilities

The land on which the irrigation network, the pumping systems and the ponds are located, as well as on which it is intended to project and locate the photovoltaic installation necessary for its self-sufficiency, is located in the municipality of Vallada. This municipality, which is located in the region of "La Costera", province of Valencia, is about 75 km from Valencia, capital of the Valencian Community and third city in Spain in terms of population and gross domestic product (GDP), and is close to other larger towns, such as Játiva and Onteniente.

Its municipal area, with an area of 6,123 ha., limits to the north with Enguera, to the east with Montesa, to the south with Aiello de Malferit and Onteniente and to the west with Mogente. Of these 6123 ha of the municipality, 2793 correspond to forest land and another 1000 (approximately) correspond to irrigated farmland.

This small municipality has a population of 3036 people (according to the census of the National Institute of Statistics of Spain) as of 2018. The coordinates to locate the town are 38 ° 53'44.2 "N 0 ° 41'25.3" W and its Postal code is 46691. As for the communication routes, it has the A-35 highway that connects Valencia, Alicante, Albacete and Madrid, as well as a bus line from Játiva and a railway connection that offers commuter, regional train services and long distance.

As for the climate, it is classified as Mediterranean / continental, with temperatures that are usually between 8 °C in January and 24 °C in August, and the average annual rainfall is around 439 m3.

On the other hand, its economy is based on two fundamental pillars:

- Firstly, the municipality is dedicated to the furniture, wicker, rattan, reed and basketry industry, its main clients being other European countries.
- Secondly, agriculture also plays a fundamental role in the economy and the maintenance of jobs for the population. In this case, olive trees, cereals, almond trees and fruit trees predominate as dry crops. Citrus and different varieties of fruit trees occupy irrigated crops.

The geographical location is the one shown below, in Figure 1.14 (its geographical context is shown in greater detail in the plan 1 in [Annex I](#)):

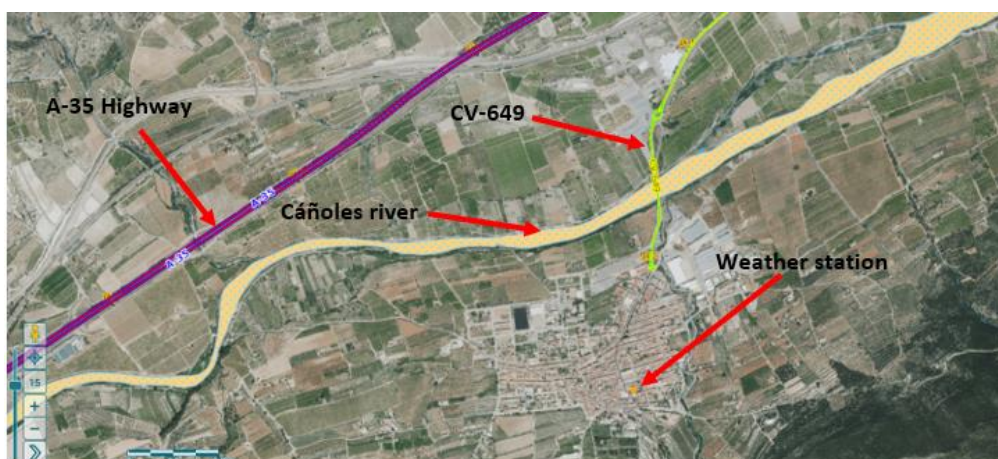


Figure 1.14- Geographical location of Vallada. Source: Adaptation from "Instituto Cartográfico Valenciano"

1.6 Available data and existing facilities

According to the data provided by the irrigation company to which the cultivation area in question belongs (Sociedad de Riego Canyoles I), in said land there are:

- 383 ha, 405 intakes and 43,98 km of pipes of various materials and diameters.
- Drip irrigation system. The change in the type of irrigation from flooding to drip irrigation occurred as a consequence of the increase in the area devoted to the cultivation of citrus fruits, which consume a greater amount of water than that of other rainfed crops (almond and olive trees), and by the lower efficiency in the use of water resources in this irrigation system.
- There are two branched networks of pipes. The first of them, the oldest, consists of the water extraction well known as "Pozo Canyoles I" that provides a maximum water flow of around 0,1 m³/s that is pumped to a reservoir located at a height of 360 m and with a capacity of around 5000 m³. The second, much more recent, consists of a water extraction point known as "Pozo el Tollo" that pumps a maximum flow of around 0,1 m³/s to a reservoir located at a level similar to the previous one (371 m) but of much greater capacity, specifically 17,000 m³.
- By default, both branched networks of pipes work independently, each one with its well and its reservoir, although if necessary it is possible to allow the communication of both basins, so that one of them can also supply water to the different irrigation points of the other pipe network.
- The pumps are submerged and therefore self-priming and not susceptible to the cavitation problem common in jet pumps. These are usually centrifugal pumps. In the present case study, both the pump located in the "Pozo Canyoles I" and the one in the "Pozo el Tollo" are semi-axial type pumps.
- Finally, the Sociedad de Regantes Canyoles I also provides an Excel file with the data on the monthly water consumption of the different intakes between 2001 and 2017. This file also contains the total monthly consumption corresponding to an average year, necessary to establish a reference year with which to carry out the study of the water needs of the area, as well as the amount per one of the total monthly consumption of this same period and the theoretical consumption of the two types of crops (orange and olives). This is represented in the graph shown below (Figure 1.15):

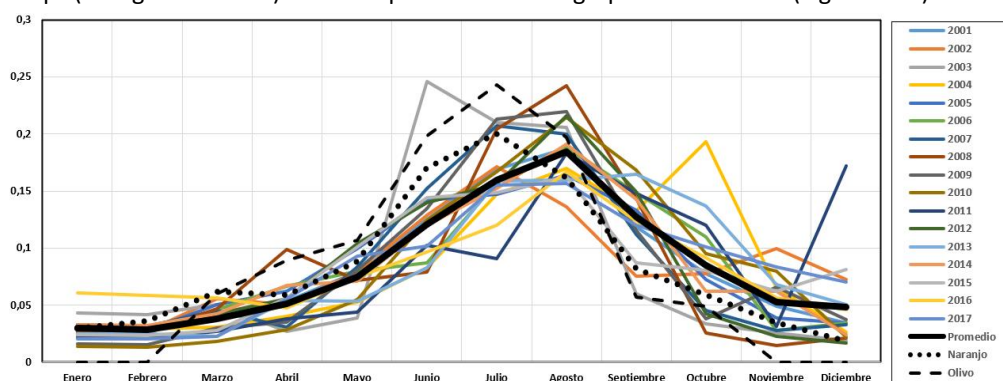


Figure 1.15- Total monthly consumption of an average year, monthly consumptions in amount per one and theoretical consumption of the orange trees and olive trees

There is also **access** to data on the required monthly volume of water and the number of hectares associated with each of the 405 intakes.

1.7 Results of the previous study

Before entering fully into the considerations and the calculation and design procedure that will be applied in this project, it is convenient to indicate and comment on certain results and conclusions obtained by Héctor Montero Ortiz in his TFM [15], since they are of great relevance when addressing the development strategy of this work. In this sense, the following points stand out:

- In function of the energy sale price, 3 scenarios were proposed: one neutral; an optimistic one, in which an increase in the sale price of energy was considered 20% higher than in the neutral case; and a pessimistic scenario in which the sale price of energy was taken 20% lower. Using as financial indicators the NPV, the IRR and the Return Period (Payback), the convenience of the installation of between 1 and 10 groups of countries was estimated, both by sectors separately and jointly and for each of these scenarios, as well as for the two objective functions proposed, one that only considers the maximization of the recovered energy (E) and another that also takes into account the economic implications of the increase in groups of installed PATs (E/PSR). The following Table 1.2 reflects the optimal results for each scenario:

Table 1.2- Results of the feasibility analysis according to scenario. Source: Adapted from Héctor Montero

Scenario	Number of groups of PATs	Objective function	Sector
Neutral	2	E/PSR	2
Optimistic	3	E/PSR	Both
Pessimistic	2	E/PSR	2

In view of the results, it was decided to proceed with the studio considering a total of two groups of PATs and the second objective function.

- Subsequently, the energy recovery was analysed through the installation of these two groups of PATs, the 2004 and 2070 lines, characterized by the circulation of large volumes of water and by high heights (pressures) respectively, those chosen for this purpose. These lines are represented below:
- On the other hand, both in the case of the group of PATs installed on the 2004 line and the one located on the 2070 line, there are 3 PATs that make it up, each of them being 3,25 kW in the group of the former. mentioned line and 1,71 kW in the case of the second. The connection of these 3 PATs is as follows (Figure 1.16):

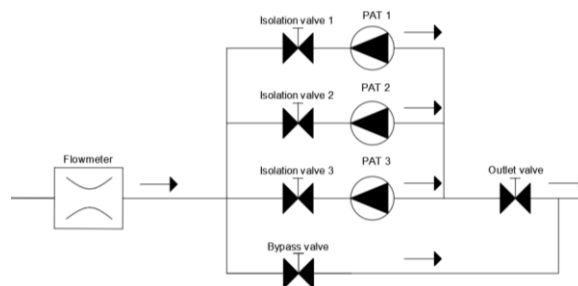


Figure 1.16- Configuration of PATs in parallel. Source: Adapted from Pérez-Sánchez et al

- The following Table 1.3 contains relevant information, obtained after the energy recovery study of the two groups of PATs of the aforementioned lines. It displays the recovered energy, as well as the percentage that it represents of the total recoverable, and the percentage that is turbine for its recovery.

Table 1.3- Energy recovery and turbinatate volume in lines 2004 and 2070

Line	Theoretical energy recovered (kWh)	Energy finally recovered (kWh)	% Energy recovery	Total volume (m ³)	Turbinatate volume (m ³)	% Turbinatate volume
2004	68833,97	29004,31	42,14	898102,95	743505,38	82,79
2070	39571,14	12665,42	32,01	281048,97	245013,57	87,18
Total	108405,10	41669,72	38,44	1179151,91	988518,95	83,83

- Finally, knowing the costs of the PATs (9336,1 €), their installation (25555,88€) and the manholes in which they will be located (15872,8€), as well as the unit operating cost (0,0145 €/kWh), the fixed discount rate (2,5%), the energy recoverable annually (41,67 MWh/año) and the sale price of the electricity considered in the scenario neutral (0,0842 €/kWh), the financial indicators mentioned in the first point of this section are applied, obtaining the results presented by Table 1.4:

Table 1.4- Real case feasibility analysis

Number of groups of PATs	NPV (€)	IRR (%)	Payback (years)
2	16445,65	4,33	19

1.8 Technical conditions. Regulations in force applied to the project

The most relevant rules and regulations that apply to this project are shown below:

- **Código Técnico de la Edificación CTE.** “Documento Básico. Seguridad Estructural. Acciones de la Edificación”, DB-SE-AE. Standard that regulates the safety conditions of the support structure.
- **Ley 31/1995**, dated November 8, on the Prevention of Occupational Risks. Law whose purpose is to promote the safety and health of workers by establishing the guarantees and responsibilities necessary to guarantee the adequate level of protection of their health.
- **Real Decreto 1627/1997**, dated October 24, establishing the minimum health and safety provisions in construction sites.
- **Real Decreto 842/2002**, dated August 2, approving the “Reglamento Electrotécnico de Baja Tensión” (REBT), which determines the conditions that the electrical installation of the project must meet.
- **Ley 24/2013**, dated December 26, of the electricity sector.
- **Norma UNE-EN 50618: 2015**, dated March 18, which establishes the parameters to be met by electrical cables for photovoltaic systems. The IEC 60529: 1991 standard is an identical international equivalent.
- **Norma UNE-EN 60364-7-712: 2017**, dated February 15, which sets the requirements for electrical installations or special low-voltage sites. Photovoltaic (PV) solar power systems.
- **Norma UNE-EN 61215-1:2017**, dated June 7, which establishes the test requirements for the qualification of the design and approval of photovoltaic modules for land use.
- **Norma UNE-EN 60529:2018**, dated April 25, which sets the degrees of protection provided by the envelopes.

- **Real Decreto 244/2019**, dated April 5, which regulates the administrative, technical and economic conditions for self-consumption of electrical energy.

In relation to equipment used in the project:

- All equipment installed must incorporate CE marking.
- The photovoltaic modules will incorporate the CE marking, according to Directive 2016/95/CE of the European Parliament and of the Council, of 12 December 2006, on the approximation of the laws of the Member States on the electrical equipment intended to be used within certain voltage limits.
- In addition, they must comply with the “Norma UNE-EN 61730”: Photovoltaic Module Safety Conditions, harmonized for Directive 2006/95/CE, and the “Norma UNE-EN 50380”: Information on data sheets and nameplates. Characteristics for photovoltaic modules. Additionally, they must meet the “Norma UNE-EN 61215”: Crystalline Silicon Photovoltaic (PV) Modules for Land Use. Design Qualification and Type Approval. They must have an IP65 protection degree and their frames, made of aluminium or stainless steel, must be grounded.
- The characterization of the inverters must be done according to the standards: UNE-EN 62093: Components of accumulation, conversion and energy management of photovoltaic systems.
- Design qualification and environmental tests, UNE-EN 61683: Photovoltaic systems. Power conditioners. Procedure for performance measurement, and according to IEC 62116. Testing procedure of islanding prevention measures for utility interactive photovoltaic inverters.
- The nominal power of the inverters must be at least 65% of the nominal power of their corresponding section of the photovoltaic generator and, at the same time, said nominal power will not exceed 1,3 times the peak power of that section of the photovoltaic generator to maintain optimal production. Furthermore, its efficiency must be at least 90% in STC and must comply with the IEC 61000-6-2 and IEC 6100-6-4 regulations, as well as the specific national regulations.
- The conductors will have the adequate section to avoid voltage drops and overheating. Specifically, for any working condition, the conductors of the direct current part will have enough section so that the voltage drop is less than 1,5% (1,2% between the photovoltaic generator and the junction boxes, and 0,3% between the junction boxes and the inverters, since no specific values are specified) and those of the alternating current part will have a section such that the voltage drop is less than 1,5%, having in both cases as reference voltages corresponding to junction boxes. This is done in accordance with [ITC-BT-40](#) [25].
- The positives and negatives of each group of modules will be conducted separately and protected according to current regulations.
- It must have the necessary length so as not to generate efforts in the various elements or the possibility of being hooked by the normal traffic of people.
- All DC wiring will be double insulated and suitable for use outdoors, in the air or in the ground, in accordance with the UNE 21123 standard and with a minimum insulation of 1000V.

Chapter 2.

Calculations for the dimensioning of the photovoltaic installation

2.1 Determination of the water needs of the sectors

As indicated in the previous chapter, the Sociedad Canyoles I provides information on the volume of water demanded by each of the intakes throughout the months of an average year; furthermore, it also provides the average annual volume consumed jointly by both sectors, both between 2001 and 2017.

Since what is intended here is to know the water needs that each sector demands separately, and that will have to be satisfied by its reservoir and corresponding pumping group, the reference value corresponding to the average annual volume per average in intakes is used, since in addition the data of each of the shots are available for each month on average, as previously commented, and that on the other hand results in an average higher than the previous ones. It results in a higher and more conservative value that will give rise to higher energy needs, so that the resulting photovoltaic installation (with or without the combination of other sources that provide electrical energy) will be able to meet the needs with greater guarantees.

However, the following clarification should be made: the exact volume with is somewhat lower, and is the result of the introduction of the data in EPANET. This is due to the fact that certain intakes that have consumption data do not have an associated area, as is the case of connection 8, or the opposite, such as connections 51 and 52, in which the cultivation area is indicated but there is no monthly water consumption. This is the one finally indicated per month and for both sectors separately, as well as the sum of both sectors and difference that these values suppose with respect to those provided in the Excel file (Table 2.1):

Table 2.1- Total monthly consumption of the intakes of each sector in an average year

Sector 1											
January	February	March	April	May	June	July	August	September	October	November	December
17559,25	17096,65	16843,79	22006,13	30572,47	49246,11	66026,67	78757,31	60598,12	43535,99	26921,23	23016,16
Sector 2											
January	February	March	April	May	June	July	August	September	October	November	December
29803,47	28812,83	42232,41	55387,13	80258,48	129859,85	173216,54	193444,08	125363,74	85655,63	55794,59	67545,62
Total											
January	February	March	April	May	June	July	August	September	October	November	December
47362,72	45909,48	59076,19	77393,26	110830,96	179105,96	239243,21	272201,38	185961,86	129191,62	82715,81	90561,77
Difference											
January	February	March	April	May	June	July	August	September	October	November	December
2008,04	1944,65	2786,61	2246,68	3969,68	5472,63	10156,47	7745,15	5250,16	3792,50	2186,11	3548,35

It is important to highlight that the data of the demand flows provided already takes into account the net crop needs, that is, the crop needs considering the historical data of average monthly rains. If this had not been the case and the volume of water required per monthly intake was not known, it would have been possible to use the information provided by the Agencia Estatal de Meteorología (AEMET) in terms of climatology (humidity, temperatures, hours of sunshine and wind characteristics), as well as from other sources for data related to the soil and the characteristics of the crops considered, and the support of software such as Cropwat for calculating the crop water requirements and irrigation needs.

On the other hand, although it is true that the volumes consumed monthly are those mentioned above for each sector, the hourly data of the flows consumed will be used (that is, the flow demanded by each sector to its respective water tank in each hour of each month of the year) because this data is available in an EPANET file. Although it results in a much larger volume of data and that makes its treatment and subsequent corresponding calculation to determine the reservoirs filling regulation strategy and the sizing of the corresponding photovoltaic installation more complex, much more accurate and therefore reliable and rigorous results are achieved.

2.2 Determination of the required pumping parameters. Commercial pump selection

It is known that the maximum flow provided by both wells is $0,1 \frac{\text{m}^3}{\text{s}}$, and it is the one that will be used to optimize the strategy for filling the reservoirs through the pumping systems.

On the other hand, the other parameter necessary to determine the power of the commercial pump to select is the head at which it must be able to provide said flow.

As is known, Bernoulli's equation (eq. 2.1) allows us to know the terms that make up the energy of the fluid along its path. By posing this equation between the points of interest, it is possible to precisely know the necessary pumping head. This equation is the one cited below:

$$z_1 + \frac{p_1}{\gamma} + \frac{v_1^2}{2 \cdot g} + h_b - \sum h_l = z_2 + \frac{p_2}{\gamma} + \frac{v_2^2}{2 \cdot g} \rightarrow E_1 + h_b - \sum h_l = E_2 \quad (2.1)$$

Where:

- **z**: Geometric elevation of the fluid. Represents the potential energy that it possesses due to having an elevation above the reference level (m)
- $\frac{p}{\gamma}$: This is the fluid pressure height, equal to the pressure divided by the specific weight of the fluid. The sum of this term and the previous one gives rise to what is known as the piezometric height of the fluid (m)
- $\frac{v}{2 \cdot g}$: Kinetic height. In water installations this term is usually negligible
- **h_b**: This is the head that the pump must provide to the fluid to overcome the losses in the pipes.
- $\sum h_l$: Sum of the total fluid losses in the pipes.
- **E**: Represents the energy available in the fluid. It is the sum of the piezometric height and the kinetic height.

Regarding the calculation of losses, the following has been done:

- To calculate the head losses due to the roughness of the walls, there are three different methods [16 and 17]:

- Hazen-Williams method (eq. 2.2): It is only valid for water, and its application is in the turbulent regime.

$$h_f = 10,674 \cdot L \cdot D^{-4,871} \cdot \left(\frac{Q}{C_{HW}} \right)^{1,852} \quad (2.2)$$

- Darcy-Weisbach method (eq. 2.3): It is the most widely used method, and it is the one used by EPANET in its calculations. It is very exact, and can be used with any liquid and regime (laminar, turbulent or transitory).

$$h_f = \frac{8 \cdot f \cdot L}{\pi^2 \cdot g \cdot D^5} \cdot Q^2 \quad (2.3)$$

- Chezy-Manning method (eq. 2.4): Used when there are free sheet flow rates.

$$h_f = 10,294 \cdot L \cdot n^2 \cdot D^{-5,33} \cdot Q^2 \quad (2.4)$$

- To calculate localized losses, also known as minor losses or local losses and which are due to turbulences that originate in elbows and other elements or connections of the hydraulic network, it was decided to increase the real lengths of the pipes in 15%. It is not an exact calculation, but it is approximate enough to justify not spending time considering each of the elbows, valves and TEs individually in the calculation of these losses. These lengths are, thus, the ones used in the D-W formula for the friction losses.

The procedure for calculating this height is detailed below, both for the system that must provide the water pumping in sector 1 and that located in sector 2:

Sector 1 (Canyoles I)

This sector is the oldest of the two that make up the cultivation area studied, as well as the smallest, both by total length of its pipes and by cultivation area covered, as well as the one with the lowest monthly water needs (an average of 30.6% with respect to the total). In this case, the pumping system is responsible for driving the water from the well to the reservoir located at a higher level, with a capacity of 5000 m³. The approximate measurements of this raft are 46x28x4 m. Figure 2.1 shows an aerial view of this sector:



Figure 2.1- Aerial view of the well and the water reservoir in Sector 1

The characteristics of pumping in this sector are in Table 2.2:

Table 2.2- Characteristics of pumping at Sector 1

Parameter	Value
$p_1 \left(\frac{N}{m^2} \right) / \gamma \left(\frac{N}{m^3} \right)$	0
$v_1^2 \left(\frac{m}{s} \right)^2 / 2 \cdot g \left(\frac{m}{s^2} \right)$	0
Losses in pipes $\left(\frac{s^2}{m^5} \right)$	2590,18
$p_2 \left(\frac{N}{m^2} \right) / \gamma \left(\frac{N}{m^3} \right)$	0
$v_2^2 \left(\frac{m}{s} \right)^2 / 2 \cdot g \left(\frac{m}{s^2} \right)$	0
Height difference (m)	99,75

Thus, the resistance curve of Sector 1 is given by eq. (2.5):

$$H^r_{Sector\ 1} = 99,75 + 2590,18 \cdot Q^2_{Sector\ 1} \quad (2.5)$$

Sector 2 (El Tollo)

Sector 2 is the main sector of the cultivation area, since in addition to having higher irrigation needs it also covers most of the cultivation area. It consists of a reservoir with a much greater capacity than that of sector 1 (17000 m³), which was built, as was the well from which the water stored in said reservoir is extracted, to meet the growing water needs of the growing area by citrus growing becomes the majority. It has a shape that resembles an isosceles triangle of about 85 m on each side and 100 m at the base. Its approximate area is 4400 m², so its depth is around 4m. Figure 2.2 shows an aerial view of this sector:



Figure 2.2- Aerial view of the well and the water reservoir in Sector 2

Whereas the characteristics of pumping in this sector are shown in Table 2.3:

Table 2.3- Characteristics of pumping at Sector 2

Parameter	Value
$p_1 \left(\frac{N}{m^2} \right) / \gamma \left(\frac{N}{m^3} \right)$	0
$v_1^2 \left(\frac{m}{s} \right)^2 / 2 \cdot g \left(\frac{m}{s^2} \right)$	0
Losses in pipes $\left(\frac{s^2}{m^5} \right)$	92,58
$p_2 \left(\frac{N}{m^2} \right) / \gamma \left(\frac{N}{m^3} \right)$	0
$v_2^2 \left(\frac{m}{s} \right)^2 / 2 \cdot g \left(\frac{m}{s^2} \right)$	0
Height difference (m)	63,07

In this case, the resistance curve of Sector 2 is given by eq. (2.6):

$$H^r_{Sector\ 2} = 63,07 + 92,58 \cdot Q^2_{Sector\ 2} \quad (2.6)$$

As can be seen, while in both sectors, due to the characteristics of the existing wells, the maximum extractable flow from them is the same, and therefore the maximum flow that each of the two pumping systems must also provide, in the case of Sector 1, the maximum required pumping head is much higher, around 200% of that of sector 1. This is due to two factors: on the one hand, the greater height difference between the water extraction point and the higher point of the network, and on the other hand, the smaller diameter and the greater length of the conduit that make the losses to overcome are much higher.

Once the maximum flow to be pumped is known (of around 0,1 m³/s, as said before), as well as the necessary head to be provided by the pump (with that maximum flow, it would be of 125,65 m and 63,99 m for Sector 1 and 2, respectively), the commercial model that satisfies them must be chosen. In this sense, after comparing two commercial models, the following has been decided [34]:

- In **Sector 1**, install **two pumps in parallel, model SDX 1,8-4**.
- In **Sector 2**, install **two pumps in parallel, model SDX 1,8-2**. Although it is true that in this case a commercial model has been found that, with a single pump, provided a maximum flow of $360 \frac{m^3}{h}$ and a maximum head above 64 m, in this case it has also been decided to install two pumps in parallel of a lower-range model to avoid that, in the event of a pump failure, this does not affect the pumping, preventing it entirely, but rather that it can continue pumping at least 50% of the requested demand.

The choice of a submersible type of pump is clear: the depth of the well is greater than 35 m. If this depth was between 8 and 35 m, a jet pump for deep wells would have been selected, in which the ejector would be located below the water level and would have two tubes directed to the well, while for depths less than 8 m, a jet pump for shallow wells would have been chosen, so that the ejector would be located in the body of the pump and there would be a single tube directed to the well. The useful life of this type of device is between 15 and 20 years. These pumps will substitute the existing ones.

On the other hand, it is necessary to have a set of accessories in the pumping groups for their correct operation and work control, such as the flow meter, the pressure switch, the air vents which function is to empty the volumes of air that can accumulate in high points of the pipeline and that hinder the correct flow of water through it, and the filters that prevent the entry of solids of certain dimensions into the pumps and, with it, the obstructions and damage that would occur in them in case of contrary.

In addition, these pumps are not going to operate 24 hours a day, nor are they going to do so by driving the same flow and providing the same head constantly. Given the need to vary the flow that each pumping group supplies, it is possible to follow two strategies: carry out a regulation at a fixed speed, or at a variable speed.

In the first case, valves which degree of opening is regulated to modify the circulation flow are used. It is a more inefficient method, in which the head also changes,

The second case, which turns out to be a more economical and efficient option, consists of using a frequency inverter. In this way, by requiring a lower flow than the one previously driven, it is possible to keep the pressure (head) constant and, therefore, the power consumed is also reduced.

In this project the second strategy is chosen, so it will be necessary to look for a suitable frequency inverter from among those commercial models found in the different internet catalogues. In this sense, considering the

operating point at a constant head, the performance increases when the frequency (and therefore the flow) decreases. However, it should be clear that below a certain frequency value, the pump is not capable of delivering the requested head.

2.3 Approach to possible alternatives

Before calculating the energy needs of the pumping groups, it is necessary to propose different alternatives that allow, with the greatest safety and lowest possible cost, to supply them. In this sense, the following possibilities have been proposed:

- **Self-supply only through solar panels:** In this case, the energy needs would be satisfied only through the photovoltaic system. Therefore, energy recovery by the PATs would not be considered, thereby losing not only the use of energy that would otherwise be dissipated by PRV, but also the reduction of greenhouse gases associated with the generation of the corresponding amount of energy in case it was obtained through non-renewable energy sources, such as coal. For this reason, it seems an undesirable scenario, in which an opportunity to optimize the obtaining of energy resources is being consciously lost. On the other hand, electricity generation is subject to certain restrictions, such as variable weather conditions, which leads to a lack of uniformity in electricity generation, or the limitation of available space for the installation of the panels.
- **Self-supply through solar panels + PATs:** This is the option that, at least a priori, is more attractive and the one that is intended to be achieved, since it achieves energy self-sufficiency, without having other expensive elements that require high maintenance and taking advantage of recoverable energy to reduce either the electricity tariff in case of grid connection, or the number of solar panels in case of not using said grid connection. As in the previous case, its difficulty lies mainly in the availability of the required space and in the climatological variability.
- **Self-supply through solar panels + PATs with or without batteries and with or without generator sets:** This scenario is undesirable and unlikely. It would try to achieve the self-sufficiency of the system through the installation of auxiliary groups, either batteries or generators. It is not desirable because they are expensive groups and they significantly complicate the maintenance of the installation.
- **Self-supply through solar panels + PATs and energy from the network:** In this case, the maximum degree of self-supply capacity would be installed and the consumptions not satisfied by the pv installation would be fed by the electricity of the grid. PATs generation is also taken into account.
- **Connection to the network of the pumping groups:** Finally, the situation arises in which the energy needs are not covered by means of the different installed elements that have been raised in the previous cases. Therefore, the connection of the pumps to the electrical network would be established so that in this way the energy requirements are met. It is the easiest solution but it would naturally have the costs associated with the electricity rate.

On the other hand, the strategy is clear: during peak hours, when the price of electricity consumed from the grid is higher, an attempt will be made to pump the maximum possible flow by means of the energy provided by the photovoltaic installation if the remaining capacity of the corresponding water tank is sufficient, so that in off-peak hours, when the cost is much lower, the energy from the network is used in case it is necessary to pump more water.

However, and as a consequence of the particularities of the water needs and of the water pumping and storage systems of each sector, the strategy differs from one to the other. In this way, with the hours in which solar radiation is available (the irradiance threshold from which it is usually considered that the received one is enough to allow the water pumping is usually between 200 and 400 W/m², so in this project, 300 W/m² has been taken as the minimum value to consider that the pumping can be carried out by photovoltaic energy) and the pumping flow of the installation of Sector 1, not only the water needs of the same can be supplied, but there is also a considerable number of hours per year in which, as no pumping is required, this solar resource can be used to generate electricity that would be poured into the grid (after conversion to alternating current) for sale, thereby generating profits while the tank is able to keep irrigation needs satisfied. On the other hand, it should be emphasized that it has been established, as a regulation strategy, not to pump during those hours in which the radiation was lower than the previously indicated minimum value, to let the tank empty and to pump again at those times when enough radiation is received until it reaches its maximum capacity, at which point it stops pumping again until its capacity is around 15% of its maximum. Therefore, in this sector, if so decided, it would be possible to supply the energy and water needs by pumping water from the well during a fraction of the annual hours in which sufficient irradiance is received without requiring the injection of electricity from the electrical network, being able to sell the energy surpluses.

In the case of Sector 2, regulation is not so simple. Due to the high water needs, in this case it is not only not possible to meet the energy and water demands not even pumping all the annual hours with sufficient radiation, but also during the months of highest consumption (May-September) it is required a certain contribution of electricity from the network to pump during the night hours. In this case, it has also been decided to pump using photovoltaic energy once 15% of the capacity of the corresponding reservoir has been reached and until it is filled, and on the other hand the energy from the network has been used when the stored volume was already scarce, 10% of capacity, during night hours.

The value of 15%, in both cases, has been set in order to ensure that the remaining capacity of the reservoirs was sufficient to supply the water needs for at least the next 6 hours in the event that solar radiation was not available in those hours (passage of a cloud or rainy day).

In this way, the "Sociedad de Riego Canyoles 1" intends to obtain a study on the technical-economic feasibility of the installation of a photovoltaic system that, to a greater or lesser extent, achieves self-sufficiency of the energy needs of the pumping systems. Apart from the economic and environmental benefits, by installing a photovoltaic solar pumping system, aid could be obtained for the modernization of irrigation systems, based on the provisions of ORDER 27/2018 of November 28, 2018, of the Consellería de Agricultura, Medioambiente, Cambio Climático and Desarrollo Rural, by which "the regulatory bases for granting aid to irrigation communities and other irrigation entities are approved, in relation to the promotion of the rational use of water".

2.4 Calculation of the power required at the input of the pump motor

To recap, there is:

- **In Sector 1** it has been decided to install two pumps in parallel, model SDX 1,8-4. The operating point at which the pumping group will work, obtained by intersecting the Q-H motor curve that defines the parallel association of two equal machines (see corresponding graph) and the resistance curve of the installation, is Q = 100,94 L/s; H = 126,14 m.

- **In Sector 2** it has been decided to install two pumps in parallel, model SDX 1.8-2. The operating point at which the pumping group will work, obtained by intersecting the Q-H motor curve that defines the parallel association of two equal machines (see corresponding graph) and the resistance curve of the installation, is $Q = 98,74$ L/s; $H = 63,97$ m.

Once the operating point corresponding to each sector is known, either through the analytical expression obtained by representing the power corresponding to each operating point of the commercial pump according to the Q-H curve attached to its catalogue, or through the traditional power formula, the physical power (or received by the fluid) can be obtained through eq. (2.7):

$$P_f = \frac{\gamma \cdot Q \cdot H}{1000} \quad (2.7)$$

Where:

- P_f : Power received by the fluid (kW)
- γ : Specific gravity of the water fluid. It has been taken from $9810 \frac{N}{m^3}$
- Q : Flow to be driven by the pump ($\frac{m^3}{s}$)
- H : Height to be supplied by the pump (m)

If in this formula, and successive formulas for obtaining the power in previous stages, the values of Q and H corresponding to the association of the pumps in parallel are entered, the total power is obtained. If values per pump are used, the power should be doubled accordingly.

Next, according to the hydraulic performance obtained for the operating point and which curve as a function of the pumped flow has also been represented for the parallel association of the two selected commercial models, the summed power is obtained on the axis of the two pumps (or power that both pumps must provide, jointly) by means of eq. (2.8):

$$P_p = \frac{\gamma \cdot Q \cdot H}{\eta_h \cdot 1000} = \frac{P_f}{\eta_h} \quad (2.8)$$

Being:

- P_p : Power that the pump(s) must provide (kW)
- η_h : Hydraulic performance of the pump (-)

After this, knowing the performance of the electric motor coupled to the pump, the power consumed by said motor is determined. This is the total power that is required at the input of both pump motors (eq. 2.9):

$$P_e = \frac{\gamma \cdot Q \cdot H}{\eta_h \cdot \eta_e \cdot 1000} = \frac{P_f}{\eta_h \cdot \eta_e} = \frac{P_p}{\eta_g} = \frac{P_p}{\eta_e} \quad (2.9)$$

In which:

- P_e : Electric power consumed by the engine(s) (kW)
- η_e : Electric performance of the engine (-)
- η_g : Global performance of the motor-pump system (-)

The results of these calculations are represented in Table 2.4 and Table 2.5 below, for both sectors and considering the parallel association of the pumps:

Sector 1 (Canyoles I)

Table 2.4- Operating point, performances and powers of the pumping groups of Sector 1

Q (L/s)	H (m)	P_f (kW)	η_h (%)	P_p (kW)	η_e (%)	η_g (%)	P_e (kW)
100,94	126,14	124,91	80,56	155,05	86	69,28	180,29

Sector 2 (El Tollo)

Table 2.5- Operating point, performances and powers of the pumping groups of Sector 2

Q (L/s)	H (m)	P_f (kW)	η_h (%)	P_p (kW)	η_e (%)	η_g (%)	P_e (kW)
98,74	63,97	61,96	80,87	76,63	86	69,54	89,10

2.5 Determination of the optimal position of the photovoltaic modules

2.5.1 Obtention of the incident solar irradiance

Now that the power that must be provided to the motors is known, it is necessary to determine the configuration and particularities of the photovoltaic installation as a whole, trying to optimize said configuration to try to maximize the obtaining of photovoltaic energy, use the least number of components and make the most of the available terrain, all this to increase the benefits obtained by the implementation of the photovoltaic system.

To do this, the first step consists in obtaining the hourly irradiance levels in the area where the photovoltaic park is wanted to be located, for each month of the year. In that sense, to obtain these (and other) data in the area, the Photovoltaic Geographical Information System (PVGIS) website is accessed (although it would be also possible to obtain these data from other sources, such as the "Instituto Nacional de Meteorología" or official autonomic institutions, PVGIS has been selected since it is the most precise and widely used source in Europe). It is an application developed by the European Commission Joint Research Center in 2001 and which has been improved and updated in subsequent years, the purpose of which is to provide reliable data on solar energy, radiation and photovoltaic performance of autonomous installations and connected to the net. This web page offers a user manual to learn more about the calculation procedure of this tool.

The first step to determine the available solar energy is, naturally, to know the coordinates of the location where the installation of the photovoltaic system would take place. In this case, these coordinates are (Table 2.6):

Table 2.6- Coordinates of the limits of the pv installation

Corner	Latitude	Length
Superior (North)	38° 54' 53.748" (38.91493°)	0° 42' 17.388" (-0.70483°)
Lower (South)	38° 54' 50.112" (38.91392°)	0° 42' 11.448" (-0.70319°)
Right (East)	38° 54' 53.892" (38.91497°)	0° 42' 12.492" (-0.70347°)
Left (West)	38° 54' 50.184" (38.91394°)	0° 42' 16.740" (-0.70465°)

The average values used for obtaining the hourly irradiance and temperature data correspond to average coordinates:

- **Latitude: 38°54'52"N (38.914°)**
- **Length: 0°42'14.4"W (-0.704°)**
- **Elevation: 318 m**

On the other hand, the irradiance values obtained throughout each of the months of the year also depend on two factors that define the position of the photovoltaic modules: their orientation or **azimuth α** and their **inclination β** . These parameters are represented in Figure 2.3:

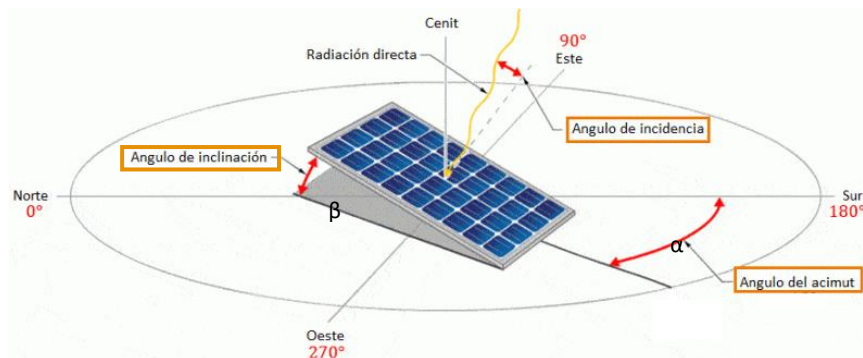


Figure 2.3- Characteristic parameters of the position of the photovoltaic module. Source: SunFields Europe

Azimuth is defined as the angle formed between the reference direction (North) and the line formed between the observer and the observed point in the same plane as the reference direction. Since in the Northern hemisphere, where the terrain on which the photovoltaic installation calculated and designed in this thesis is projected, the panels must be oriented towards the South to optimally take advantage of the incident solar radiation, it is sought that the azimuth angle is 0, that is $\alpha_{opt} = 0^\circ$, so that the installed panels have said optimal orientation that maximizes the radiation captured.

For its part, the inclination of a module is interpreted as the angle that its surface forms with the horizontal terrain. This factor is key, since it largely determines the solar energy capture that can be achieved. As is logical, since the height of the sun in the celestial vault varies throughout the year, and the more it will vary the closer it is to the poles, the optimal inclination of these modules is also different in each month of the year.

For this reason, photovoltaic systems with 1 or 2-axis solar tracking offer a substantial improvement in the annual capture of solar energy, although their cost is higher and their maintenance is more complex. However, as usually happens in isolated type solar installations, in this case it is initially decided to choose an installation with a fixed structure, without solar tracking on any axis. In this way, a compromise solution must be reached that allows the energy received to be maximized by maintaining a fixed angle of inclination throughout the year and, in turn, satisfying energy needs.

2.5.2 Criteria for the selection of the optimal inclination angle

Once the irradiance levels are known at the location of interest and for the different inclinations considered in the study, the next step is to apply a method or criterion that allows determining the optimal angle of inclination of the photovoltaic panels, so that maintaining this angle throughout the year, the dimensioned photovoltaic system guarantees the coverage of energy needs. In order to obtain this optimal angle of inclination, four possible criteria are contemplated:

- **Criterion of the critical month:** The purpose of this criterion is to establish the optimum angle of inclination of the photovoltaic modules in such a way as to guarantee the necessary energy supply in the worst month, in terms of radiation received. This criterion consists of three steps, which are the following:
 - Firstly, the quotient between the average hourly energy per month required by the pumping system and the value of hourly irradiance received in the corresponding month is calculated for each of the inclinations considered in the study and each month of the year.

- Next, the maximum quotient for each of the inclinations must be identified. In this way, the critical month is the one that groups a greater number of the highest value of these ratios for the different inclinations.
- Finally, the optimal inclination is the one that corresponds, within the month identified as critical, with the smallest value of its quotients.

In this way, what this criterion does is, in the first place, to know the month for which it is more difficult to satisfy the energy needs (since the quotient between said needs and the incident radiation is higher) and, once known, to determine the inclination that allows a greater capture of solar energy (that is why the quotient is, in this case, the lowest).

The results of the application of this method give $\beta_{opt} = 20^\circ$ as the optimum angle.

- **Criterion of maximum annual energy capture:** For its part, this criterion consists of two steps:
 - The first step is to know the annual mean value of daily radiation for each inclination.
 - The second one consists in proceeding, in a similar way to the previous criterion, to calculate the quotient between the average needs, in this case annual, of daily energy, and said annual average values of daily radiation. In this way, the smallest quotient corresponds to the optimum inclination of the photovoltaic modules.

Table 2.7- Annual mean value of daily radiation for each inclination

		H (β) Average year										
		0°	10°	20°	30°	35°	36°	40°	50°	60°	70°	80°
Year		4,852	5,237	5,507	5,648	5,669	5,670	5,658	5,536	5,277	4,887	4,383

In this way, it is observed how the optimal angle of inclination (according to this criterion) that allows a greater annual energy capture is 36° , since it provides the maximum annual average value of daily radiation captured. On the other hand, it can be checked how this value is the same that PVGIS provides as the optimal inclination.

Therefore, in this case, $\beta_{opt} = 36^\circ$.

- **Statistical criterion:** The following formula is based on statistical analysis of annual solar radiation on surfaces with different inclinations located in places of different latitudes and provides the optimal inclination as a function of the latitude of the place (eq. 2.10):

$$\beta_{opt} = 3,7 + 0,69 \cdot |\Phi| \quad (2.10)$$

Where:

- $|\Phi|$: Latitude of the place, in absolute value ($^\circ$)

According to this criterion, the optimal angle would be: $\beta_{opt} = 3,7 + 0,69 * |38,9| \rightarrow \beta_{opt} = 30,5^\circ$.

- **Design period criterion:** This criterion is set out in the “Pliego de Condiciones Técnicas de Instalaciones Aisladas de Red” (IDAE), Table 2.8:

Table 2.8- Optimal inclination of the photovoltaic panel depending on the design period. Source: IDAE

Design period	Optimal inclination
December (winter)	Latitude +10°
July (summer)	Latitude -20°
Annual	Latitude -10°

In this case, the optimal inclination would be: $\beta_{opt} = 38,9 - 10 \rightarrow \beta_{opt} = 28,9^\circ$

The criterion finally chosen has been the second one (maximum annual energy capture), so the optimal inclination angle established for this project is $\beta_{opt} = 36^\circ$. However, the calculations are approached using $\beta =$

35°. This is due to the inclination angles with which the commercial models of support structures for photovoltaic modules are offered (from 5°, to 30 or 35°, usually, 5 in 5). The radiation levels received on an annual average are really close (around 99.97%) and their monthly variation is also minimal (around 1% at most), so it does not affect the installation.

2.6 Calculation of the power to install in the photovoltaic generator

Now, the performance of the inverter must be used to determine the power required at the input of said component. Initially, the inverter (and battery if used) performance used values are chosen by estimation, using usual values. This is because in order to calculate in the first instance the energy that the photovoltaic installation must provide, it is necessary to use these parameters. As will be developed in the following points, the photovoltaic generator must then be dimensioned according to the position (orientation and inclination) and the arrangement of the panels (the separation that is left between rows of panels in their 4 directions).

The performance initially considered was 97,5% until the most appropriate commercial model was subsequently selected, at which point the calculations were redone (eq. 2.11):

$$P_{inv} = \frac{P_e}{\eta_{inv}} \quad (2.11)$$

In which:

- P_{inv} : Power required at the inverter input (kW)
- η_{inv} : Inverter energy efficiency (-)

And in case of those systems in which batteries are installed to store part of the energy produced, the formula that would provide the value of the power required at the output of the pv generator would be (eq. 2.12):

$$P_{inv} = \frac{P_e}{\eta_{inv} \cdot \eta_{bat}} \quad (2.12)$$

Being:

- η_{bat} : Battery energy efficiency (-)

Finally, by setting a PR of the photovoltaic solar generator until the losses of the wiring sections (and others) are known and obtained with more precision, the power that must be installed in the photovoltaic field is known. The initial value chosen has been 0,75, which is a common value in installations without batteries (0,7-0,8 generally, achieving values of 0,85 or even more in some cases). To establish this starting value of PR, the following percentages of the different losses that take place in these energy systems have been estimated:

- Orientation and tilt losses: 3,5% (the panels face south, then the orientation is optimal, and the slope is almost identical to optimal).
- Shadow losses: 7,5%.
- Cell temperature losses: 2,5% These losses were already considered before, so they are not included now.
- Losses due to mismatch effect: 2%.
- Losses due to dust: 1,5%.
- Angular and spectral losses: 1,5%.
- Losses due to non-compliance with nominal power: 5%.
- Ohmic losses in the DC section: 1,5% (voltage drop limit value according to [ITC-BT-40 \[25\]](#)).

- Losses in the MPPT system: 1,5%.
- Losses in the DC/AC converter: 2,5%. These losses were already considered before, so they are not included now (the complete PR would be 70%).
- Ohmic losses in the AC section: 1,5% (voltage drop limit value according to [ITC-BT-40](#) [25]).
- Other losses: 2,5%.

So, the power of the pv generator is given by the following eq. (2.13):

$$P_{pv\ gen} = \frac{P_{inv}}{PR} \quad (2.13)$$

Where:

- $P_{pv\ gen}$: Required power of the pv generator (kW)
- PR : Performance Ratio of the installation (-)

When the inverter is selected, and the new losses obtained with the commercial section of the DC and AC cabling are taken into account, a new PR is calculated (this time including the efficiency of the inverter but not the losses due to temperature, they are applied apart to know the power that the module is capable of delivering). An updated value of the PR is obtained and used to obtain the new annual profits/expenses.

The results of these calculations are represented in Table 2.9 and Table 2.10 below, for both sectors and considering the parallel association of the pumps:

Sector 1 (Canyoles I)

Table 2.9- Performances and powers required at the photovoltaic system of Sector 1

P_e (kW)	η_{inv} (%)	P_{inv} (kW)	PR (%)	$P_{pv\ gen}$ (kW)
180,29	99,1	181,93	75	242,58

Sector 2 (El Tollo)

Table 2.10- Performances and powers required at the photovoltaic system of Sector 2

P_e (kW)	η_{inv} (%)	P_{inv} (kW)	PR (%)	$P_{pv\ gen}$ (kW)
89,10	99,1	89,91	75	119,88

2.7 Photovoltaic generator sizing

After determining the power that the photovoltaic generator to install must have in each sector, as well as the optimal orientation and inclination of the panels, it is time to establish the arrangement of the panels on the surface in which they are going to be located and select the comercial model that is considered most appropriate, as well as the total number of panels theoretically necessary and the one finally set. These calculations will be addressed in this section.

2.7.1 Commercial PV panels compared

For the selection of the panel, the power it is capable to generate, its performance, dimensions and price have been taken into account, all with the aim of maximizing the electrical production of the solar field and, therefore, the economic benefit, as well as occupy the least possible surface and spend as few money as possible.

With this objective, in this section, after comparing some commercial models, the dimensions and functional characteristics of three of them are detailed below (Table 2.11 and Table 2.12):

Table 2.11- Mechanical data of the comercial pv panels compared

Mechanical data			
Parameter	Panel 1	Panel 2	Panel 3
Length (m)	1,623	1,979	1,960
Width (m)	1,048	1,002	992
Thickness (mm)	35	40	40
Mass (Kg)	18,5	22,5	22,1
Front Glass (mm)	3,2	3,2	3,2
Framework	Anodized aluminium	Al hollow-chamber on each side	Anodized aluminium

Table 2.12- Characteristics of the comercial pv panels compared

Panel characteristics			
Parameter	Panel 1	Panel 2	Panel 3
Rated power-Pmax (W)	335	400	330
Nominal Power Tolerance (W)	4,99	-	5
Voltage at point Pmax-VMPP (V)	37,05	41,7	37,7
Current at point Pmax-IMPP (A)	9,05	9,60	8,76
Open Circuit Voltage-VOC (V)	45,15	49,8	45,8
Short Circuit Current-ISC (A)	9,49	10,36	9,22
Module efficiency η_m (%)	19,70%	20,17%	17,00%
Nominal Operation Celule Temperature -NOCT (°C)	45	45	42
Variation of the maximum generator power (% / °C) γ_p	-0,37%	-0,57%	-0,38%
Temperature factor of the open circuit voltage (% / °C) β_V	-0,28%	-0,38%	-0,33%
Temperature factor of the short-circuit current (% / °C) α_I	0,05%	0,03%	0,07%

Where:

- **Panel 1:** Seraphim Eclipse SRP-335-E01B-HV (unit price: 151,84 €)
- **Panel 2:** ERA Solar ESPSC400 (unit price: 135,65 €)
- **Panel 3:** Suntech STP330 (unit price: 135,18 €)

2.7.2 Minimum distance between rows of modules

In addition to the azimuthal angle and inclination, which, as previously indicated, determine the position of the photovoltaic module, the separation between said modules is another determining factor when it comes to maximizing solar irradiance capture. By optimizing this parameter, what is sought is to minimize the shadows that some photovoltaic panels (or another type of element or obstacle) can project on others that are in their vicinity. These shadows have a lower incidence in summer, since the path of the sun is much more vertical.

On the other hand, depending on whether the placement of the panels is portrait or landscape, the shadows generated will be greater or less respectively, but it will also influence the use of the available space, in this case being greater and less, respectively. Figure 2.4 clarifies this difference:



Figure 2.4- Portrait vs Landscape disposition of the solar panels. Source: Conermex

In this way, both the “Código Técnico de la Edificación” (CTE) and the “Pieglos de Condiciones Técnicas” of the IDAE specify that “the distance d , measured on the horizontal, between a row of collectors and an obstacle of height h , which can produce shadows on the installation, you must guarantee a minimum of 4 hours of sunshine around noon of the winter solstice”. Said distance, represented in Figure 2.5, between rows of modules must be greater than the value d , provided by the expression shown below (eq. 2.14) [18]:

$$d = \frac{h}{\tan(61^\circ - \Phi)} \quad (2.14)$$

Where:

- d : Distance between rows of modules (m)
- h : Height of the module or obstacle, or the difference in heights between the top of one row and the bottom of the next (m)
- Φ : Latitude of the place ($^\circ$)

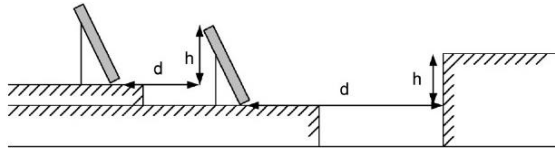


Figure 2.5- Distance between rows of panels

At the same time, since:

$$k = \frac{1}{\tan(61^\circ - \Phi)} \quad (2.15)$$

And

$$h = L \cdot \sin \beta \quad (2.16)$$

Where:

- L : Length of the side of the pv module with β inclination with respect to the horizontal (m). This will be the longest side of the panel, if portrait configuration is adopted, whereas it will be the shortest in case landscape configuration is chosen. Obviously, $\beta = \beta_{opt}$ in these calculations.

Thus, the formula of distance (eq. 2.14) “ d ” can be also expressed this way (eq. 2.17):

$$d = k \cdot h = k \cdot (L \cdot \sin \beta) \quad (2.17)$$

On the other hand, to know the horizontal projection that the photovoltaic panel makes on the ground, the following expression is used (eq. 2.18):

$$b = L \cdot \cos \beta \quad (2.18)$$

Therefore, depending on whether the panels are installed in portrait or landscape configuration, the values of these parameters, as well as the area required by each of them, will be slightly different.

On the other hand, it is also relevant to know both the area occupied by the projection of the panels on the ground (A_s) and the surface necessary to maintain the minimum distance between rows of panels (A_{bm}). These areas, as well as the sum of both and representing the surface that each panel requires for its installation (A_t), are also reflected in the following Table 2.13:

Table 2.13 Geometric parameters related to the arrangement of photovoltaic panels

Parameter	Panel 1		Panel 2		Panel 3	
	Portrait config	Landscape config	Portrait config	Landscape config	Portrait config	Landscape config
β (°)	35					
Φ (°)	38,92					
L (m)	1,62	1,05	1,98	1,00	1,96	0,99
h (m)	0,93	0,60	1,14	0,57	1,12	0,57
k (-)	2,46	2,46	2,46	2,46	2,46	2,46
d (m)	2,29	1,48	2,80	1,42	2,77	1,40
b (m)	1,33	0,86	1,62	0,82	1,61	0,81
a (m)	1,05	1,62	1,00	1,98	0,99	1,96
A_s (m ²)	1,39	1,39	1,62	1,62	1,59	1,59
A_{bm} (m ²)	2,40	2,40	2,80	2,80	2,75	2,75
A_t (m ²)	3,80	3,80	4,43	4,43	4,34	4,34

It has been decided to arrange the panels in a **portrait configuration**.

2.7.3 Comparison of the commercial modules and selection of the best option

In first place, it is necessary to determine the maximum power that each module is capable of providing at each operating moment based on the irradiance and temperature of the place. For this the following function, eq. (2.19), is used, which expresses the variation of the maximum power that the module is capable of delivering in STC and which is provided in its corresponding commercial catalogue when the temperature and irradiance values are different from these standard values:

$$P_{m\ mod} = P_{m\ mod\ (STC)} \cdot \frac{G_{loc}(\alpha, \beta)}{G_{STC}} \cdot \left[1 + \frac{\gamma_p}{100} \cdot (T_{cel} - T_{cel\ (STC)}) \right] \quad (2.19)$$

Being:

- $P_{m\ mod}$: Maximum power that the module is capable of delivering depending on the irradiance received and the ambient temperature (W)
- $P_{m\ mod\ (STC)}$: Maximum power that the module is capable of delivering in STC (W)
- $G_{loc}(\alpha, \beta)$: Effective irradiance received by the solar collector surface according to its orientation and inclination (W/m²)
- G_{STC} : Irradiance under standard test conditions (STC). Its value is equal to 1000 W/m²
- γ_p : Coefficient of variation of the maximum power of the module with its temperature (%/°C)
- $T_{cel\ (STC)}$: Temperature of the photovoltaic cell in STC (°C). Its value is equal to 25 °C.
- T_{cel} : Temperature of the photovoltaic cell depending on the ambient temperature of the site and the irradiance received (°C). The value of this parameter is obtained by means of the following formula (eq. 2.20):

$$T_{cel} = T_{loc} + \frac{NOCT - 20}{800} \cdot G_{loc}(\alpha, \beta) \quad (2.20)$$

Where, in turn:

- T_{loc} : Ambient temperature of the location (°C)
- **NOCT** : Nominal Operating Cell Temperature of photovoltaic cells= 45 °C. Conditions: Irradiance: 800 W/m²; AM 1,5 G spectral distribution; ambient temperature: 20 °C; wind speed: 1 m / s

At the same time, the minimum number of modules that must be installed to achieve the required power is given by eq. (2.21):

$$N_T = \frac{P_{pv\ gen}}{P_{m\ mod}} \quad (2.21)$$

Taking into account the 3 commercial panels previously selected for their comparison, this has been carried out as follows: for each hour of each day, the maximum power that the module is capable of delivering is different due to the variation in irradiance and the temperature, so the number of modules theoretically necessary to achieve to produce the corresponding necessary power in each one of the sectors is remarkably different. In this sense, for each hour of the year in which the irradiance threshold considered as a minimum (300 W/m²) is reached and water pumping is required, it has been calculated, for each of the 3 commercial panels compared and in the two sectors of the study, the number of panels necessary to reach this power. In addition, the acquisition cost of said number of panels and the occupied surface have also been calculated. Due to the large amount of data (a matrix of 8760x12 for each sector), only the results of these calculations for two days of the year (January 1st and July 15th, due to their irradiance and temperature disparities) are attached, as an illustration, for both sectors. They are represented in Table 2.14, Table 2.15, Table 2.16 and Table 2.17:

Sector 1 (Canyoles I)

Table 2.14- Maximum deliverable power and number of modules required each hour depending on the conditions of irradiance and temperature, cost and occupied surface. January 1st. Sector 1

Hour (h)	$P_{pv\ gen}$ (kW)	$P_{m\ mod}$ (W)	N_r (-)	Cost (€)	S (m ²)	$P_{m\ mod}$ (W)	N_r (-)	Cost (€)	S (m ²)	$P_{m\ mod}$ (W)	N_r (-)	Cost (€)	S (m ²)
9	242,58	116,60	2081	315969,68	7903,04	140,75	1724	233863,19	7632,96	115,47	2101	284021,58	9120,87
10	242,58	182,34	1331	202093,05	5054,76	216,61	1120	151929,68	4958,77	180,99	1341	181281,74	5821,55
11	242,58	205,45	1181	179317,73	4485,10	241,98	1003	136058,45	4440,76	204,10	1189	160733,78	5161,69
12	242,58	142,92	1698	257816,68	6448,52	169,96	1428	193710,34	6322,43	141,63	1713	231570,19	7436,48
13	242,58	176,22	1377	209077,48	5229,45	208,07	1166	158169,65	5162,43	174,85	1388	187635,39	6025,59
14	242,58	135,67	1789	271633,71	6794,11	161,50	1502	203748,55	6650,06	134,40	1805	244007,12	7835,87
15	242,58	104,41	2324	352865,70	8825,89	125,02	1941	263299,56	8593,73	103,32	2348	317412,03	10193,15

Table 2.15- Maximum deliverable power and number of modules required each hour depending on the conditions of irradiance and temperature, cost and occupied surface. July 15th. Sector 1

Hour (h)	$P_{pv\ gen}$ (kW)	$P_{m\ mod}$ (W)	N_r (-)	Cost (€)	S (m ²)	$P_{m\ mod}$ (W)	N_r (-)	Cost (€)	S (m ²)	$P_{m\ mod}$ (W)	N_r (-)	Cost (€)	S (m ²)
8	242,58	148,28	1636	248402,88	6213,06	172,27	1409	191132,96	6238,31	146,89	1652	223323,97	7171,67
9	242,58	203,58	1192	180987,92	4526,87	232,59	1043	141484,51	4617,85	202,13	1201	162355,98	5213,79
10	242,58	250,63	968	146976,76	3676,19	281,64	862	116931,59	3816,48	249,40	973	131534,03	4223,99
11	242,58	277,10	876	133007,90	3326,80	307,72	789	107029,03	3493,28	276,12	879	118826,74	3815,92
12	242,58	288,22	842	127845,49	3197,68	317,69	764	103637,75	3382,59	287,36	845	114230,48	3668,32
13	242,58	280,47	865	131337,71	3285,02	309,61	784	106350,78	3471,14	279,53	868	117339,71	3768,16
14	242,58	252,44	961	145913,92	3649,60	280,93	864	117202,90	3825,34	251,21	966	130587,74	4193,60
15	242,58	209,03	1161	176281,02	4409,15	235,48	1031	139856,70	4564,73	207,57	1169	158030,10	5074,87
16	242,58	149,73	1621	246125,35	6156,09	171,90	1412	191539,92	6251,59	148,29	1636	221161,02	7102,21

Sector 2 (El Tollo)

Table 2.16- Maximum deliverable power and number of modules required each hour depending on the conditions of irradiance and temperature, cost and occupied surface. January 1st. Sector 2

Hour (h)	$P_{pv\ gen}$ (kW)	$P_{m\ mod}$ (W)	N_r (-)	Cost (€)	S (m ²)	$P_{m\ mod}$ (W)	N_r (-)	Cost (€)	S (m ²)	$P_{m\ mod}$ (W)	N_r (-)	Cost (€)	S (m ²)
9	119,88	116,60	1029	156238,73	3907,85	140,75	852	115575,08	3772,21	115,47	1039	140456,18	4510,51
10	119,88	182,34	658	99907,76	2498,90	216,61	554	75150,93	2452,82	180,99	663	89626,99	2878,22
11	119,88	205,45	584	88671,93	2217,86	241,98	496	67283,14	2196,03	204,10	588	79488,19	2552,63
12	119,88	142,92	839	127389,98	3186,28	169,96	706	95769,96	3125,80	141,63	847	114500,85	3677,00
13	119,88	176,22	681	103399,98	2586,24	208,07	577	78270,92	2554,65	174,85	686	92736,22	2978,07
14	119,88	135,67	884	134222,58	3357,18	161,50	743	100789,06	3289,61	134,40	892	120584,13	3872,35
15	119,88	104,41	1149	174458,99	4363,57	125,02	959	130089,79	4245,95	103,32	1161	156948,62	5040,14

Table 2.17- Maximum deliverable power and number of modules required each hour depending on the conditions of irradiance and temperature, cost and occupied surface. July 15th. Sector 2

Hour (h)	$P_{pv\ gen}$ (kW)	$P_{m\ mod}$ (W)	N_r (-)	Cost (€)	S (m^2)	$P_{m\ mod}$ (W)	N_r (-)	Cost (€)	S (m^2)	$P_{m\ mod}$ (W)	N_r (-)	Cost (€)	S (m^2)
8	119,88	148,28	809	122834,92	3072,35	172,27	696	94413,44	3081,52	146,89	817	110445,33	3546,76
9	119,88	203,58	589	89431,11	2236,85	232,59	516	69996,17	2284,58	202,13	594	80299,30	2578,68
10	119,88	250,63	479	72729,20	1819,10	281,64	426	57787,54	1886,10	249,40	481	65023,50	2088,12
11	119,88	277,10	433	65744,77	1644,41	307,72	390	52904,09	1726,71	276,12	435	58805,04	1888,42
12	119,88	288,22	416	63163,57	1579,85	317,69	378	51276,27	1673,58	287,36	418	56506,91	1814,62
13	119,88	280,47	428	64985,59	1625,42	309,61	388	52632,78	1717,86	279,53	429	57993,94	1862,38
14	119,88	252,44	475	72121,86	1803,91	280,93	427	57923,19	1890,53	251,21	478	64617,95	2075,10
15	119,88	209,03	574	87153,58	2179,89	235,48	510	69182,27	2258,01	207,57	578	78136,35	2509,22
16	119,88	149,73	801	121620,24	3041,97	171,90	698	94684,75	3090,38	148,29	809	109363,86	3512,03

In the previous tables the results for panel 1 are in red, for panel 2 in green, and for panel 3 in blue.

Once these results are obtained, it can be found that, in the most unfavourable hour (lower irradiance and / or very high temperatures), the values of these parameters are, for each commercial panel and each sector (and in total), the ones shown in Table 2.18, Table 2.19 and Table 2.20:

Sector 1 (Canyoles I)

Table 2.18- Maximum number of required panels, cost and occupied area in Sector 1

	Panel 1	Panel 2	Panel 3
Max number of required panels (-)	2530	2193	2560
Max cost of panels (€)	384.143,82	297.483,74	346.071,04
Max occupied surface (m^2)	9608,22	9709,45	11113,48

Sector 2 (El Tollo)

Table 2.19- Maximum number of required panels, cost and occupied area in Sector 2

	Panel 1	Panel 2	Panel 3
Max number of required panels (-)	1165	1084	1266
Max cost of panels (€)	189.794,38	147.046,23	171.142,94
Max occupied surface (m^2)	4747,14	4799,38	5495,96

Total

Table 2.20- Total maximum number of required panels, cost and occupied area

	Panel 1	Panel 2	Panel 3
Max number of required panels (-)	3695	3277	3826
Max cost of panels (€)	573.938,19	444.529,97	517.213,98
Max occupied surface (m^2)	14355,36	14508,83	16609,45

At this point the final choice of panel 2 seems obvious, but it is not, since several factors must be weighed:

Panel 3 is ruled out from the outset, since it is the one that gives rise not only to the largest number of modules required to achieve the necessary power, but also to the largest surface area necessary for its installation. As for the other two panels, panel 1 requires more units than panel 2, and the cost is also much higher. The surface occupied by the total of panels 2 is higher, but slightly. In this way, with panel 2 it is possible to reach the total power of the photovoltaic field with a smaller number of panels and a significantly lower investment, being in fact the smallest of all of them and with a significant difference. It is a panel that, with a very close unit price to the smallest one, produces a considerably higher power (16,41% compared to panel 1 and 18,89% compared to

panel 3). This means that with a significantly lower number of panels, the required generator power is reached, what also reduces the necessary wiring between panels and the probability of failure or shading of any of them.

Although it is true that all of the aforementioned are advantages of panel 2, a disadvantage must be taken into account, which in hot climates such as Valencia's between the months of June and September is relevant, and is the factor of loss of the maximum power with temperature. This factor is 54% higher than that of the other panels, which will mean that, if the panels determined as strictly necessary are installed, the power of the photovoltaic generator is lower in these months than that which would be obtained with the installation of the number of panels types 1 and 3, and therefore it would be required either to install a few more panels or to request a greater injection of current from the network.

Therefore, with all this, it has finally been decided to select **panel 2 (ERA Solar ESPSC400)** [27] for its installation in the photovoltaic solar field.

2.8 Inverter calculations

The calculation of the parameters that define the operation of the inverter and its subsequent commercial selection are addressed in this section. After choosing the commercial panel and establishing the number of panels that must (and can) be used, the necessary parameters can now be calculated to be able to choose a specific commercial inverter also based on the type of photovoltaic system configuration chosen, so it is an iterative process. The values shown correspond to the performance of the commercial inverter.

First, it is necessary to set the number of modules that can be connected in series to this component. To do this, the following equations (eq. 2.22 and eq. 2.23) establish the limits of the interval of this number of modules:

$$N_{S \max} = \frac{V_{DC \text{ inv max}}}{V_{OC \text{ mod } (T_{\min \text{ mod}})}} \quad (2.22)$$

$$N_{S \min} = \frac{V_{MPPT \min}}{V_{M \text{ mod } (T_{\max \text{ mod}})}} \quad (2.23)$$

And, at the same time:

$$V_{OC \text{ mod } (T_{\min \text{ mod}})} = V_{OC \text{ mod}} + \beta_V \cdot (T_{\min \text{ mod}} - 25^\circ C) \cdot V_{OC \text{ mod}} \quad (2.24)$$

$$V_{M \text{ mod } (T_{\max \text{ mod}})} = V_{M \text{ mod}} + \beta_V \cdot (T_{\max \text{ mod}} - 25^\circ C) \cdot V_{OC \text{ mod}} \quad (2.25)$$

In which:

- $N_{S \max}$: Maximum number of modules that can be connected in series to the inverter. The result, if it is decimal, is rounded to the next lower integer.
- $V_{DC \text{ inv max}}$: Maximum voltage value that can be admitted at the input of the inverter (V)
- $V_{OC \text{ mod } (T_{\min \text{ mod}})}$: Maximum voltage value that can be reached in the module (V). It coincides with the open circuit voltage of the module with 1000 W/m², but the lowest temperature expected for the module.
- $V_{OC \text{ mod}}$: Open circuit voltage of the module (V) in STC.
- $T_{\min \text{ mod}}$: Lowest temperature expected for the module (°C)

- $N_{S \min}$: Minimum number of modules that can be connected in series to the inverter. The result, if it is decimal, is rounded to the next higher integer.
- $V_{MPPT \min}$: Minimum voltage value that can be admitted at the input of the inverter MPPT system (V)
- $V_{M \text{ mod}} (T_{\max \text{ mod}})$: Minimum voltage value that can be reached in the module (V). It coincides with the voltage of the module at its maximum power point with 1000 W/m², but the highest temperature expected for the module.
- $V_{M \text{ mod}}$: Voltage of the module at its maximum power point (V)
- $T_{\max \text{ mod}}$: Highest temperature expected for the module (°C)
- β_V : Temperature coefficient of open circuit voltage of the module (% / °C)

Whereas the maximum number of modules that can be connected in parallel to the inverter is given by the expression shown below (eq. 2.26):

$$N_{P \max} = \frac{I_{DC \text{ inv max}}}{I_{SC \text{ mod}} (T_{\max \text{ mod}})} \quad (2.26)$$

And, at the same time:

$$I_{SC \text{ mod}} (T_{\max \text{ mod}}) = I_{SC \text{ mod}} + \alpha_I \cdot (T_{\max \text{ mod}} - 25^\circ\text{C}) \cdot I_{SC \text{ mod}} \quad (2.27)$$

Being:

- $N_{P \max}$: Maximum number of modules that can be connected in parallel to the inverter.
- $I_{DC \text{ inv max}}$: Maximum current value that can be admitted at the input of the inverter (A)
- $I_{SC \text{ mod}} (T_{\max \text{ mod}})$: Maximum current value that can be provided by the module (A). It coincides with the short circuit current of the module with 1000W/m², but the highest temperature expected for the module.
- α_I : Temperature coefficient of short circuit current of the module (% / °C)
- $I_{SC \text{ mod}}$: Short circuit current of the module (A)

In addition to the maximum number of modules that can be connected in series and parallel, and related to this, it is necessary to set limits on both the maximum voltage and the open circuit voltage and the short-circuit current that can reach the inverter, and that they must respect the capacity values of this component established in their commercial datasheet:

$$V_{M \text{ string}} = N_S \cdot V_{M \text{ mod}} \in (V_{MPPT \min}, V_{MPPT \max}) \quad (2.28)$$

$$V_{OC \text{ string}} = N_S \cdot V_{OC \text{ mod}} < V_{M \text{ adm inv}} \quad (2.29)$$

$$I_{SC \text{ sos}} = N_P \cdot I_{SC \text{ mod}} < I_{M \text{ adm inv}} \quad (2.30)$$

Where:

- $V_{M \text{ string}}$: Maximum voltage of the string (V)
- $V_{OC \text{ string}}$: Open circuit voltage of the string (V)
- N_S : Number of modules that are finally connected in series in the string that leads to the inverter.
- $V_{M \text{ adm inv}}$: Maximum allowable voltage of the inverter (V)
- $I_{SC \text{ sos}}$: Short circuit current of the set of strings (A)
- N_P : Number of strings that are finally connected in parallel to the inverter.

On the other hand, it is relevant to analyse the possible alternatives proposed when choosing the most appropriate inverter configuration:

- A possible configuration would result in choosing a large commercial inverter with connection capacity for a large number of photovoltaic modules, to establish a central inverter-type connection for all photovoltaic modules, that is, for those that supply the pumping system of the sector and as those that feed the sector 2.
- In a similar way, it was also thought to establish a central inverter, this time separately, one of them corresponding to the photovoltaic system of sector 1 and the other central inverter connected to the photovoltaic field that feeds the pumping system of the sector 2.
- A third possibility would be to carry out a multi-string type configuration for all the photovoltaic panels of the complete photovoltaic installation.
- Finally, it was proposed to use two individual multi-string systems, each one associated with the photovoltaic installation of the corresponding sector. This is the chosen scenario.

The configuration of grid connection inverters chosen is the 'multi-string' type, due to the reduction of the safety and reliability problems associated with this type in comparison with a central inverter. Furthermore, said configuration presents greater modularity. Additionally, it should be mentioned that the production problems (shading, breakdown, etc.) of each module affect the entire string, but not the installation as a whole. Finally, it is necessary to clarify that those strings which are connected to the same inverter must have the same number of panels connected in series. There will be two individual multi-string inverter systems, as said before.

Once the inverter configuration to be established has been determined, a comparison of the performance of 3 different commercial models has been carried out in a similar way as was done in the case of photovoltaic modules, in order to choose the model that meet the requirements demanded by the photovoltaic system at the lowest possible cost. The table that contains the most relevant technical data of these 3 commercial models is shown below (Table 2.21):

Table 2.21- Characteristics of the commercial inverters compared

Inverter characteristics			
	Inverter 1	Inverter 2	Inverter 3
Input parameters (DC)			
Recommended maximum power of the photovoltaic field (kWp)	159,5	120	37,8
MPPT voltage range (V)	627-850	450-820	580-850
Maximum voltage (V) $V_{DC\ inv\ max}$	1100	900	1000
Maximum current (A) $I_{DC\ inv\ max}$	185	258	47,7
Number of connections (-)	24	8	6
Output parameters (AC)			
Nominal output power (kW)	110	100	27
Nominal output voltage (V)	440	400 ($\pm 10\%$)	400 (+20% - 30%)
Output frequency (Hz)	50 - 60	50 - 60	50 - 60
Nominal output current (A)	145	145	39
Power factor $\cos \Phi$ (-)	1 (adjustable)	0.95 inductive - 0.95 capacitive (adjustable)	0 - 1 inductive / capacitive
Other technical parameters			
Nominal maximum efficiency (%)	99,1	97,1	98,3
European Performance (%)	98,5	96,5	98
Standby consumption (W)	20	<40	20
Dimensions (mm)	905x720x315	1700x1440x1040	725x510x225
Permissible ambient temperature range (°C)	-25°C / +60°C	-20°C / +50°C	-25°C / +60°C
Degree of protection (-)	IP65 ¹ /NEMA 4	IP54	IP66

Where:

- **Inverter 1:** Ingeteam INGECON SUN 3Play 100TL PRO (unit price: 9144,99 €)
- **Inverter 2:** Freesun LVT FS0100_T (unit price: 11860,55 €)
- **Inverter 3:** Fronius Eco 27.0-3-S (unit price: 3358,29 €)

¹The [IPxy degree of protection](#) depends on the digits it has.

On the other hand, using the equations previously described, these limit values are represented in the Table 2.22 shown below:

Table 2.22- Values for the configuration of the string connections to the compared inverter commercial models

Parameter	Inverter 1 (Ingeteam INGECON SUN 3Play 100TL PRO)	Inverter 2 (Freesun LVT FS0100_T)	Inverter 3 (Fronius Eco 27.0-3-S)
$T_{min\ mod}$ (°C)	18,65	18,65	18,65
$T_{max\ mod}$ (°C)	63,35	63,35	63,35
$V_{OC\ mod}(T_{min\ mod})$ (V)	51,00	51,00	51,00
$V_{M\ mod}(T_{max\ mod})$ (V)	34,44	34,44	34,44
$N_{S\ max}$ (-)	21,57	17,65	19,61
$N_{S\ max\ ent}$ (-)	21	17	19
$N_{S\ min}$ (-)	18,20	13,07	16,84
$N_{S\ min\ ent}$ (-)	19	14	17
$I_{SC\ mod}(T_{max\ mod})$ (A)	10,48	10,48	10,48
$N_{P\ max}$ (-)	17,65	24,62	4,55
$N_{P\ max\ ent}$ (-)	17	24	4

Next, it is necessary to define a certain number of modules to be installed in order to know what their optimal configuration should be in relation to the commercial inverter to which they are connected (or inverters, if more than one is required) prior connection to the DC connection box.

This allowed to choose the commercial inverter that best suits the number of panels needed, in addition to its voltage and current parameters, as well as the number of units of this component that are necessary.

Operating with several percentages and comparing the results, the **inverter 1 (INGECON SUN 3Play 100TL PRO)** [28], of the company **Ingeteam** has been selected for the pv installation. Despite the fact that in some cases the number of necessary inverters was one unit higher than the number of required inverters if they corresponded to the Inverter 2, in all the cases studied the total cost managed to be lower than both the cost of the necessary inverters 2 and 3. On the other hand, it should be noted that Inverter 3, due to its more limited features, was only capable to receive the connection of a much smaller number of panels, resulting in a much higher number of units needed and, in turn, in a higher cost.

2.9 Evaluation of alternatives in the sizing of the photovoltaic system

Once the commercial models of the photovoltaic module and the inverter are known, it is necessary to decide what will be the final number of modules to install and, consequently, also of inverters. At this point, it is necessary to take into account a series of conditioning factors that must be weighed in order to make an informed decision.

Therefore, at this point we have proceeded as follows, for each of the sectors:

- First, an Excel sheet has been generated in which the necessary power to install in the photovoltaic field has been set, as well as the maximum power that the module (panel 2) is capable of delivering and the number of modules theoretically necessary to reach this power in every hour of operation.
- Next, a series of tables have been generated in which the following parameters have been represented:
 - Percentage of modules installed.
 - Number of modules installed.
 - Acquisition cost of the modules.
 - Extra (+) or missing (-) panels with respect to the required quantity.
 - Percentage of the necessary energy produced by the installed modules compared to the necessary.
 - Benefits obtained from the sale of surpluses. These benefits also take into account the sale of energy at times when irradiance is less than 300 W/m² and when it is higher than that value but pumping is not taking place.
 - Expenses derived from the purchase of unmet needs.
 - Total cost, sum of the cost of the necessary panels and the costs of purchasing electricity each hour.

After this, and as indicated in the section corresponding to the calculation of the parameters that define the inverter and the optimal configuration of the strings which current they receive, it has been proceeded for each of these percentages to determine the number of necessary inverters of the chosen model, in addition to calculating the cost of their purchase.

Then, with these investment expenses in the purchase of panels and inverters, as well as the annual incomes obtained from the sale of surplus energy and the annual expenses due to the purchase of the necessary energy, the cash flows, updated cash flows and updated accumulated cash flows are obtained for the next 25 years (with a $k=2,5\%$), since it is the time horizon that has been taken for the project and that is a usual value. This is intended to visualize, in the absence of the complete economic study (developed in [Document 4](#)) with the NPV, TIR and PP in which other expenses and incomes are taken into account, such as pumps and PATs and the sale of energy that they recover, as well as the annually saved money, and other expenses such as cabling and protection elements against overvoltages and overcurrents, the evolution of expenses/income in the following years since the materialization of the project according to its initial dimensions. Thus, it is intended to select a suitable number of panels (and their corresponding inverters).

It is worth mentioning that at this point it has been tried to be as rigorous as possible. For this, not only the progressive annual reduction in the power generated by the panels has been taken into account (1% annual for 10 years and 0,67% annual for 15 years) and therefore the reduction in the energy sold and the increase in the purchase of energy, but also the evolution of the sale price of energy.

In this context, 0,05 €/kWh has been taken as the energy sale price. It is a price somewhat lower than the average of last 10 years that, according to the Statista website¹, is around 0,0553 €/kWh. However, the price considered in this document has taken into account the small (but existing) additional expenses in the sale of energy. These are, on the one hand, the cost of representation, which takes into account the expense incurred by requiring a representative in the electricity market to manage the sale of the customer's energy by negotiating its sale price to obtain the maximum benefit in the transaction, and on the other hand, the generation access toll which reason is the corresponding payment that must be made to the electricity distribution company for using its facilities to transport electricity. The expenses considered have been 0,00082 €/kWh and 0,0005 €/kWh,

respectively. As explained in the economic analysis section, an increase in the sale price of the surplus electricity, as well as in the purchase rate, of 2% per year, similar to the CPI of 2,2%, is considered.

These economical parameters have also been applied in the economic analysis of the [Document 4](#).

These tables have been prepared for different percentages of the number of modules determined as necessary at the worst hour.

¹ <https://es.statista.com/estadisticas/993787/precio-medio-final-de-la-electricidad-en-espana/>

2.10 Number of panels and inverters finally installed, total power and cost

Once the ideal inclination of the commercial pv panel model selected and the minimum separation between rows are established, knowing their dimensions, as well as the direction in which they should be located to have an optimal orientation ($\alpha_{opt} = 0^\circ$, which being in the northern hemisphere means that the panels are oriented towards the south) it is possible to configure the number of rows of panels in said terrain, as well as the number of panels per row.

As said before, the panels are arranged in a **portrait configuration**, which means that the edges parallel to the ground (perpendicular to the support structure) are the shortest. The panels implemented in the field have a fixed structure, in such a way that a minimum separation between modules has been omitted, so the panels that make up each row are adjacent to each other.

Based on the results of the previous section, it has been decided to install around 70,8% of the total number of panels required in both sectors. Therefore, in Sector 1 1560 panels will be installed (24 more than 70% to correctly adjust the connection of the strings to the inverters and feed the pumps identically) and 6 inverters, and in Sector 2 a total of 760 panels (1 more than 70 % for the same reason) and 4 inverters. This seeks, with a large but reasonable investment, to satisfy the energy needs without the need to purchase energy from the network in a high percentage of the necessary pumping hours and, at the same time, to obtain a profit in the years following the initial investment.

Furthermore, the total area required for each photovoltaic module is known, as well as the number of modules that will be installed for feeding each sector, so it is possible to calculate the surface required for their installation. The results of this simple calculation were reflected in the tables of the previous point. Their sum is 10277,6 m².

But beyond knowing the area required by the installation of the modules, it is worth asking: is it possible to install all the necessary modules in each sector, with the land available for that purpose? Or can only a fraction of the total be installed, requiring the assistance of an additional source to complete the necessary energy supply?

To answer this question, the AutoCAD software tool is used. Since for the development of this master thesis there is a .dwg file that represents both the irrigable plots and the surface area of the polygons in which these plots are located, in addition to the pipe networks and a cartographic representation of the terrain, it is possible to determine the area of the plots of land intended for the implementation of the photovoltaic modules required in each sector.

The reasons for choosing these plots of land have been the following:

- It is a land with a not excessive surface, but sufficient to house a large number of photovoltaic panels, as well as other elements of the installation. In this way, the decrease in the arable area and the

demand for water in each sector is practically imperceptible, not affecting the water needs that serve as the basis for estimating the energy needs of the installation.

- The land for the installation of these components is located in a perimeter area of the existing plots, so there is direct access through dirt roads on at least one of its sides.
- It has been tried to select a land close to the location of the water extraction wells in order to minimize the length of the wiring as well as the losses due to current circulation. At the same time, care has been taken that this terrain is not too close to the mountains, to avoid further losses due to shading.

This surface is visualized in the following Figure 2.6:

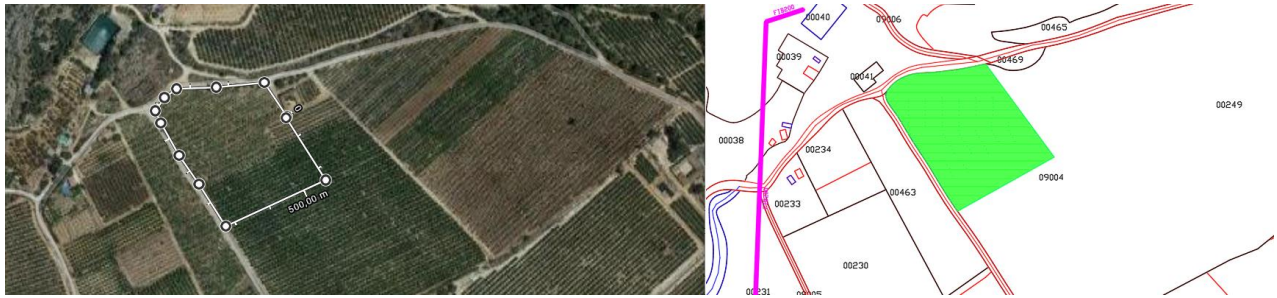


Figure 2.6- Available surface for the installation of the pv panels that feed the pumping systems of Sectors 1 and 2

Once the available area is known (around 21314,08 m²), the value of the area occupied by each module is used individually to determine the number of modules that could be installed on said land.

The results of these calculations are as follows (Table 2.23):

Table 2.23- Surface finally occupied by the panels and number of panels installed in total

		Sector 1	Sector 2	Total
Panel 2	Surface finally occupied by the panels (m ²)	9709,45	4799,38	14508,83
	Number of panels that could be installed (u)	2300	1105	2405

2.11 Panel structure

The panel support structure must be calculated to ensure that it is able to withstand the stresses applied to it in good conditions, thereby guaranteeing the firmness and stability to the photovoltaic module. Its design depends on the weight of the panels, the intensity of the wind that they must support and the type of anchoring used. The calculations presented here are based on the indications of the DB-SE AE.

Therefore, to carry out its calculation, the geometric parameters, mass and inclination (β_{opt}) of the commercial panel to be installed must be known, as well as the conditions of the place where the photovoltaic park is located. The considered temperature is the most unfavourable one, that is, the one that increases the density of the air to its maximum (the lowest temperature reached during the year)

Considering the dimensions of the solar panels, their inclination of 35° and their arrangement with respect to the horizontal, an appropriate commercial model must be chosen. In this sense, it has been decided to select the pre-assembled **CVA915XL model**, from the company **SUNFER** [35].

2.12 Calculation of cabling

As mentioned in chapter 1, although the cabling calculation follows common guidelines, the specific procedure and the standards applied are particular and specific depending on whether we speak of direct current (DC) or alternating current (AC) cabling.

In both cases, the sizing of the cabling has been carried out using the two existing selection criteria: the maximum admissible voltage drop criterion and the maximum admissible current criterion. The reason for this has been to size and select the commercial cabling in the last instance based on the criterion that provides a more conservative result, that is, a cabling with a larger section, to guarantee that the transport of electric current is adequate despite unfavourable operating conditions for this occurred and, in turn, reduce losses due to voltage drops, which lead to an increase in temperature that can lead in turn to a faster deterioration of the wiring or even a higher risk of fire.

Both criteria are included in [ITC-BT-40 \[25\]](#) (point 5) of the “*Reglamento Electrotécnico de Baja Tensión (REBT)*”. These criteria are developed in later sections, depending on the type of current flowing through the cables whose section is to be calculated. The different lines must be marked with the standard colours: phases in brown, black and grey; neutral in blue and protection cable, for grounding, in yellow-green.

2.12.1 DC Cabling

This set consists of the cables that connect the photovoltaic modules to each other in series and those that connect the output of the different strings that make up the photovoltaic field with their corresponding junction boxes, as well as the cables that connect the output of these junction boxes with the input of the inverters, in parallel, and through which direct current circulates.

2.12.1.1 DC cabling of the strings

In this case, the application of the aforementioned criteria is carried out by means of the equations developed below. The wiring that connects the modules in series will be placed on a wire mesh cable tray, while the wiring that connects the ends of the strings with their corresponding junction boxes will run underground.

Criterion of the maximum admissible voltage drop

The calculation of the minimum necessary cable section in case of applying this criterion is obtained by the eq. (2.31):

$$S_{vd\ DC\ st} = \frac{2 \cdot L_{DC\ st} \cdot I_{mp}}{\sigma_{T^{\circ}C} \cdot \frac{e_{st}}{100} \cdot N_S \cdot V_{M\ mod}} = \frac{2 \cdot L_{DC\ st} \cdot I_{mp}}{\sigma_{x^{\circ}C} \cdot \frac{e_{st}}{100} \cdot V_{M\ string}} \quad (2.31)$$

Where:

- $S_{vd\ DC\ st}$: Section of the string cable according to the maximum admissible voltage drop criterion (mm²)
- $L_{DC\ st}$: Cable length of the string (m)
- I_{mp} : String current at its maximum power point (A). Since a string consists of a series connection of the modules, this is the current of one module at its maximum power point in STC.
- e_{st} : Maximum allowable voltage drop between the photovoltaic generator and the connection point to the Public Distribution Network or to the indoor installation. The [ITC-BT-40 \[25\]](#) specifies that a value of 1,5% has to be adopted (V); thus, a value of 1,2% will be used for those cables that connect the strings and the junction boxes.

- $\sigma_{T^{\circ}C}$: Conductivity of the material that makes up the cable, at temperature T ($m/\Omega \cdot mm^2$). In order to calculate this conductivity as a function of its T, the following eq. (2.32) is applied:

$$\sigma_{T^{\circ}C} = \frac{\sigma_{20^{\circ}C}}{[1 + \alpha \cdot (T - 20)]} \quad (2.32)$$

Where:

- $\sigma_{20^{\circ}C}$: Conductivity of the material at 20°C. In case of copper conductors, its value is 58 $m/\Omega \cdot mm^2$, whereas the value of this parameter is 35,714 $m/\Omega \cdot mm^2$ when it comes to aluminium conductors [26].
- α : Coefficient of variation of conductivity with temperature. Its value for copper and aluminium is 0,00393 $^{\circ}C^{-1}$ and 0,00407 $^{\circ}C^{-1}$ respectively [26].
- **T**: Temperature of the conductor ($^{\circ}C$). Since copper cables will be used, and the maximum temperature that they will reach is 90°C, the value of this parameter is 45,49 ($m/\Omega \cdot mm^2$)
- $V_{M\ string}$: String voltage at its maximum power point (V). Since a string consists of a series connection of the modules, this is the voltage of one module at its maximum power point in STC multiplied by the number of modules connected in series.

The reason for doubling the length of the string lies in the fact that there are two cables, one that connects the positive poles and the other that connects the negative poles. This is due to the fact that the current in this section is direct (DC) so it has a single direction of circulation, from the positive to the negative pole (conventional direction, the real direction is from negative to positive), whereas AC current has two directions of circulation, so the electrons "oscillate" on both sides continuously.

Once the section of the cables is calculated, it must be normalized to the immediately higher value. For this, the following Table 2.24, which shows the nominal sections of the commercial cables, is used:

Table 2.24- Nominal cross section of unipolar conductors. Source: Ingemecánica

Normalized sections of commercial cables							
1,5	2,5	4	6	10	16	25	35
50	70	95	120	150	185	240	300

Due to the symmetrical arrangement of the modules, the calculations can be halved. Thus, the results of the application of this criterion are the following Table 2.25 for Sector 1 and Table 2.26 for Sector 2):

Table 2.25- Calculation of the section of the wiring of the strings of the PV installation corresponding to Sector 1.
Criterion of the maximum allowable voltage drop

Sector 1									
String	Ldcst (m)	I mp (A)	$\sigma \tau$ (m/Ω·mm ²)	e st (%)	N s	V M string (V)	S vd DC st (mm ²)	S vd DC st norm (mm ²)	e st (%) with S norm
S1-1-1	502,25	9,6	45,49	1,2%	20	834	21,18	25	1,017%
S2-1-1	502,25	9,6	45,49	1,2%	20	834	21,18	25	1,017%
S3-1-1	496,85	9,6	45,49	1,2%	20	834	20,96	25	1,006%
S4-1-1	496,85	9,6	45,49	1,2%	20	834	20,96	25	1,006%
S5-1-1	491,45	9,6	45,49	1,2%	20	834	20,73	25	0,995%
S1-2-1	596,19	9,6	45,49	1,2%	20	834	25,15	35	0,862%
S2-2-1	590,8	9,6	45,49	1,2%	20	834	24,92	25	1,196%
S3-2-1	590,8	9,6	45,49	1,2%	20	834	24,92	25	1,196%
S4-2-1	585,09	9,6	45,49	1,2%	20	834	24,68	25	1,184%
S5-2-1	585,09	9,6	45,49	1,2%	20	834	24,68	25	1,184%
S6-2-1	579,38	9,6	45,49	1,2%	20	834	24,44	25	1,173%
S7-2-1	579,38	9,6	45,49	1,2%	20	834	24,44	25	1,173%
S8-2-1	574,6	9,6	45,49	1,2%	20	834	24,23	25	1,163%
S9-2-1	574,6	9,6	45,49	1,2%	20	834	24,23	25	1,163%
S10-2-1	569,82	9,6	45,49	1,2%	20	834	24,03	25	1,154%
S11-2-1	569,82	9,6	45,49	1,2%	20	834	24,03	25	1,154%
S12-2-1	565,04	9,6	45,49	1,2%	20	834	23,83	25	1,144%
S13-2-1	565,04	9,6	45,49	1,2%	20	834	23,83	25	1,144%
S14-2-1	560,26	9,6	45,49	1,2%	20	834	23,63	25	1,134%
S15-2-1	560,26	9,6	45,49	1,2%	20	834	23,63	25	1,134%
S16-2-1	547,35	9,6	45,49	1,2%	20	834	23,09	25	1,108%
S17-2-1	547,35	9,6	45,49	1,2%	20	834	23,09	25	1,108%
S1-3-1	622,73	9,6	45,49	1,2%	20	834	26,26	35	0,900%
S2-3-1	622,73	9,6	45,49	1,2%	20	834	26,26	35	0,900%
S3-3-1	617,95	9,6	45,49	1,2%	20	834	26,06	35	0,894%
S4-3-1	617,95	9,6	45,49	1,2%	20	834	26,06	35	0,894%
S5-3-1	613,07	9,6	45,49	1,2%	20	834	25,86	35	0,887%
S6-3-1	613,07	9,6	45,49	1,2%	20	834	25,86	35	0,887%
S7-3-1	608,29	9,6	45,49	1,2%	20	834	25,66	35	0,880%
S8-3-1	608,29	9,6	45,49	1,2%	20	834	25,66	35	0,880%
S9-3-1	603,5	9,6	45,49	1,2%	20	834	25,45	35	0,873%
S10-3-1	603,5	9,6	45,49	1,2%	20	834	25,45	35	0,873%
S11-3-1	598,57	9,6	45,49	1,2%	20	834	25,25	35	0,866%
S12-3-1	598,57	9,6	45,49	1,2%	20	834	25,25	35	0,866%
S13-3-1	592,91	9,6	45,49	1,2%	20	834	25,01	35	0,857%
S14-3-1	592,91	9,6	45,49	1,2%	20	834	25,01	35	0,857%
S15-3-1	587,17	9,6	45,49	1,2%	20	834	24,76	25	1,189%
S16-3-1	587,17	9,6	45,49	1,2%	20	834	24,76	25	1,189%
S17-3-1	581,66	9,6	45,49	1,2%	20	834	24,53	25	1,178%
S1-4-1	575,74	9,6	45,49	1,2%	20	834	24,28	25	1,166%
S2-4-1	570,9	9,6	45,49	1,2%	20	834	24,08	25	1,156%
S3-4-1	570,9	9,6	45,49	1,2%	20	834	24,08	25	1,156%
S4-4-1	565,97	9,6	45,49	1,2%	20	834	23,87	25	1,146%
S5-4-1	565,97	9,6	45,49	1,2%	20	834	23,87	25	1,146%
S6-4-1	560,31	9,6	45,49	1,2%	20	834	23,63	25	1,134%
S7-4-1	560,31	9,6	45,49	1,2%	20	834	23,63	25	1,134%
S8-4-1	554,56	9,6	45,49	1,2%	20	834	23,39	25	1,123%
S9-4-1	554,46	9,6	45,49	1,2%	20	834	23,39	25	1,122%
S10-4-1	549	9,6	45,49	1,2%	20	834	23,15	25	1,111%
S11-4-1	549	9,6	45,49	1,2%	20	834	23,15	25	1,111%
S12-4-1	543,32	9,6	45,49	1,2%	20	834	22,92	25	1,100%
S13-4-1	543,32	9,6	45,49	1,2%	20	834	22,92	25	1,100%
S14-4-1	537,6	9,6	45,49	1,2%	20	834	22,67	25	1,088%
S15-4-1	537,6	9,6	45,49	1,2%	20	834	22,67	25	1,088%
S16-4-1	531,9	9,6	45,49	1,2%	20	834	22,43	25	1,077%
S17-4-1	531,9	9,6	45,49	1,2%	20	834	22,43	25	1,077%
S1-5-1	615,79	9,6	45,49	1,2%	20	834	25,97	35	0,890%
S2-5-1	611,07	9,6	45,49	1,2%	20	834	25,77	35	0,884%
S3-5-1	611,07	9,6	45,49	1,2%	20	834	25,77	35	0,884%
S4-5-1	606,14	9,6	45,49	1,2%	20	834	25,56	35	0,877%
S5-5-1	606,14	9,6	45,49	1,2%	20	834	25,56	35	0,877%
S6-5-1	600,48	9,6	45,49	1,2%	20	834	25,33	35	0,868%
S7-5-1	600,48	9,6	45,49	1,2%	20	834	25,33	35	0,868%
S8-5-1	594,73	9,6	45,49	1,2%	20	834	25,08	35	0,860%
S9-5-1	594,73	9,6	45,49	1,2%	20	834	25,08	35	0,860%
S10-5-1	589,17	9,6	45,49	1,2%	20	834	24,85	25	1,193%
S11-5-1	589,17	9,6	45,49	1,2%	20	834	24,85	25	1,193%
S12-5-1	583,49	9,6	45,49	1,2%	20	834	24,61	25	1,181%
S13-5-1	583,49	9,6	45,49	1,2%	20	834	24,61	25	1,181%
S14-5-1	577,77	9,6	45,49	1,2%	20	834	24,37	25	1,170%
S15-5-1	577,77	9,6	45,49	1,2%	20	834	24,37	25	1,170%
S16-5-1	572,07	9,6	45,49	1,2%	20	834	24,13	25	1,158%
S17-5-1	572,07	9,6	45,49	1,2%	20	834	24,13	25	1,158%
S1-6-1	520,02	9,6	45,49	1,2%	20	834	21,93	25	1,053%
S2-6-1	520,02	9,6	45,49	1,2%	20	834	21,93	25	1,053%
S3-6-1	514,3	9,6	45,49	1,2%	20	834	21,69	25	1,041%
S4-6-1	514,3	9,6	45,49	1,2%	20	834	21,69	25	1,041%
S5-6-1	508,6	9,6	45,49	1,2%	20	834	21,45	25	1,030%

Table 2.26- Calculation of the section of the wiring of the strings of the PV installation corresponding to Sector 2.
Criterion of the maximum allowable voltage drop

Sector 2										
String	L _{DC st} (m)	I _{mp} (A)	σ_T (m/Ω·mm ²)	e _{st} (%)	N _s	V _{M string} (V)	S _{vd DC st} (mm ²)	S _{vd DC st norm} (mm ²)	e _{st} (%) with S norm	
S1-1-2	464,52	9,6	45,49	1,2%	20	834	19,59	25	0,94%	
S2-1-2	464,52	9,6	45,49	1,2%	20	834	19,59	25	0,94%	
S3-1-2	469,3	9,6	45,49	1,2%	20	834	19,79	25	0,95%	
S4-1-2	469,3	9,6	45,49	1,2%	20	834	19,79	25	0,95%	
S5-1-2	474,08	9,6	45,49	1,2%	20	834	20,00	25	0,96%	
S6-1-2	474,08	9,6	45,49	1,2%	20	834	20,00	25	0,96%	
S7-1-2	478,86	9,6	45,49	1,2%	20	834	20,20	25	0,97%	
S8-1-2	478,86	9,6	45,49	1,2%	20	834	20,20	25	0,97%	
S9-1-2	483,64	9,6	45,49	1,2%	20	834	20,40	25	0,98%	
S10-1-2	483,64	9,6	45,49	1,2%	20	834	20,40	25	0,98%	
S11-1-2	488,41	9,6	45,49	1,2%	20	834	20,60	25	0,99%	
S12-1-2	488,41	9,6	45,49	1,2%	20	834	20,60	25	0,99%	
S13-1-2	493,19	9,6	45,49	1,2%	20	834	20,80	25	1,00%	
S14-1-2	493,19	9,6	45,49	1,2%	20	834	20,80	25	1,00%	
S15-1-2	497,97	9,6	45,49	1,2%	20	834	21,00	25	1,01%	
S1-2-2	431,21	9,6	45,49	1,2%	20	834	18,19	25	0,87%	
S2-2-2	431,21	9,6	45,49	1,2%	20	834	18,19	25	0,87%	
S3-2-2	435,99	9,6	45,49	1,2%	20	834	18,39	25	0,88%	
S4-2-2	435,99	9,6	45,49	1,2%	20	834	18,39	25	0,88%	
S5-2-2	440,77	9,6	45,49	1,2%	20	834	18,59	25	0,89%	
S6-2-2	440,77	9,6	45,49	1,2%	20	834	18,59	25	0,89%	
S7-2-2	445,55	9,6	45,49	1,2%	20	834	18,79	25	0,90%	
S8-2-2	445,55	9,6	45,49	1,2%	20	834	18,79	25	0,90%	
S9-2-2	450,33	9,6	45,49	1,2%	20	834	18,99	25	0,91%	
S10-2-2	450,33	9,6	45,49	1,2%	20	834	18,99	25	0,91%	
S11-2-2	455,1	9,6	45,49	1,2%	20	834	19,19	25	0,92%	
S12-2-2	455,1	9,6	45,49	1,2%	20	834	19,19	25	0,92%	
S13-2-2	459,88	9,6	45,49	1,2%	20	834	19,40	25	0,93%	
S14-2-2	459,88	9,6	45,49	1,2%	20	834	19,40	25	0,93%	
S15-2-2	464,66	9,6	45,49	1,2%	20	834	19,60	25	0,94%	
S1-3-2	424,78	9,6	45,49	1,2%	20	834	17,92	25	0,86%	
S2-3-2	424,78	9,6	45,49	1,2%	20	834	17,92	25	0,86%	
S3-3-2	429,56	9,6	45,49	1,2%	20	834	18,12	25	0,87%	
S4-3-2	429,56	9,6	45,49	1,2%	20	834	18,12	25	0,87%	
S1-4-2	514,37	9,6	45,49	1,2%	20	834	21,69	25	1,04%	
S2-4-2	514,37	9,6	45,49	1,2%	20	834	21,69	25	1,04%	
S3-4-2	519,15	9,6	45,49	1,2%	20	834	21,90	25	1,05%	
S4-4-2	519,15	9,6	45,49	1,2%	20	834	21,90	25	1,05%	

So, there would be 24 strings with a 35 mm² normalized section and 92 strings with a 25 mm² normalized section. The last two columns of the tables show the normalized sections of the cables and the corresponding voltage drop for each one, respectively. It can be seen how, as it is logical, the voltage drop is lower than the voltage drop allowed.

The channelling of underground lines or trenches have been designed taking into account the following conditions:

- First, the radius of curvature after the cable is laid will be at least 10 times the external diameter. These radii of curvature of the cables are made in order to avoid mechanical stress in the corners, when it is necessary to make a change of direction (turn).
- Second, road crossings will be perpendicular to the axis of the road or road, trying to avoid them if possible.

The previously indicated lengths of the strings correspond to those obtained when measuring the cable sections in the corresponding CAD file, but with an increase of 2% in order to capture the effect that the realization of the radii of curvature of said buried cables would have in its final length.

Criterion of the maximum admissible current

This criterion, also called thermal criterion, expresses that the connection cables must be sized to allow the circulation of a current at least 25% higher than the value of the maximum intensity that could circulate

through the considered cabling section, according to the provisions of the “Norma UNE-HD 60364-7-712”, dated 15th February 2017. Therefore, this intensity is expressed by eq. (2.33):

$$I_C = 1,25 \cdot I_{SC\ mod} \leq I_{adm} \quad (2.33)$$

Where:

- I_C : Minimum current for which the connection cables between the strings and their corresponding junction boxes must be dimensioned, equal to the maximum current that may circulate through the cable (A)
- $I_{SC\ mod}$: Short-circuit current of the photovoltaic panel, for cables in the rows of panels in series (strings) (A)
- I_{adm} : Maximum admissible current of the cable (A) between the strings and their corresponding junction boxes

Since $I_{SC\ mod} = 10,36$ A, the value of the maximum current is $I_C = 12,95$ A. applying eq. 2.33.

In other words, this criterion seeks to size the conductor so that it does not exceed the maximum admissible temperature that its insulation can withstand in normal operation, being said temperature equal to 70°C in the case that the insulation is thermoplastic (PVC), or 90°C if it is thermosetting type (XLPE or EPR) (this last is the case in this thesis).

In the case of this type of cabling, first of all, it is necessary go to Table B.52-1 of the “Norma UNE-HD 60364-5-52” (which cancels UNE 20460-5-523: 2004) to know which the code corresponding to the reference installation method used in the project is. In this case, since as said before those cables that connect the strings and the junction boxes will run underground, the installation method is D1.

On the other hand, since there is a single conductor per cable but there is no column for that value, and XLPE insulation is used in these cables, the column corresponding to two conductors and with this type of insulation is taken. With this, and the installation method, the table and column of said table to which it is necessary to go to are known, depending on the section obtained with the previous criterion, check the maximum admissible current (to which it is subsequently necessary to apply the CF).

Therefore, the results are taken from Table C.52-2 bis (Table 2.27), **column 5**.

Table 2.27- Table B.52-1 of the UNE-HD 60364-5-52 (2014). Reference installation methods

Instalación de referencia			Tabla y columna				
			Intensidad admisible para los circuitos simples				
			Aislamiento PVC		Aislamiento XLPE o EPR		
			Número de conductores				
			2	3	2	3	
	Local	Conductores aislados en un conducto en una pared térmicamente aislante	A1	Tabla C.52-1 bis columna 4	Tabla C.52-1 bis columna 3	Tabla C.52-1 bis columna 7b	Tabla C.52-1 bis columna 6b
	Local	Cable multiconductor en un conducto en una pared térmicamente aislante	A2	Tabla C.52-1 bis columna 3	Tabla C.52-1 bis columna 2	Tabla C.52-1 bis columna 6b	Tabla C.52-1 bis columna 5b
		Conductores aislados en un conducto sobre una pared de madera o mampostería	B1	Tabla C.52-1 bis columna 6a	Tabla C.52-1 bis columna 5a	Tabla C.52-1 bis columna 10b	Tabla C.52-1 bis columna 8b
		Cable multiconductor en un conducto sobre una pared de madera o mampostería	B2	Tabla C.52-1 bis columna 5a	Tabla C.52-1 bis columna 4	Tabla C.52-1 bis columna 8b	Tabla C.52-1 bis columna 7b
		Cables unipolares o multipolares sobre una pared de madera o mampostería	C	Tabla C.52-1 bis columna 8a	Tabla C.52-1 bis columna 6a	Tabla C.52-1 bis columna 11	Tabla C.52-1 bis columna 9b
		Cable multiconductor en conductos enterrados	D1	Tabla C.52-2 bis columna 3	Tabla C.52-2 bis columna 4	Tabla C.52-2 bis columna 5	Tabla C.52-2 bis columna 6
		Cables con cubierta unipolares o multipolares directamente en el suelo	D2				
		Cable multiconductor al aire libre Distancia al muro no inferior a 0,3 veces el diámetro del cable	E	Tabla C.52-1 bis columna 9a	Tabla C.52-1 bis columna 7a	Tabla C.52-1 bis columna 12	Tabla C.52-1 bis columna 10b
		Cables unipolares en contacto al aire libre Distancia al muro no inferior al diámetro del cable	F	Tabla C.52-1 bis columna 10a	Tabla C.52-1 bis columna 8a	Tabla C.52-1 bis columna 13	Tabla C.52-1 bis columna 11
		Cables unipolares espaciados al aire libre Distancia entre ellos como mínimo el diámetro del cable	G	Ver UNE-HD 60364-5-52			

XLPE: Polietileno reticulado (90°C) EPR: Etileno-propileno (90°C) PVC: Policloruro de vinilo (70°C)

Cobre: $\rho_{20} = 1/56 \Omega \text{mm}^2/\text{m}$; Aluminio: $\rho_{20} = 1/35 \Omega \text{mm}^2/\text{m}$

$\rho = K_0 \cdot \rho_{20}$ Para el cobre y el aluminio: $\theta = 70^\circ\text{C} \rightarrow K_0 = 1,20$; $\theta = 90^\circ\text{C} \rightarrow K_0 = 1,28$

POTENCIAS NORMALIZADAS DE TRANSFORMADORES (EN kVA):

5, 10, 15, 20, 30, 50, 75, 100, 125, 160, 200, 250, 315, 400, 500, 630, 800, 1000, 1250, 1600, 2000

FACTORES DE MAYORACIÓN K_G : 1,25 para motores y 1,8 para lámparas de descarga

In this case, Table A.52-2 of the UNE 20460-5-523: 2004 standard is used (even though it is cancelled by the UNE-HD 60364-5-52 standard, there is no access to the equivalent updated table, the C.52-2 bis, so these values, which should be very close, are the ones used) to obtain the normalized sections. This is due to the D installation method is not found in the Table C.52-1 bis (Table 2.28).

Table 12.28- Table A.52-2 bis of the UNE 20460-5-523 (2004). Admissible currents for buried cables for a temperature of 25 °C in the ground (A)

Método de instalación	Sección mm ²	Número de conductores cargados y tipo de aislamiento			
		PVC2	PVC3	XLPE2	XLPE3
D 	Cobre				
	1,5	20,5	17	24,5	21
	2,5	27,5	22,5	32,5	27,5
	4	36	29	42	35
	6	44	37	53	44
	10	59	49	70	58
	16	76	63	91	75
	25	98	81	116	96
	35	118	97	140	117
	50	140	115	166	138
	70	173	143	204	170
	95	205	170	241	202
	120	233	192	275	230
	150	264	218	311	260
	185	296	245	348	291
	240	342	282	402	336
300	387	319	455	380	

Although the values for the maximum admissible current are extracted from the previous table based on the standard sections of the cables installed on the surface obtained and shown in Table 47 (Sector 1) and Table 48 (Sector 2), this current carrying capacity will be diminished by the installation conditions, therefore, it must be corrected by two corresponding reduction factors. In this way, we have the following expression (eq. 2.34):

$$I_{adm} = CF_1 \cdot CF_2 \cdot I_0 \quad (2.34)$$

Being:

- **CF₁**: Correction factor corresponding to the bundling level of the cables. To determine the value of this factor, Table B.52.17 (Table 2.29) of the UNE HD 60364-5-52 standard is used, which includes the values that can be adopted according to the number of circuits or multipolar cables in the installation.

Table 2.29- Table B.52.17 of the UNE-HD 60364-5-52 (2014). Correction factors according to the number of bundled cables

Punto	Disposición (En contacto)	Número de circuitos o de cables multipolares:											Para usarse con las corrientes admisibles, referencia	
		1	2	3	4	5	6	7	8	9	12	16		20
1	Agrupados en el aire, sobre una superficie, empotrados o en el interior de una envolvente	1,00	0,80	0,70	0,65	0,60	0,57	0,54	0,52	0,50	0,45	0,41	0,38	B.52.2 a B.52.13 Métodos A a F

The criterion is to consider that point of the installation where the grouping of cables is maximum. This point corresponds to the final section, that is, to the entrance of the junction boxes. In inverters 2, 3,4 and 5 of Sector 1, the number of cables that arrive at their respective junction boxes is 34 (2x17), and in the case of inverters 1 and 6 it is 10 (2x5). On the other hand, in inverters 1 and 2 of Sector 2, the number of cables that reach their respective junction boxes is 30 (2x15) and 8 (2x4) arrive to the junction box of inverters 3 and 4. Therefore, the CF1s are:

- Junction boxes 2,3,4,5-1: 0,38
- Junction box 1,6-1: 0,483 (linear interpolation between 0.50 and 0.45)
- Junction boxes 1,2-2: 0,38
- Junction boxes 3,4-2: 0,52
- **CF₂**: Correction factor for operating temperature other than 60 °C. In this project a maximum operating temperature of 90 °C has been considered, so the value of this factor is, according to Table A.4 (Table 2.30) of UNE-EN 50618 standard, 0,75.

Table 2.30- Table A.4 of the UNE-EN 50618 (2015) standard. Correction factors for an operating temperature different to 60°C

Temperatura ambiente °C	Factor de conversión
Hasta 60	1,00
70	0,92
80	0,84
90	0,75

- **I₀**: Maximum admissible current of the cable in permanent service at 60 °C of the individual conductor (A). It is the current obtained from Table A.52-2 above.

Therefore, the maximum admissible current based on the installation conditions, I_{adm} , will be, applying eq. (2.34):

Sector 1 (Canyoles I)

- Junction box 1-1
 - Cables with S_{vdDCst} norm of 25 mm²:

$$I_{adm} = 0,483 \cdot 0,75 \cdot 116 \rightarrow I_{adm} = 42,02 A > I_C = 12,95 A$$
- Junction box 2-1
 - Cables with S_{vdDCst} norm of 35 mm²:

$$I_{adm} = 0,38 \cdot 0,75 \cdot 140 \rightarrow I_{adm} = 39,9 A > I_C = 12,95 A$$
 - Cables with S_{vdDCst} norm of 25 mm²:

$$I_{adm} = 0,38 \cdot 0,75 \cdot 116 \rightarrow I_{adm} = 33,06 A > I_C = 12,95 A$$
- Junction box 3-1
 - Cables with S_{vdDCst} norm of 35 mm²:

$$I_{adm} = 0,38 \cdot 0,75 \cdot 140 \rightarrow I_{adm} = 39,9 A > I_C = 12,95 A$$
 - Cables with S_{vdDCst} norm of 25 mm²:

$$I_{adm} = 0,38 \cdot 0,75 \cdot 116 \rightarrow I_{adm} = 33,06 A > I_C = 12,95 A$$
- Junction box 4-1
 - Cables with S_{vdDCst} norm of 25 mm²:

$$I_{adm} = 0,38 \cdot 0,75 \cdot 116 \rightarrow I_{adm} = 33,06 A > I_C = 12,95 A$$
- Junction box 5-1
 - Cables with S_{vdDCst} norm of 35 mm²:

$$I_{adm} = 0,38 \cdot 0,75 \cdot 140 \rightarrow I_{adm} = 39,9 A > I_C = 12,95 A$$
 - Cables with S_{vdDCst} norm of 25 mm²:

$$I_{adm} = 0,38 \cdot 0,75 \cdot 116 \rightarrow I_{adm} = 33,06 A > I_C = 12,95 A$$
- Junction box 6-1
 - Cables with S_{vdDCst} norm of 25 mm²:

$$I_{adm} = 0,483 \cdot 0,75 \cdot 116 \rightarrow I_{adm} = 42,02 A > I_C = 12,95 A$$

Sector 2 (El Tollo)

- Junction box 1-2
 - Cables with S_{vdDCst} norm of 25 mm²:

$$I_{adm} = 0,38 \cdot 0,75 \cdot 116 \rightarrow I_{adm} = 33,06 A > I_C = 12,95 A$$
- Junction box 2-2
 - Cables with S_{vdDCst} norm of 25 mm²:

$$I_{adm} = 0,38 \cdot 0,75 \cdot 116 \rightarrow I_{adm} = 33,06 A > I_C = 12,95 A$$
- Junction box 3-2
 - Cables with S_{vdDCst} norm of 25 mm²:

$$I_{adm} = 0,52 \cdot 0,75 \cdot 116 \rightarrow I_{adm} = 45,24 A > I_C = 12,95 A$$
- Junction box 4-2
 - Cables with S_{vdDCst} norm of 25 mm²:

$$I_{adm} = 0,52 \cdot 0,75 \cdot 116 \rightarrow I_{adm} = 45,24 A > I_C = 12,95 A$$

Hence, with the sections previously obtained by the criterion of the m.a.v.d., the condition of maximum allowable intensity is also met. So, there will be two types of cables for the strings, specifically 25 and 35 mm² in section, all of them being single-pole, made of copper, with XLPE insulation and PVC cover. The

model **Exzhellent Solar XZ1FA3Z-K (AS)** [29], from the company **General Cable**, has been chosen in this case.

2.12.1.2 DC cabling between the junction boxes and the inverters

Criterion of the maximum admissible voltage drop

This formula is identical to that used in the DC cabling of the strings, with the difference that the number of parallel strings reaching these inverters must be taken into account. Therefore, in this case the following expression (eq. 2.35) should be applied to obtain the minimum necessary cable section:

$$S_{vd DC inv} = \frac{2 \cdot L_{DC inv} \cdot N_P \cdot I_{mp}}{\sigma_{T^{\circ}C} \cdot \frac{e_{inv}}{100} \cdot N_S \cdot V_{M mod}} = \frac{2 \cdot L_{DC inv} \cdot N_P \cdot I_{mp}}{\sigma_{x^{\circ}C} \cdot \frac{e_{inv}}{100} \cdot V_{M string}} \quad (2.35)$$

In which:

- $S_{vd DC inv}$: Section of the cable that goes from the junction box to its corresponding inverter according to the maximum admissible voltage drop criterion (mm^2).
- $L_{DC inv}$: Cable length that goes from the junction box to its corresponding inverter (m).
- e_{inv} : Maximum allowable voltage drop between the photovoltaic generator and the connection point to the Public Distribution Network or to the indoor installation. The [ITC-BT-40](#) [25] specifies that a value of 1,5% has to be adopted (V); thus, a value of 0,3% will be applied in case of the cables that connect the junction boxes and the inverters.

The protection boxes (junction boxes) will be installed, as they have an underground connection, in accordance with ITC-BT-13, in a niche in the wall, closed with a metal door, with protection degree IK 10 according to UNE-EN 50.102 protected against corrosion and raised at least 30 cm from the ground.

As in the previous case, once the section of the cables is calculated, it must be normalized to the immediately higher value. Next, the new voltage drop is obtained. Table 2.31 (Sector 1) and Table 2.32 (Sector 2) contain these results.

Table 2.31- Calculation of the section of the wiring between the junction boxes and the inverters of the PV installation corresponding to Sector 1. Criterion of the maximum allowable voltage drop

Sector 1									
Cabling zone	$L_{DC inv}$ (m)	N_p	I_{mp} (A)	σ_T ($m/\Omega \cdot mm^2$)	e_{inv} (%)	$V_{M string}$ (V)	$S_{vd DC inv}$ (mm^2)	$S_{vd DC inv norm}$ (mm^2)	e_{inv} (%) with S_{norm}
CC1-1-1	2,68	5	9,6	45,49	0,3%	834	2,26	2,5	0,13%
CC2-2-1	2,68	17	9,6	45,49	0,3%	834	7,70	10	0,11%
CC3-3-1	2,68	17	9,6	45,49	0,3%	834	7,70	10	0,11%
CC4-4-1	2,68	17	9,6	45,49	0,3%	834	7,70	10	0,11%
CC5-5-1	2,68	17	9,6	45,49	0,3%	834	7,70	10	0,11%
CC6-6-1	2,68	5	9,6	45,49	0,3%	834	2,26	2,5	0,13%

Table 2.32- Calculation of the section of the wiring between the junction boxes and the inverters of the PV installation corresponding to Sector 2. Criterion of the maximum allowable voltage drop

Sector 2									
Cabling zone	$L_{DC inv}$ (m)	N_p	I_{mp} (A)	σ_T ($m/\Omega \cdot mm^2$)	e_{inv} (%)	$V_{M string}$ (V)	$S_{vd DC inv}$ (mm^2)	$S_{vd DC inv norm}$ (mm^2)	e_{inv} (%) with S_{norm}
CC1-1-2	2,68	15	9,6	45,49	0,3%	834	6,79	10	0,10%
CC2-2-2	2,68	15	9,6	45,49	0,3%	834	6,79	10	0,10%
CC3-3-2	2,68	4	9,6	45,49	0,3%	834	1,81	2,5	0,11%
CC4-4-2	2,68	4	9,6	45,49	0,3%	834	1,81	2,5	0,11%

According to this criterion, it would be necessary to install 6 cables of 10 mm² normalized section and 4 cables of 2,5 mm² normalized section.

However, it is by means of the criterion of the maximum admissible current that it is determined whether the previously obtained sections are adequate or whether, on the contrary, it is necessary to use larger sections.

Criterion of the maximum admissible current

The application of this criterion is analogous to that of the DC wiring of the strings but, as was the case with the previous criterion, on this occasion the number of branches in parallel that reach each inverter must be considered. Therefore, the next formula (eq. 2.36) is defined:

$$I_{C\ jb-inv} = 1,25 \cdot N_p \cdot I_{SC\ mod} \leq I_{adm\ jb-inv} \quad (2.36)$$

Being:

- $I_{C\ jb-inv}$: Minimum current for which the connection cables between the junction boxes and their corresponding inverters must be dimensioned, equal to the maximum current that may circulate through the cable (A)
- $I_{adm\ jb-inv}$: Maximum admissible current of the cable (A) between the junction boxes and their corresponding inverters

However, in this case, the corresponding installation **method** is **C**. This is because the cables would be installed on a wall, in vertical sections, and horizontally on the ceiling. Furthermore, since there is a single conductor per cable but there is no column for that value, and XLPE insulation is used in these cables, the column corresponding to two conductors and with this type of insulation is taken, being now **column 11**. With this, and the installation method, it is necessary to go the Table C.52-1 bis (Table 2.33), column 11 and, depending on the section obtained with the previous criterion, obtain the maximum admissible current (to which it is subsequently necessary to apply the CF).

Table 2.33- Table C.52-1 bis of the UNE-HD 60364-5-52 (2014). Admissible currents (A)

Intensidades admisibles en amperios Temperatura ambiente 40 °C en el aire																		
Método de instalación de la tabla B.52-1	Número de conductores cargados y tipos de aislamiento																	
	A1	PVC 3	PVC 2	PVC 3	PVC 2	PVC 3	PVC 2	PVC 3	PVC 2	PVC 3	PVC 2	PVC 3	PVC 2	PVC 3				
A2	PVC 3	PVC 2	PVC 3	PVC 2	PVC 3	PVC 2	PVC 3	PVC 2	PVC 3	PVC 2	PVC 3	PVC 2	PVC 3	PVC 2				
B1																		
B2																		
C																		
E																		
F																		
1	2	3	4	5a	5b	6a	6b	7a	7b	8a	8b	9a	9b	10a	10b	11	12	13
Sección mm²																		
Cobre																		
1,5	11	11,5	12,5	13,5	14	14,5	15,5	16	16,5	17	17,5	19	20	20	20	21	23	-
2,5	15	15,5	17	18	19	20	20	21	22	23	24	26	27	26	28	30	32	-
4	20	20	22	24	25	26	28	29	30	31	32	34	36	36	38	40	44	-
6	25	26	29	31	32	34	36	37	39	40	41	44	46	46	49	52	57	-
10	33	36	40	43	45	46	49	52	54	54	57	60	63	65	68	72	78	-
16	45	48	53	59	61	63	66	69	72	73	77	81	85	87	91	97	104	-
25	59	63	69	77	80	82	86	87	91	95	100	103	108	110	115	122	135	146
35	-	-	-	95	100	101	106	109	114	119	124	127	133	137	143	153	168	182
50	-	-	-	116	121	122	128	133	139	145	151	155	162	167	174	188	204	220
70	-	-	-	148	155	155	162	170	178	185	193	199	208	214	223	243	262	282
95	-	-	-	180	188	187	196	207	216	224	234	241	252	259	271	298	320	343
120	-	-	-	207	217	216	226	240	251	260	272	280	293	301	314	350	373	397
150	-	-	-	-	-	247	259	276	289	299	313	322	337	343	359	401	430	458
185	-	-	-	-	-	281	294	314	329	341	356	368	385	391	409	460	493	523
240	-	-	-	-	-	330	345	368	385	401	419	435	455	468	489	545	583	617
Aluminio																		
2,5	11,5	12	13	14	15	16	16,5	17	17,5	18	19	20	20	20	21	23	25	-
4	15	16	17	19	20	21	22	22	23	24	25	26	28	27	29	31	34	-
6	20	20	22	24	25	27	29	28	30	31	32	33	35	36	38	40	44	-
10	26	27	31	33	35	38	40	40	41	42	44	46	49	50	52	56	60	-
16	35	37	41	46	48	50	52	53	55	57	60	63	66	66	70	76	82	-
25	46	49	54	60	63	63	66	67	70	72	75	78	81	84	88	91	98	110
35	-	-	-	74	78	78	81	83	87	89	93	97	101	104	109	114	122	136
50	-	-	-	90	94	95	100	101	106	108	113	118	123	127	132	140	149	167
70	-	-	-	115	121	121	127	130	136	139	145	151	158	162	170	180	192	215
95	-	-	-	140	146	147	154	159	166	169	177	183	192	197	206	219	233	262
120	-	-	-	161	169	171	179	184	192	196	205	213	222	228	239	254	273	306
150	-	-	-	-	-	196	205	213	222	227	237	246	257	264	276	294	314	353
185	-	-	-	-	-	222	232	243	254	259	271	281	293	301	315	337	361	406
240	-	-	-	-	-	261	273	287	300	306	320	332	347	355	372	399	427	482
Aislamientos termoestables (90°C)																		
Aislamientos termoplásticos (70°C)																		
XLPE: Polietileno reticulado						EPR: Etileno-propileno						PVC: Policloruro de vinilo						

Carrying out the correction of the maximum admissible current obtained from Table A.3 using again the corresponding correction factors in eq. (2.37):

$$I_{adm\ jb-inv} = CF_1 \cdot CF_2 \cdot I_{0\ jb-inv} \quad (2.37)$$

Where:

- $I_{0\ jb-inv}$: Maximum admissible current of the cable between the junction boxes and their corresponding inverters in permanent service at 60 °C of the individual conductor (A). It is the current obtained from Table C.52-1 bis.

Regarding to the values of both correction factors, they are in this case:

- $CF_1 = 1$, since now there is no bundle of cables
- $CF_2 = 1$, since Table C.52-1 bis is already tabulated for an operating temperature of 90 °C.

Using in first instance the normalized sections previously obtained with the maximum admissible voltage drop criterion, it was proven that the maximum admissible current criterion was not satisfied. Thus, it was necessary to increase the section of the cables until the admissible current is higher than the maximum current, in other words, until the admissible current is sufficient. In this case, if the 70, 10 and 6 mm² sections are selected instead of 10, 2,5 (Canyoles) and 2,5 (El Tollo) mm² respectively, the previous condition is met: (eq. 2.36 and 2.37):

Sector 1 (Canyoles I)

- Junction box 1-1 to inverter 1-1
 - Cables with $S_{vd DC st norm}$ of 10 mm²:
$$I_{adm jb-inv} = 1 \cdot 1 \cdot 72 \rightarrow I_{adm jb-inv} = 72 A > I_{C jb-inv} = 1,25 \cdot 5 \cdot 10,36 = 64,75 A$$
- Junction box 2-1 to inverter 2-1
 - Cables with $S_{vd DC st norm}$ of 70 mm²:
$$I_{adm jb-inv} = 1 \cdot 1 \cdot 243 \rightarrow I_{adm jb-inv} = 243 A > I_{C jb-inv} = 1,25 \cdot 17 \cdot 10,36 = 220,15 A$$
- Junction box 3-1 to inverter 3-1
 - Cables with $S_{vd DC st norm}$ of 70 mm²:
$$I_{adm jb-inv} = 1 \cdot 1 \cdot 243 \rightarrow I_{adm jb-inv} = 243 A > I_{C jb-inv} = 1,25 \cdot 17 \cdot 10,36 = 220,15 A$$
- Junction box 4-1 to inverter 4-1
 - Cables with $S_{vd DC st norm}$ of 70 mm²:
$$I_{adm jb-inv} = 1 \cdot 1 \cdot 243 \rightarrow I_{adm jb-inv} = 243 A > I_{C jb-inv} = 1,25 \cdot 17 \cdot 10,36 = 220,15 A$$
- Junction box 5-1 to inverter 5-1
 - Cables with $S_{vd DC st norm}$ of 70 mm²:
$$I_{adm jb-inv} = 1 \cdot 1 \cdot 243 \rightarrow I_{adm jb-inv} = 243 A > I_{C jb-inv} = 1,25 \cdot 17 \cdot 10,36 = 220,15 A$$
- Junction box 6-1 to inverter 6-1
 - Cables with $S_{vd DC st norm}$ of 10 mm²:
$$I_{adm jb-inv} = 1 \cdot 1 \cdot 72 \rightarrow I_{adm jb-inv} = 72 A > I_{C jb-inv} = 1,25 \cdot 5 \cdot 10,36 = 64,75 A$$

Sector 2 (El Tollo)

- Junction box 1-2 to inverter 1-2
 - Cables with $S_{vd DC st norm}$ of 70 mm²:
$$I_{adm jb-inv} = 1 \cdot 1 \cdot 243 \rightarrow I_{adm jb-inv} = 243 A > I_{C jb-inv} = 1,25 \cdot 15 \cdot 10,36 = 194,25 A$$
- Junction box 2-2 to inverter 2-2
 - Cables with $S_{vd DC st norm}$ of 70 mm²:
$$I_{adm jb-inv} = 1 \cdot 1 \cdot 243 \rightarrow I_{adm jb-inv} = 243 A > I_{C jb-inv} = 1,25 \cdot 15 \cdot 10,36 = 194,25 A$$
- Junction box 3-2 to inverter 3-2
 - Cables with $S_{vd DC st norm}$ of 6 mm²:
$$I_{adm jb-inv} = 1 \cdot 1 \cdot 52 \rightarrow I_{adm jb-inv} = 52 A > I_{C jb-inv} = 1,25 \cdot 4 \cdot 10,36 = 51,8 A$$
- Junction box 3-2 to inverter 3-2
 - Cables with $S_{vd DC st norm}$ of 6 mm²:
$$I_{adm jb-inv} = 1 \cdot 1 \cdot 52 \rightarrow I_{adm jb-inv} = 52 A > I_{C jb-inv} = 1,25 \cdot 4 \cdot 10,36 = 51,8 A$$

In this way, there are 16,11 m of 70 mm² section cable (six cables), 5,37 m of 10 mm² section cable (two cables) and 5,37 m of 6 mm² section cable (two cables). Once the necessary sections of the DC cabling have been obtained, it is time to select a commercial model. The model **Energy RV-K FOC 0,6/1 kV XLPE** [30], from the company **General Cable**, has been chosen in this case.

2.12.2 AC Cabling

This kind of cabling includes those sections that distribute the current from the output of each inverter to the corresponding AC measurement and protection panel, as well as the cables that connect said panels to the Low Voltage Panel (LVP), through which the current is alternating. Subsequently, the power line to the pumps goes from the LVP, at 400 V.

The protection and measurement box will be installed, as it has an underground connection, in accordance with the ITC-BT-13, in a niche in the wall, closed with a metal door, with IK 09 protection degree according to UNE-EN 50.102 protected against corrosion and with a height of the measuring equipment housed between 0.7 and 1,80 m.

As said before, the calculation of the necessary section of the AC wiring follows some general lines common to the calculation of the DC wiring, but it has its peculiarities. The following is the procedure for calculating AC wiring sections using the two criteria already mentioned:

Criterion of the maximum admissible voltage drop

Taking into account that the current is triphasic, the formula (eq. 2.38) to be used in this case is the following:

$$S_{vd AC triph} = \frac{\sqrt{3} \cdot L_{AC} \cdot I_{out inv AC} \cdot \cos \varphi}{\sigma_{T^{\circ}C} \cdot \frac{e_{AC}}{100} \cdot V_{net}} \quad (2.38)$$

In which:

- $S_{vd AC triph}$: Section of the AC cable according to the maximum admissible voltage drop criterion (mm²)
- L_{AC} : Length of the AC cable (m)
- $I_{out inv AC}$: Nominal current of the inverter in the alternating part (output) (A)
- $\cos \varphi$: Inverter power factor, which results from the quotient between active power (P) and apparent power (S). This parameter, according to the commercial catalogue of the inverter, is adjustable, so it has been assigned the ideal value, that is $\cos \varphi = 1$ ($\varphi = 0^{\circ}$)
- e_{st} : Maximum allowable voltage drop between the photovoltaic generator and the connection point to the Public Distribution Network or to the indoor installation. The [ITC-BT-40](#) [25] and the IDAE specify that a value of 1,5% has to be adopted (V)
- V_{net} : Voltage between phases of the network to which the installation is connected (V). The value of this parameter is 400 V.

The obtained sections are shown in Table 2.34 (Sector 1) and Table 2.35 (Sector 2), as well as the normalized sections and the new voltage drops:

Table 2.34 Calculation of the section of the wiring between the inverters and the AC measurement and protection panel of the PV installation corresponding to Sector 1. Criterion of the maximum allowable voltage drop

Sector 1									
Cabling zone	L _{AC} (m)	I _{out inv AC} (A)	cos φ (°)	σ _T (m/Ω·mm ²)	e _{AC} (%)	V _{net} (V)	S _{vd AC triph} (mm ²)	S _{vd AC triph norm} (mm ²)	e _{AC} (%) with S _{norm}
Inv 1-1	3,37	145	1	45,49	1,5%	400	3,10	4	1,16%

Inv 2-1	2,87	145	1	45,49	1,5%	400	2,64	4	0,99%
Inv 3-1	2,91	145	1	45,49	1,5%	400	2,68	4	1,00%
Inv 4-1	3,48	145	1	45,49	1,5%	400	3,20	4	1,20%
Inv 5-1	2,91	145	1	45,49	1,5%	400	2,68	4	1,00%
Inv 6-1	2,87	145	1	45,49	1,5%	400	2,64	4	0,99%

Table 2.35- Calculation of the section of the wiring between the inverters and the AC measurement and protection panel of the PV installation corresponding to Sector 2. Criterion of the maximum allowable voltage drop

Sector 1									
Cabling zone	L _{AC} (m)	I _{out inv AC} (A)	cos φ (°)	σ _T (m/Ω·mm ²)	e _{AC} (%)	V _{net} (V)	S _{vd AC triph} (mm ²)	S _{vd AC triph norm} (mm ²)	e _{AC} (%) with S _{norm}
Inv 1-2	2,98	145	1	45,49	1,5%	400	2,74	4	1,03%
Inv 2-2	3,56	145	1	45,49	1,5%	400	3,28	4	1,23%
Inv 3-2	3,51	145	1	45,49	1,5%	400	3,23	4	1,21%
Inv 4-2	2,93	145	1	45,49	1,5%	400	2,70	4	1,01%

According to this criterion, it would be necessary to install 10 cables of 4 mm² normalized section.

Criterion of the maximum admissible current

Now, according to Table B.52-1 of the “Norma UNE-HD 60364-5-52”, since these cables would be installed on a wall, in vertical sections, and horizontally on the ceiling, the installation **method** is **C**.

On the other hand, since there are 3 conductors per cable (this is the AC section, so current is triphasic and each phase runs through one conductor of the cable) and XLPE is the applied insulation, the column corresponding to three conductors and with this type of insulation is taken. With this, and the installation method, it is possible to obtain the results from Table C.52-1 bis, **column 9b**.

Again, the maximum current that may circulate through the cable is obtained by the expression shown below (eq. 2.39):

$$I_{C AC} = 1,25 \cdot I_{AC inv max} \leq I_{adm AC} \quad (2.39)$$

Where:

- **I_{C AC}**: Minimum current for which the AC connection cables must be dimensioned, equal to the maximum current that may circulate through them (A)
- **I_{AC inv max}**: Maximum current value that will circulate from output of the inverter (A)
- **I_{adm AC}**: Maximum admissible current of the AC cable (A)

So now, taking into account the following formula (eq. 2.40):

$$I_{adm AC} = CF_1 \cdot CF_2 \cdot I_{0 AC} \quad (2.40)$$

Where:

- **I_{0 AC}**: Maximum admissible current of the AC cable (A). To check the maximum admissible current, once again it is necessary to refer to the Table C.52-1 bis of the “Norma UNE-HD 60364-5-52”.

Regarding to the values of both correction factors, they are in this case:

- **CF₁** = 0,7 for the AC measurement and protection panels of inverters 1,2,3-1 and of inverters 4,5,6-1 (three bundled cables to each panel) and 0,8 for the AC measurement and protection panels of inverters 1,3-2 and 2,4-2 (two bundled cables to each panel).

- $CF_2 = 0,75$ since in this project the maximum operating temperature has been considered of 90 °C

Using in first instance the normalized sections previously obtained with the maximum admissible voltage drop criterion, it was proven that the maximum admissible current criterion was not satisfied. Thus, it was necessary to increase the section of the cables until the admissible current is higher than the maximum current, in other words, until the admissible current is sufficient. In this case, if the 185 and 150 mm² sections are selected instead of 4 (Canyoles) and 4 (El Tollo) mm² respectively, the following maximum admissible currents are obtained and the previous condition is met (eq. 2.39 and 2.40):

Sector 1 (Canyoles I)

- Inverters 1,2,3-1 to AC m.a.p panel 1,2,3-1
 - Cable with $S_{vd AC st norm}$ of 185 mm²
 $I_{adm AC} = 0,70 \cdot 0,75 \cdot 385 \rightarrow I_{adm AC} = 202,13 A > I_{C AC} = 1,25 \cdot 145 = 181,25A$
- Inverters 4,5,6-1 to AC m.a.p panel 4,5,6-1
 - Cable with $S_{vd AC st norm}$ of 185 mm²
 $I_{adm AC} = 0,70 \cdot 0,75 \cdot 385 \rightarrow I_{adm AC} = 202,13 A > I_{C AC} = 1,25 \cdot 145 = 181,25A$

Sector 2 (El Tollo)

- Inverters 1,3-2 to AC m.a.p panel 1,3-2
 - Cable with $S_{vd AC st norm}$ of 150 mm²
 $I_{adm AC} = 0,80 \cdot 0,75 \cdot 337 \rightarrow I_{adm AC} = 202,2 A > I_{C AC} = 1,25 \cdot 145 = 181,25A$
- Inverters 1,3-2 to AC m.a.p panel 1,3-2
 - Cable with $S_{vd AC st norm}$ of 150 mm²
 $I_{adm AC} = 0,80 \cdot 0,75 \cdot 337 \rightarrow I_{adm AC} = 202,2 A > I_{C AC} = 1,25 \cdot 145 = 181,25A$

On the other hand, the dimensioning AC wiring section consists of three phase conductors and a neutral. The section of said neutral conductor is determined by means of Table 1 of ITC-BT-07 (Table 2.36). Although the table refers to the lines of underground low-voltage distribution facilities, these values have been assumed for the case of an AC line of a low-voltage generation facility as the values corresponding to this type of facility are not specified.

Table 2.36-Table 1 of the ITC-BT-07. Section of the neutral conductor as a function of the section of the phase conductors (mm²)

Conductores fase (mm²)	6 (Cu)	10 (Cu)	16 (Cu)	16 (Al)	25	35	50	70	95	120	150	185	240	300	400
Sección neutro (mm²)	6	10	10	16	16	16	25	35	50	70	70	95	120	150	185

Therefore, in conclusion, the AC section will need six triphasic lines of three conductors of 185 mm² and a neutral of 95 mm² each (Sector 1), and four triphasic lines of three conductors of 150 mm² and a neutral of 70 mm² each (Sector 2). The model **Energy RV-K FOC 0,6/1 kV XLPE** [30], from the company **General Cable**, has been chosen in this case.

2.13 Protection tubes

Protection tubes are used to protect cables within building materials or the terrain they run through. Although it is true that, just as two types of cabling were distinguished, it is necessary to differentiate the protection tubes corresponding to DC cables and AC cables, in this case the procedure is identical for both types of protection tubes.

2.13.1 Protection tubes for DC cabling

First of all, the outer diameter of the protection tubes corresponding to the cabling that connects the end of the strings and the junction boxes must be obtained, for which, as indicated in the section corresponding to the calculation of the minimum necessary wiring sections circulates CC. Specifically, for the dimensioning of this element, Table 9 of the [ITC-BT-21](#) [22] (Table 2.37) (REBT) is used, since it corresponds to the tubes inside buried canalizations. This table is shown below:

Table 2.37- Table 9 of the ITC-BT-21 [22]. Minimum external diameters for buried cable protection tubes (mm)

Sección nominal de los conductores unipolares (mm ²)	Diámetro exterior de los tubos (mm)				
	Número de conductores				
	< 6	7	8	9	10
1,5	25	32	32	32	32
2,5	32	32	40	40	40
4	40	40	40	40	50
6	50	50	50	63	63
10	63	63	63	75	75
16	63	75	75	75	90
25	90	90	90	110	110
35	90	110	110	110	125
50	110	110	125	125	140
70	125	125	140	160	160
95	140	140	160	160	180
120	160	160	180	180	200
150	180	180	200	200	225
185	180	200	225	225	250
240	225	225	250	250	--

In this way, taking into account the sections and number of the cables that come from the strings and arrive to the connection boxes, it is concluded that it would be necessary to acquire:

Sector 1 (Canyoles I)

- Junction box 1-1
 - 5 Cables with $S_{vd DC st norm}$ of 25 mm² → 90 mm external diameter tube
- Junction box 2-1
 - 16 Cables with $S_{vd DC st norm}$ of 25 mm² and 1 of 35 mm² → 110 mm (10) external diameter tube and 90 mm (6+1) external diameter tube
- Junction box 3-1
 - 3 Cables with $S_{vd DC st norm}$ of 25 mm² and 14 of 35 mm² → 110 mm (3+5) external diameter tube and 110 mm (9) external diameter tube
- Junction box 4-1
 - 17 Cables with $S_{vd DC st norm}$ of 25 mm² → 110 mm (9) external diameter tube and 90 mm (8) external diameter tube
- Junction box 5-1
 - 8 Cables with $S_{vd DC st norm}$ of 25 mm² and 9 of 35 mm² → 90 mm (8) external diameter tube and 110 mm (9) external diameter tube

- Junction box 6-1
 - 5 Cables with $S_{vd DC st norm}$ of $25 \text{ mm}^2 \rightarrow 90 \text{ mm}$ external diameter tube

Sector 2 (El Tollo)

- Junction box 1-2
 - 15 Cables with $S_{vd DC st norm}$ of $25 \text{ mm}^2 \rightarrow 90 \text{ mm}$ external diameter tube (8) and 90 mm external diameter tube (7)
- Junction box 2-2
 - 15 Cables with $S_{vd DC st norm}$ of $25 \text{ mm}^2 \rightarrow 90 \text{ mm}$ external diameter tube (8) and 90 mm external diameter tube (7)
- Junction box 3-2
 - 4 Cables with $S_{vd DC st norm}$ of $25 \text{ mm}^2 \rightarrow 90 \text{ mm}$ external diameter tube
- Junction box 4-2
 - 4 Cables with $S_{vd DC st norm}$ of $25 \text{ mm}^2 \rightarrow 90 \text{ mm}$ external diameter tube

In conclusion, 11 tubes of 90 mm external diameter (5592,38 m) and 5 tubes of 110 mm external diameter (2992,36 m) are needed. 5 tubes of 90 mm and other 5 of 110 mm will be in Sector 1, and the other 6 tubes of 90 mm will be in Sector 2. Finally, these amounts must be doubled, since there are two poles (positive and negative) and the previous results are obtained for each sense of the current (remember when the correction factor CF1 was defined). The commercial models have been selected from **IBK cables** [31].

2.13.2 Protection tubes for AC cabling

On the other hand, for the dimensioning of the protective tube between the AC measurement and protection panel, the same table is used as in the previous case, since it also involves buried cables. Therefore, taking into account the diameter of these sections, it has been decided to use a tube with an external diameter of 225 mm , which will be able to accommodate the $3 \times 185 \text{ mm}^2 + 1 \times 95 \text{ mm}^2$ and the $3 \times 150 \text{ mm}^2 + 1 \times 70 \text{ mm}^2$. However, a **250 mm outer diameter** tube has finally been selected since the manufacturer has diameters of 200 and 250 , but not 225 mm [31].

2.14 Protection devices specifications

In this section, the aim is to define the minimum necessary performance of the system protection elements required in the installation, both in the DC and in the AC part, as well as to select the commercial models that satisfy them at the lowest possible cost.

2.14.1 DC Protection devices

In this chapter, the protections corresponding to the part of the installation in which direct current circulates are dimensioned, and the corresponding commercial models are chosen.

2.14.1.1 Protection against overcurrents and short circuits

According to what is stated in the first chapter of this document, they must not only be capable of protecting against overcurrents, but also against short circuits, and must be dimensioned accordingly. For

this, the [ITC-BT-22 \[23\]](#) of the REBT is used, which establishes the following conditions to be met (eq. [2.41](#) and [2.42](#)):

$$I_d \leq I_{nf} \leq I_{adm} \quad (2.41)$$

$$I_{opg} \leq 1,45 \cdot I_{adm} \quad (2.42)$$

Being:

- I_d : Current for which the circuit or line has been designed. Since what reaches each of the fuses housed in each junction box is the set of modules connected in series that form the string they protect, said current is that corresponding to a photovoltaic module at its maximum power point (I_{Mmod}) (A). Thus, the value of this parameter is 9,6 A.
- I_{nf} : This is the rated current of the protection device; in this case, it is the nominal current of the fuse (A). It is the parameter to obtain.
- I_{adm} : Maximum admissible current of the cable depending on the installation method used. Its value was obtained in the chapter corresponding to cabling sizing (A) of [DC cabling of the strings](#).
 - For cables with $S_{vdDCstnorm}$ of 25 mm²:
 - If the number of cables that arrive at their respective junction boxes is 34 (2x17) or 30 (2x15), $I_{adm} = 33,06$ A.
 - If the number of cables that arrive at their respective junction boxes is 10 (2x5), $I_{adm} = 42,02$ A.
 - If the number of cables that arrive at their respective junction boxes is 8 (2x4), $I_{adm} = 45,24$ A.
 - For cables with $S_{vdDCstnorm}$ of 35 mm², since the number of cables that arrive at their respective junction boxes is 34 (2x17), $I_{adm} = 39,90$ A
- I_{opg} : Current that ensures the effective operation of the protection device (fuse). According to the UNE-60269 standard, the value will be taken for the case of a gG type fuse since the standard does not specify values for gPV fuses. Therefore, the value of this parameter must be:

$$\circ \quad I_{opg} = \begin{cases} 1,6 \cdot I_{nf} & \text{if } I_{nf} \geq 16 \text{ A} \\ 1,9 \cdot I_{nf} & \text{if } 4 \text{ A} < I_{nf} < 16 \text{ A} \\ 2,1 \cdot I_{nf} & \text{if } I_{nf} \leq 4 \text{ A} \end{cases} \quad (2.43)$$

Therefore, based on the values in this case, the previous expressions (eq. [2.41](#), [2.42](#) and [2.43](#)) would be as follows:

- For cables with $S_{vdDCstnorm}$ of 25 mm²:
 - If the number of cables that arrive at their respective junction boxes is 34 (2x17) or 30 (2x15):
 - $9,6 \leq I_{nf} \leq 33,06 \text{ A}; 1,9 \cdot I_{nf} \leq 1,45 \cdot 33,06 \text{ A} \rightarrow I_{nf} \leq 25,23 \text{ A}$
 - If the number of cables that arrive at their respective junction boxes is 10 (2x5):
 - $9,6 \leq I_{nf} \leq 42,02 \text{ A}; 1,9 \cdot I_{nf} \leq 1,45 \cdot 42,02 \text{ A} \rightarrow I_{nf} \leq 32,07 \text{ A}$
 - If the number of cables that arrive at their respective junction boxes is 8 (2x4):
 - $9,6 \leq I_{nf} \leq 45,24 \text{ A}; 1,9 \cdot I_{nf} \leq 1,45 \cdot 45,24 \text{ A} \rightarrow I_{nf} \leq 34,53 \text{ A}$
- For cables with $S_{vdDCstnorm}$ of 35 mm², since the number of cables that arrive at their respective junction boxes is 34 (2x17):
 - $9,6 \leq I_{nf} \leq 39,90 \text{ A}; 1,9 \cdot I_{nf} \leq 1,45 \cdot 39,90 \text{ A} \rightarrow I_{nf} \leq 30,45 \text{ A}$

Observing the values obtained, gPV-type fuses with a nominal intensity of 15 A, cutting power equal to or greater than 10 kA and a nominal voltage greater than 125% of the open circuit voltage of the photovoltaic field, which is will 996 V in each junction box since all of them receive strings of 20 modules with an open circuit voltage of 49,8 V (so with a nominal voltage greater than 1245 V) be installed on the DC side. Finally, it has been decided to select fuses of 1500 Vdc nominal voltage, 30 kA cutting power and nominal intensity of 15 A.

In addition, it can be observed that the two first conditions are met.

The above calculations determine the values that the chosen commercial fuses must achieve to satisfy the overcurrent protection conditions. However, as mentioned previously, these devices must also protect against short circuits. For this, and again in accordance with the provisions of [ITC-BT-22](#) [23], the following conditions (eq. 2.44, 2.45 and 2.46) must be met:

$$P_{fb} \geq I_{SCmaxf} \quad (2.44)$$

$$I_{SCadmcond} > I_{opf5} \quad (2.45)$$

$$I_{SCminf} > I_{opf5} \quad (2.46)$$

In which:

- P_{fb} : Fuse breaking capacity (A)
- I_{SCmaxf} : Maximum short-circuit current that can be generated downstream of the fuse (A)
- $I_{SCadmcond}$: Admissible short-circuit current (A). Represents the maximum current that the cable can withstand for 5 seconds without deterioration. From the [ITC-BT-22](#) [23] the next equation (eq. 2.47) is obtained, which allows to calculate this parameter:

$$I_{SCadmcond} = k \cdot \frac{S}{\sqrt{t}} \quad (2.47)$$

Where, in turn:

- k : Coefficient that depends on the material of which the conductor is made and the insulation it has. In case of using copper cable with XLPE insulation, its value is 143 (consult the [UNE 20460-4-43](#) standard)
- S : Cable section (mm^2)
- t : Maximum duration of the short circuit, during which the equipment must guarantee the protection of the installation. It has been set at 5 s.
- I_{opf5} : Minimum current capable of making the fuse act in a time not exceeding 5s (A). It is therefore the fusing current in 5 seconds of the selected fuse.
- I_{SCminf} : Minimum short-circuit current that can be generated downstream of the fuse (A). Its value is calculated using the simplified expression (eq. 2.48) found in the "[Guía BT Anexo 3](#)":

$$I_{SCminf} = \frac{0,8 \cdot U}{Z_L} \quad (2.48)$$

Being:

- U : According to the "[Guía BT Anexo 3](#)", the phase-neutral supply voltage is taken, which is 230 V. This is because it is considered as the most unfavourable.

- Z_L : Line impedance, which is calculated, again, under the most unfavourable conditions, which in this case correspond to those with the highest service temperature (Ω). The equation that allows obtaining its value is the following eq. (2.49):

$$Z_L = \sqrt{R_L^2 + X_L^2} \quad (2.49)$$

Where, in turn:

- R_L : Line resistance. It is obtained by means of the next formula (eq. 2.50) (Ω):

$$R_L = \frac{L_L \cdot \rho_{90^\circ C}}{S_L} = \frac{L_L}{\sigma_{90^\circ C} \cdot S_L} \quad (2.50)$$

- L_L : Length of the line (m). To calculate this parameter, the length of the longest string is taken, since this is the most unfavourable case, to ensure compliance with any of the other strings. In this case, it is 622,73 m.
- $\rho_{90^\circ C}$: Resistivity of the material that makes up the cable. At 90°C (highest service temperature) and for copper, its value is 0,02198 ($\Omega \cdot \text{mm}^2/\text{m}$).
- $\sigma_{90^\circ C}$: Conductivity of the material that makes up the cable. At 90°C (highest service temperature) and for copper, its value is 45,49 ($\text{m}/\Omega \cdot \text{mm}^2$) [26].
- S_L : Section of the line conductor (mm^2). Equal to S.

- X_L : Line inductive reactance (Ω). Its obtaining is carried out using the following eq. (2.51):

$$X_L = L_L \cdot 2 \cdot \pi \cdot f \cdot L = L_L \cdot \omega \cdot L \quad (2.51)$$

- f : Current frequency (Hz). In Europe, its value is 50 Hz.
- L : Coil inductance (H). Its value is assumed in 0,5 μH .
- ω : Angular frequency (Rad)

For cables which section does not exceed 120 mm^2 , the value of this parameter in the line can be considered negligible. The cables have a section that do not exceed 35 mm^2 , so $X_L \cong 0 \rightarrow Z_L = R_L$.

Therefore, since the breaking capacity of the fuses selected in the first instance ($P_{fb} = 30$ kA) is far greater than the maximum short-circuit current that could occur not only in the string that each one protects (10,36 A) but also in the set of strings of the photovoltaic field that reach the DC junction box in which it is found in the worst case in which through said DC junction box all the current of the strings converges in a single branch (176,12 in the table that receives more branches in parallel, 17 in total), the first condition is fulfilled in all cases more than enough.

Regarding the second condition, using eq. (2.45) and (2.47), there is:

$$I_{SC \text{ adm cond } 25 \text{ mm}^2} = k \cdot \frac{S}{\sqrt{t}} = 143 \cdot \frac{25}{\sqrt{5}} = 1598,79 \text{ A} > I_{op f 5, 15 \text{ A}} = 90 \text{ A}$$

$$I_{SC \text{ adm cond } 35 \text{ mm}^2} = k \cdot \frac{S}{\sqrt{t}} = 143 \cdot \frac{35}{\sqrt{5}} = 2238,30 \text{ A} > I_{op f 5, 15 \text{ A}} = 90 \text{ A}$$

So, it is also satisfied.

Finally, regarding the third condition eq. (2.46) and (2.48):

$$I_{SC \text{ min } f 25 \text{ mm}^2} = \frac{0,8 \cdot 230}{\frac{622,73}{45,39 \cdot 25}} = \frac{0,8 \cdot 230}{0,549} = 335,29 \text{ A} > I_{op f 5, 15 \text{ A}} = 90 \text{ A}$$

$$I_{SC \text{ min } f 35 \text{ mm}^2} = \frac{0,8 \cdot 230}{\frac{622,73}{45,39 \cdot 25}} = \frac{0,8 \cdot 230}{0,549} = 469,40 \text{ A} > I_{op f 5, 15 \text{ A}} = 90 \text{ A}$$

So, as this condition is also met, the initial choice is corroborated, and the fuses selected in the first instance are the ones finally chosen [32].

2.14.1.2 Protection against overvoltages. Surge arresters

[ITC-BT-23](#) establishes that the device in charge of this type of protection must reduce overvoltages (transient) to a value that is admissible and endurable by the equipment it protects downstream. Based on this, the DC junction box has to include Type 2 surge protection devices, characterized by the following properties:

- The nominal discharge current must be greater than 5 kA. The overvoltages protection element must be capable of grounding high currents characterized by an 8/20 μ s curve, as established in UNE HD 60364-5-53 standard.
- Since of the four categories of overvoltages contemplated in this standard depending on the equipment it protects, in the case of the equipment of the installation that is the subject of this document, these can be included in Category III ("equipment and materials that are part of the electrical installation fixed and other equipment for which a high level of reliability is required", such as elevators, switches, distribution cabinets, etc.), the associated protection level must be $U_p \leq 4 \text{ kV}$ (consult the [ITC-BT-23](#) standard).
- They are the most widely used because they offer a level of protection compatible with most equipment that is connected to the power supply network.
- The connection between the protection element and its earth connection must be made by means of a copper conductor of at least 4 mm² section.
- The voltage applied to the protection device in permanent service U_c must be less than the maximum voltage supported by it continuously.

Following these conditions, it has been decided to install a Type 2 overvoltage protection device, with $I_n=20 \text{ kA}$ at 8/20 μ s (current capable of bypassing the Type 2 protector at least 20 times), $I_{max}=40 \text{ kA}$ at 8/20 μ s (maximum current capable of shifting to ground only once), $U_p \leq 4 \text{ kV}$, nominal voltage $U_c = 1000 \text{ V}$ and a maximum working voltage of 1170 V.

These devices are considered to comply with the prescriptions of devices with similar characteristics established in UNE-EN 61643-11: 2013 / A11: 2018 [33].

2.14.1.3 Protection against direct and indirect contacts. DC side grounding

The pv generator will be grounded in floating mode. The [UNE-HD 60364-4-41: 2018](#) standard sets out the minimum specifications that a system that uses the **IT installation scheme** [19 and 24] must meet for grounding. First, it is established that all the masses of the pv installation must be grounded, either individually, in groups or together; in this case it has been decided to connect these masses in groups. In the DC section the frames of the modules will be connected to earth via copper rods. Their configuration

must be round, highly resistant, ensuring maximum rigidity to facilitate their introduction into the ground and preventing them from bending due to the force of the hits.

An effort will be made to ensure that the grounding resistance of the set of 2 m long copper rods and the 35 mm² bare copper wiring that interconnects them is a maximum of 10 - 12 Ω. To do this, the calculus is done as it is shown in the following:

The resistance of each rod is given by eq. (2.52):

$$R_{vgr} = \frac{\rho_t}{L_{vgr}} \quad (2.52)$$

Being:

- R_{vgr} : Resistance of a vertical grounding rod (Ω)
- ρ_t : Resistivity of the terrain, with a value of 160 Ω·m. The following Table 2.38 shows the typical values of this parameter according to the characteristics of the terrain:

Table 2.38- Approximate average values of resistivity as a function of the terrain. Source: ITC-BT-18 [21]

Naturaleza terreno	Resistividad en Ohm.m
Terrenos pantanosos	de algunas unidades a 30
Limo	20 a 100
Humus	10 a 150
Turba húmeda	5 a 100
Arcilla plástica	50
Margas y Arcillas compactas	100 a 200
Margas del Jurásico	30 a 40
Arena arcillosas	50 a 500
Arena silícea	200 a 3.000
Suelo pedregoso cubierto de césped	300 a 5.00
Suelo pedregoso desnudo	1500 a 3.000
Calizas blandas	100 a 300
Calizas compactas	1.000 a 5.000
Calizas agrietadas	500 a 1.000
Pizarras	50 a 300
Roca de mica y cuarzo	800
Granitos y gres procedente de alteración	1.500 a 10.000
Granito y gres muy alterado	100 a 600
Naturaleza del terreno	Valor medio de la resistividad Ohm.m
Terrenos cultivables y fértiles, terraplenes compactos y húmedos	50
Terraplenes cultivables poco fértiles y otros terraplenes	500
Suelos pedregosos desnudos, arenas secas permeables	3.000

- L_{vgr} : Length of the vertical grounding rod (m), with a value of 2 m

For its part, the resistance of the bare copper conductor is obtained by means of eq. (2.53):

$$R_{bcc} = \frac{2 \cdot \rho_t}{L_{bcc}} \quad (2.53)$$

In which:

- R_{bcc} : Resistance of the bare copper conductor (Ω)
- L_{bcc} : Length of the ring of bare copper cable (m)

In addition, it is necessary to know the total resistance of the set of rods (eq. 2.54):

$$R_{tvgr} = \frac{1}{n \cdot \frac{1}{R_{vgr}}} \quad (2.54)$$

Where:

- $R_{t v g r}$: Resistance of the set of vertical grounding rods (Ω)
- n : Number of grounding rods in the installation.

And together with the resistance offered by the bare copper conductor, there is (eq. 2.55):

$$R_{v g r n} = \frac{1}{\frac{1}{R_{t v g r}} \cdot \frac{1}{R_{b c c}}} \leq 10 \Omega \quad (2.55)$$

Being:

- $R_{v g r n}$: Resistance of the network of vertical grounding rods and bare copper conductor (Ω)

Finally, substituting the known data and combining the previous equations, the minimum number of grounding rods necessary is determined:

$$\frac{1}{\frac{1}{n \cdot \frac{1}{L_{v g r}}} \cdot \frac{1}{\frac{2 \cdot \rho_t}{L_{b c c}}}} = \frac{1}{\frac{1}{n \cdot \frac{1}{\frac{160}{2}}} \cdot \frac{1}{\frac{2 \cdot 160}{20}}} \leq 10 \rightarrow n \geq 3$$

So, 3 grounding copper rods will be used, for every group of protected masses.

On the other hand, it is worth mentioning that the [ITC-BT-18 \[21\]](#) establishes recommendations to set the minimum required section of the protection conductors (grounding) that connect the masses with the main grounding terminal, in such a way that protection and grounding is guaranteed, based on the cross-section of the phase conductors. These protective conductors are housed in the same conduit as the active conductors and are made of the same material. The following Table 2.39, extracted from said ITC, reflects these values:

Table 2.39- Relationship between the sections of the protective conductors and the phase conductors. Source: ITC-BT-18

Sección de los conductores de fase de la instalación S (mm^2)	Sección mínima de los conductores de protección S_p (mm^2)
$S \leq 16$	$S_p = S$
$16 < S \leq 35$	$S_p = 16$
$S > 35$	$S_p = S/2$

Since the cables that connect the strings with the junction boxes have a section of 25 or 35 mm^2 , according to the previously mentioned table, in any case, $S_p = 16 \text{ mm}^2$.

In view of the large number of strings that exist in the photovoltaic generator, as well as the limited space available for the correct arrangement of the different wiring, the following has been decided: a series of sets of strings have been established each one of which has its own grounding system consisting, as previously calculated, of 3 interconnected rods. In this way, the frames of the modules that make up each string will be connected to earth through the mentioned 16 mm^2 cable, to a system of 3 vertical rods of 2 m length interconnected with each other by about 20 m of bare copper cable with a section of 35 mm^2 . The commercial model, from **Sofamel** company, can be searched in [38].

Only in the IT system a first insulation failure does not cause a system shutdown.

In addition, it is necessary to install an insulation controller, whose function is to warn of a first fault and allow disconnection to prevent a second fault from occurring that would already lead to dangerous fault voltages. This function is carried out by inverters.

Fourth, it is necessary to have devices that eliminate a second fault that could be due to short circuits. The installation also meets this condition, thanks to the systems incorporated by the selected commercial inverter and the DC connection box with the fuses.

Finally, as an additional measure to guarantee people's safety, all elements of the photovoltaic field (modules, cables, connection boxes ...) will be equipped with Class II insulation.

2.14.2 AC Protection devices

In this chapter, the protections corresponding to the part of the installation in which alternating current circulates are dimensioned, and the corresponding commercial models are chosen.

Said calculation, as can be seen later, is analogous to that developed in the direct current part of the installation, since the elements that carry out the protection of the AC part are also protected in indoor installations.

2.14.2.1 Protection against overcurrents and short circuits

A type C magnetothermal switch will be placed, as said in Chapter 1. Hence, the conditions to meet are expressed by the eq. (2.56) and eq. (2.57):

$$I_{d AC} \leq I_{n ms} \leq I_{M adm cond AC} \quad (2.56)$$

$$1,3 \cdot I_{n ms} \leq 1,45 \cdot I_{M adm cond AC} \quad (2.57)$$

Being:

- $I_{d AC}$: Line design current, equal to the inverter's maximum AC current (A). In this case, the value of this parameter is 145 A.
- $I_{n ms}$: This is the rated current of the protection device; in this case, it is the nominal current of the magnetothermal switch (A), which is necessary to determine.
- $I_{M adm cond AC}$: Maximum admissible current of the cable depending on the installation method used. Its value was obtained in the chapter corresponding to the [AC cabling sizing](#) (A). It was of 202,13 A for the AC m.a.p panels of Sector 1, and 202,2 A for those of Sector 2.

Therefore, based on the values in this case, the previous eq. (2.56) and (2.57) would be as follows:

Sector 1 (Canyoles I)

- AC m.a.p panel 1,2,3-1

$$145 \leq I_{n ms} \leq 202,13$$

$$1,3 \cdot I_{n ms} \leq 1,45 \cdot 202,13 \rightarrow I_{n ms} \leq 225,45 A$$

- AC m.a.p panel 4,5,6-1

$$145 \leq I_{n ms} \leq 202,13$$

$$1,3 \cdot I_{n ms} \leq 1,45 \cdot 202,13 \rightarrow I_{n ms} \leq 225,45 A$$

Sector 2 (El Tollo)

- AC m.a.p panel 1,3-2

$$145 \leq I_{n\ ms} \leq 202,2$$

$$1,3 \cdot I_{n\ ms} \leq 1,45 \cdot 202,2 \rightarrow I_{n\ ms} \leq 225,53\ A$$

- AC m.a.p panel 2,4-2

$$145 \leq I_{n\ ms} \leq 202,2$$

$$1,3 \cdot I_{n\ ms} \leq 1,45 \cdot 202,2 \rightarrow I_{n\ ms} \leq 225,53\ A$$

Thus, the two first conditions are met in any case.

The above calculations determine the values that the chosen commercial magnetothermal switch must achieve to satisfy the overcurrent protection conditions. However, as mentioned previously, these devices must also protect against short circuits. For this, and again in accordance with the provisions of [ITC-BT-22 \[23\]](#), the conditions to meet are expressed by the eq. (2.58) and eq. (2.59):

$$P_{ms\ b} \geq I_{SC\ max\ ms} \quad (2.58)$$

$$I_{SC\ min\ ms} > I_{mt} \quad (2.59)$$

In which:

- $P_{ms\ b}$: Magnetothermal switch breaking capacity (A).
- $I_{SC\ max\ ms}$: Maximum short-circuit current that can occur at the point where the magnetothermal switch is located (A). The distribution company responsible for the area where the installation is located establishes the value of this parameter, since it is in the AC part. In the province of Valencia, the distribution company is IBERDROLA. The document MT 2.00.12 (13-09) of the company establishes a minimum value of 4500 A, as well as the [ITC-BT-17 \[20\]](#), section 1.3, and the [ITC-BT-22 \[23\]](#), section 1.1. In this case, a value of 12 kA is taken, to be more conservative.
- I_{mt} : Magnetic tripping current of the protection device (A). From the [ITC-BT-22 \[23\]](#) the following eq. (2.60) is obtained, which allows to calculate this parameter:

$$k^2 \cdot S^2 > I_{mt}^2 \cdot t \quad (2.60)$$

Where, in turn:

- k : Coefficient that depends on the material of which the conductor is made and the insulation it has. In case of using copper cable with XLPE insulation, its value is 143, according to the following table taken from the UNE 20460-4-43 standard:
 - S : Cable section (mm^2)
 - t : Maximum duration of the short circuit during which the equipment must guarantee the protection of the installation. It has been set at 0,1 s.
- $I_{SC\ min\ ms}$: Minimum short-circuit current that can be generated downstream of the magnetothermal switch (A). Its value is calculated using the simplified expression (eq. 2.61) found in the [BT Guide Annex 3](#).

$$I_{SC\ min\ ms} = \frac{0,8 \cdot U}{Z_L + Z_N} \quad (2.61)$$

Being:

- U : Simple voltage, value 230 V. It is the phase-neutral supply voltage.
- Z_N : Neutral impedance, which is calculated, again, under the most unfavourable conditions, which in this case correspond to those with the highest service temperature (Ω). The equation that allows obtaining its value is the following eq. (2.62):

$$Z_N = \sqrt{R_N^2 + X_N^2} \quad (2.62)$$

Where, in turn:

- R_N : Neutral resistance. It is obtained by means of the next formula (Ω) (eq. 2.63):

$$R_N = \frac{L_L \cdot \rho_{90^\circ C}}{S_N} = \frac{L_L}{\sigma_{90^\circ C} \cdot S_N} \quad (2.63)$$

Equation 1. Neutral resistance

- S_N : Section of the neutral conductor (mm^2). Equal to S.
- X_N : Neutral inductive reactance (Ω). Its obtaining is carried out using the following eq. (2.64):

$$X_N = L_c \cdot 2 \cdot \pi \cdot f \cdot L = L_c \cdot \omega \cdot L \quad (2.64)$$

With all these formulas and the known data:

Sector 1 (Canyoles I)

- AC m.a.p panels 1,2,3-1 and 4,5,6-1
 - $R_L = \frac{L_L}{\sigma_{90^\circ C} \cdot S_L} = \frac{3,48}{45,49 \cdot 185} \rightarrow R_L = 413,52 \cdot 10^{-6} \Omega$
 - $R_N = \frac{L_N}{\sigma_{90^\circ C} \cdot S_N} = \frac{3,48}{45,49 \cdot 95} \rightarrow R_N = 805,27 \cdot 10^{-6} \Omega$
 - $X_L = L_L \cdot 2 \cdot \pi \cdot f \cdot L = 5 \cdot 10^{-5} \cdot \pi \cdot 3,48 \rightarrow X_L = 546,64 \cdot 10^{-6} \Omega$
 - $X_N = 0 \Omega$ (Since the section is smaller than 120 mm^2)
 - $Z_L = \sqrt{R_L^2 + X_L^2} = \sqrt{(413,52 \cdot 10^{-6})^2 + (546,64 \cdot 10^{-6})^2} \rightarrow Z_L = 685,43 \cdot 10^{-6} \Omega$
 - $Z_N = \sqrt{R_N^2 + X_N^2} = \sqrt{(805,27 \cdot 10^{-6})^2} \rightarrow Z_N = 805,27 \cdot 10^{-6} \Omega$
 - $I_{SC \min ms} = \frac{0,8 \cdot U}{Z_L + Z_N} = \frac{0,8 \cdot 230}{685,43 \cdot 10^{-6} + 805,27 \cdot 10^{-6}} \rightarrow I_{SC \min ms} = 123.426,19 A$
 - $I_{mt} < 143 \cdot \frac{185}{\sqrt{0,1}} \rightarrow I_{mt} < 83.658,06 A$

So, to summarize:

- $P_{ms b} \geq 12 kA$
- $I_{SC \min ms} = 123.426,19 A > I_{mt} = 83.658,06 A$

Sector 2 (El Tollo)

- AC m.a.p panels 1,3-2 and 2,4-2
 - $R_L = \frac{L_L}{\sigma_{90^\circ C} \cdot S_L} = \frac{3,56}{45,49 \cdot 150} \rightarrow R_L = 521,73 \cdot 10^{-6} \Omega$
 - $R_N = \frac{L_N}{\sigma_{90^\circ C} \cdot S_N} = \frac{3,56}{45,49 \cdot 70} \rightarrow R_N = 1,12 \cdot 10^{-3} \Omega$
 - $X_L = L_L \cdot 2 \cdot \pi \cdot f \cdot L = 5 \cdot 10^{-5} \cdot \pi \cdot 3,56 \rightarrow X_L = 559,20 \cdot 10^{-6} \Omega$
 - $X_N = 0 \Omega$ (Since the section is smaller than 120 mm^2)
 - $Z_L = \sqrt{R_L^2 + X_L^2} = \sqrt{(521,73 \cdot 10^{-6})^2 + (559,20 \cdot 10^{-6})^2} \rightarrow Z_L = 764,79 \cdot 10^{-6} \Omega$

- $Z_N = \sqrt{R_N^2 + X_N^2} = \sqrt{(1,12 \cdot 10^{-3})^2} \rightarrow Z_N = 1,12 \cdot 10^{-3} \Omega$
- $I_{SC \min ms} = \frac{0,8 \cdot U}{Z_L + Z_N} = \frac{0,8 \cdot 230}{764,79 \cdot 10^{-6} + 1,12 \cdot 10^{-3}} \rightarrow I_{SC \min ms} = 97.722,30 A$
- $I_{mt} < 143 \cdot \frac{150}{\sqrt{0,1}} \rightarrow I_{mt} < 67.830,85 A$

So, to summarize:

- $P_{msb} \geq 12 kA$
- $I_{SC \min ms} = 97.722,30 A > I_{mt} = 67.830,86 A$

As these two conditions are also met, it will be sufficient to select a magnetothermal switch that has a breaking capacity of at least 12 kA and a nominal current of between 145 and 203 A. It has been selected the **DPX³** commercial model with $I_{nms} = 160 A$ and $P_{msb} = 16 kA$ from **Legrand** company [39].

2.14.2.2 Protection against direct and indirect contacts

For this kind of protection, differential switches are the most widely used devices. Since the differential switch is sized basing on the characteristics of the chosen magnetothermal switch determined in the previous point, the selected commercial ID must comply with the following expressions eq (2.65) and eq. (2.66):

$$I_{nds} \geq I_{nms} = 160 A \quad (2.65)$$

$$P_{dsb} \geq P_{msb} = 16 kA \quad (2.66)$$

In which:

- I_{nds} : This is the rated current of the protection device; in this case, it is the nominal current of the magnetothermal switch (A)
- P_{dsb} : Differential switch breaking capacity (A)

The selected commercial model of magnetothermal switch also includes, according to the manufacturer Legrand [39], the differential protection function, so the above conditions are met.

On the other hand, another important parameter, and that is necessary to determine, is the sensitivity of the DS, since as seen in the next point the choice of this value will determine the value of the grounding resistance and with it the characteristics of electrode to use. A value of 300 mA is chosen, which implies that the DS allows the passage of fault currents of up to 0,3 A, which does not pose a risk to human health.

2.14.2.3 AC side grounding

In the AC section the inverters and the protection boxes will be connected to earth via copper rods, following a **TT scheme** in this case. The calculation of the grounding resistance of the AC masses can be found in the [ITC-BT-18](#) [21] standard of the REBT.

By means of a procedure very similar to that one described in the [DC side grounding section](#), the number of grounding roads will be, for each protected element, of $n \geq 1$.

If, once the resistivity of the terrain has been verified, it is higher than the value considered, the number of grounding rods could be increased to ensure that the value established as the limit is not exceeded.

Same commercial product is chosen that in [DC section](#) [38].

In a TT scheme, the neutral of the line must be grounded. Since the AC line is connected to the existing LV panel of the transformation centre and the transformer of said centre already has its neutral grounded, it is not necessary to ground this line. However, although not strictly necessary, this grounding could be reinforced by grounding the neutral of the AC line at an intermediate point between the inverter output and the C.T. This is done in the AC measurement and protection boxes.

2.15 Maintenance of the hydraulic-photovoltaic installation

In all types of facilities, both industrial and domestic and on a small or large scale, it is necessary to carry out a minimum periodic maintenance, not only because of the benefits that this entails, but also because of the existence of laws that oblige it.

The installation of this project is not an exception. Therefore, it is necessary to define a series of periodic maintenance guidelines, both corrective and preventive:

- **Corrective maintenance:** Consists of using the device in question until failure, after which it must be repaired or, if necessary, replaced. It requires no planning or inspection and the investment is minimal, but it offers little security. This includes the periodically necessary changes of the various components of the installation. Based on this, it is estimated that every 5 years it will be necessary to replace between 5 and 7% of the solar panels, and a further 350 € amount per year is reserved for other types of minor repairs or replacements such as some sections of cabling or protection elements that have become unusable after having acted.
- **Preventive maintenance:** It consists of carrying out a planning of the necessary inspections and interventions of the installation in order to avoid important damages that result in a significant reduction in the activity of the plant or pose a danger to its integrity. To select the actuation times, it is possible to resort to the data of the manufacturers, with which the statistical laws of failure (MTBF and probability density function) can be determined. In this sense, during the first ten years of the project's useful life, a complete review of the state of the projected photovoltaic installation will be carried out every two years. Said review will be carried out annually in subsequent years. The estimated annual cost is € 400. On the other hand, frequent cleaning of the panels will also be carried out to mitigate losses due to dust and dirt as well as their scratch. Its annual cost will be estimated at € 1000.

To efficiently manage maintenance tasks based on the elements to be maintained, the operations carried out, their useful lifetime and other necessary parameters, the option of using a CMMS is interesting, although it is left to the customer's discretion if it should finally be use this methodology.

Considering these and other expenses, it is decided to allocate an annual amount of 4000 € to maintenance and replacements. However, the possible effect of inflation (sustained and generalized increase in the level of prices and services) must be taken into account, for which the CPI ("Consumer Price Index") is taken as a reference. It is taken as [2,2% per year](#) until the end of the project's life period. It does not only affect the expenses due to maintenance, replacements and insurance, but also the selling price and the purchase price (for these two last prices a 2% is considered).

Although it would also affect electricity prices, both the electricity tariff and the surplus sale price, specific variations have been considered for these.

Chapter 3.

Economic analysis

3.1 Introduction

For this thesis, two economic studies were carried out:

- First, a project budget was drawn up, detailing the different costs of both the materials and components to be installed and the work force and machinery that must be used for the development of the works. To avoid an excessive length of the document, this economic evaluation has not been included, but only the different budgets, obtained by means of the program *Arquímedes*, have been described and specified:

The sum of the costs of the measurement and budget table reflects the Material Execution Budget (PEM in Spanish), which must be provided in capital letters and figures. In this budget, the I.V.A. is not taken into account, since it is applied afterwards (in the PEM attached in this document it has been considered, so in the economic analysis it was discounted).

The Material Execution Budget amounts to the expressed amount of ONE MILLION ONE HUNDRED EIGHTY-FIVE THOUSAND FIVE HUNDRED SIX EUROS AND THIRTY-FOUR CENTS.

Discounting the I.V.A, it amounts to NINE HUNDRED SEVENTY-NINE THOUSAND SEVEN HUNDRED FIFTY-SEVEN EUROS AND THIRTY-ONE CENTS

MATERIAL EXECUTION BUDGET..... 979.757,31 €

Next, a certain percentage of General Expenses and Construction Management and another of Industrial Benefit must be applied (13% and 6% have been taken respectively, since they are very common values) to, added to the previous budget, obtain the Execution Budget by Contract (PEC in Spanish).

General Expenses (13%)..... 127.368,45 €

Industrial Benefit (6%)..... 58.785,44 €

EXECUTION BUDGET BY CONTRACT..... 1.165.911,20€

Finally, adding 21% of I.V.A., the Tender Base Budget (PBL in Spanish) is calculated, which again must be provided both in figures and in capital letters.

I.V.A (21%)..... 244.841,35 €

TENDER BASE BUDGET..... 1.410.752,56 €

The projected budget amounts to the expressed amount of:

ONE MILLION FOUR HUNDRED TEN THOUSAND SEVEN HUNDRED FIFTY-TWO EUROS AND FIFTY-SIX CENTS.

- Second, an economic viability analysis was carried out, which reflects the expected evolution of the cash flows based on the benefits obtained both from the saving of energy consumed from the network and from the sale of surplus energy, in the event of exist, so that the suitability of the execution of said project can be analysed intuitively based on the expected benefits.

In this way, the Promoter could decide, based on fairly solid results, if the effort made to disburse the necessary investment in year 0 is compensated in an appropriate period and proportion.

3.2 Economic feasibility analysis

The production of electrical energy through the photovoltaic generator is associated with savings. In certain periods the energy production will be enough to cover the demand and the surplus will be poured into the grid, obtaining profits from its sale, and in other periods, even if the energy consumption exceeds the photovoltaic production, there will be savings due to the reduction of energy consumed from the grid.

On the other hand, the main stumbling block when it comes to guaranteeing the final profitability of any project is the initial investment involved in the construction and start-up of the facility.

First of all, the following Table 3.1 shows the monthly and annual consumptions of the two sectors of the irrigation area for which the photovoltaic installation has been designed. As it is not an industrial building, these consumptions are not distributed in a practically uniform way in the different months of the year, but there are very noticeable variations in those months in which said consumptions rise as a consequence of the greater irrigation needs.

Table 3.1- Monthly and annual consumptions (kWh) of the pumping systems of Sector 1, 2 and total

Month	Sector 1 (kWh)	Sector 2 (kWh)
January	11358,54	8731,71
February	9555,60	8018,92
March	11178,25	7484,32
April	11900,01	14523,15
May	19652,08	15859,63
June	29748,57	29669,99
July	38582,99	40450,97
August	45614,47	45173,22
September	35878,58	29313,59
October	23618,56	21294,68
November	15865,90	12028,37
December	12800,90	14255,85
Annual	265754,45	246804,40
Total	512558,85	

Similarly, energy production by the photovoltaic system will not be constant throughout the year, reaching higher production in the months closer to the summer period, where solar radiation is considerably higher (the increase in power generated as a consequence the increase in irradiance received more than compensates for the reduction in said power due to the higher temperatures reached in the cells of the photovoltaic modules).

It should be emphasized that, when determining the benefits, a distinction is made, on the one hand, that is indirectly due to the annual economic savings associated with the reduction in consumption of electrical energy from the network and, on the other hand, that due to the sale of the energy surpluses in the electricity market

in those moments in which photovoltaic generation exceeds the consumption of the pumping groups. The corresponding expressions of these benefits are given by eq. (3.1) and eq. (3.2):

- Benefit associated to the reduction in the consumption of electrical energy from the network:

$$Saving_{month\ i}(\text{€}) = \begin{cases} E_{prod\ month\ i}(\text{kWh}) \cdot price_{purchase} \left(\frac{\text{€}}{\text{kWh}} \right) & \text{if } E_{prod\ month\ i} < E_{cons\ month\ i} \\ E_{cons\ month\ i}(\text{kWh}) \cdot price_{purchase} \left(\frac{\text{€}}{\text{kWh}} \right) & \text{if } E_{prod\ month\ i} > E_{cons\ month\ i} \end{cases} \quad (3.1)$$

Here, the annual savings due to the use of the energy recovered by the PATs (around 4500 €/year) has been taken into account.

- Benefit associated to the sale of surpluses:

$$Benefits_{month\ i}(\text{€}) = \left(E_{prod\ month\ i}(\text{kWh}) - E_{cons\ month\ i}(\text{kWh}) \right) \cdot price_{sale} \left(\frac{\text{€}}{\text{kWh}} \right) \quad (3.2)$$

The sale price of the energy considered is, as indicated in the previous document, 0,05 €/kWh initially, with an annual increase of 2%, close to the considered CPI (2,2%). This difference is considered in order to have into account the impact that the entrance of new energies could have in the sale price of the energy; however, it must be said that it is a conservative value (most of the sources consulted apply a CPI of 3% to energy, what would result in higher benefits). Regarding the purchase price of energy from the grid, it is taken equal to 0,0934 €/kWh; this is an average price based on the various types of rates that exist and the powers contracted, to which the 2% annual increase is also applied due to the IPC expected evolution.

Table 3.2 shown below lists the values used for the various variables that need to be taken into account to carry out the economic analysis of the project:

Table 3.2- Considerations for the cash flows and economic indicators (NPV, IRR and PP)

Parameter	Unit	Value
Investment (TBB)	€	1.410.752,56
Maintenance, replacements and insurance	€	4000
Useful life	Years	25
Production (first year)	kWh	1.385.509,74
Consumption	kWh	512.558,85
Consumption from pv energy	kWh	459.062,91
Surplus energy	kWh	926.446,84
CPI (for maintenance and insurance)	%	2,2
CPI (for sale and purchase price)	%	2
k	%	2,5
Annual power loss (%) first 10 years	%	1
Annual power loss (%) last 15 years	%	0,67
Cost of representation	€/kWh	0,00082
Generation access toll	€/kWh	0,0005
Sale price of energy (first year)	€/kWh	0,05
Purchase price of energy (first year)	€/kWh	0,0934

On the other hand, two relevant aspects are assumed: firstly, it is assumed that the hourly irradiance levels with which it has been worked will be relatively constant in future years, and that the solar irradiance will remain at a similar intensity (for example, currently the sun is in a period of low activity); secondly, that the water needs, and therefore energy needs, will be the same in the years for which the useful life of the installation has been projected.

The following graphs illustrate the energy flows in the hydraulic-photovoltaic installation, the savings and benefits obtained in the first year, the cash flows and the updated accumulated cash flows in the case of installing the designed photovoltaic system ($\approx 70\%$ of required modules).

Regarding the results of the NPV, IRR and PP, they are shown in the following Table 3.3:

Table 3.3- Results of the financial indicators of the economic analysis

NPV (€)	267.747,46 €
IRR (%)	4,0207%
PP	20,309

As can be seen, the NPV of the project is 267.747,46 €, so it is positive and produces benefits within the 25-year term considered. In turn, the IRR is 4,021%, so it is higher than both the discount rate k (2,5%) and the Equivalent Annual Rate (2%) in case of requesting a bank loan for this type of investment (see attached table below), so it would be feasible to finance the investment through said loan.

With these parameters it is possible, in principle, to guarantee that the project is profitable, and that therefore it is advisable to carry out its execution and start-up. Specifically, according to the PP, this project will report benefits from the year 20; this result is the least promising, since a return on investment ends very far from year 0, and it is desirable and usual for benefits to be reported between the eighth and the twelfth year of operation.

On the other hand, it should be noted what has already been said above, and that is that the energy and water needs of the analyzed system and the irradiance levels received have been considered constant, and the evolution of the prices of sale and purchase of energy, as well as the discount rate and interest rate of the bank loan (TAE) applied, have been taken basing on a personal criterion, although as objective and well-founded as possible, which variation would have a direct and notable influence on the financial indicators obtained, which could result in both an unprofitable project and a project with higher profits than expected. See Table 3.4 for more information.

Table 3.4- Evolution of the last 5 years of the EAR interest rates for new operations. Loans and credits to households and NPISHs and non-financial corporations. Credit institutions and EFC. Source: Banco de España [40]

	TAE						
	Hogares e ISFLSH			Sociedades no financieras			
	Vivienda	Consumo (c)	Otros Fines	Otros créditos hasta 250 mil euros	Otros créditos entre 250 mil y 1 millón de euros	Otros créditos de más de 1 millón de euros	
	1	2	3	4	5	6	
10	R	2,66	7,47	5,64	4,55	3,89	2,71
11		3,66	9,11	6,29	5,57	4,79	3,53
12		2,93	8,31	6,23	5,67	4,27	3,00
13		3,16	9,52	5,92	5,54	4,03	2,83
14		2,64	9,10	4,93	4,52	2,91	2,10
15		2,31	8,45	4,19	3,59	2,20	2,07
16		2,18	8,05	4,27	3,28	1,91	1,63
17		2,05	8,27	4,01	2,93	1,80	1,56
18		2,24	8,31	3,72	2,67	1,70	1,59
19		1,93	7,91	3,47	2,58	1,55	1,26
20	Jun	1,92	7,64	3,10	2,37	1,76	1,58
	Jul	1,92	8,01	3,67	3,02	1,81	1,79
	Ago	1,98	8,20	3,71	2,70	1,65	1,52
	Sep	1,91	7,78	3,46	2,73	1,62	1,40
	Oct	1,91	7,52	3,94	3,11	1,69	1,44
	Nov	1,82	6,98	3,74	2,74	1,66	1,32
	Dic	1,67	7,57	3,12	2,55	1,66	1,43
21	Ene	1,74	7,52	4,32	3,48	1,78	1,16
	Feb	1,69	7,54	3,80	2,65	1,62	1,18

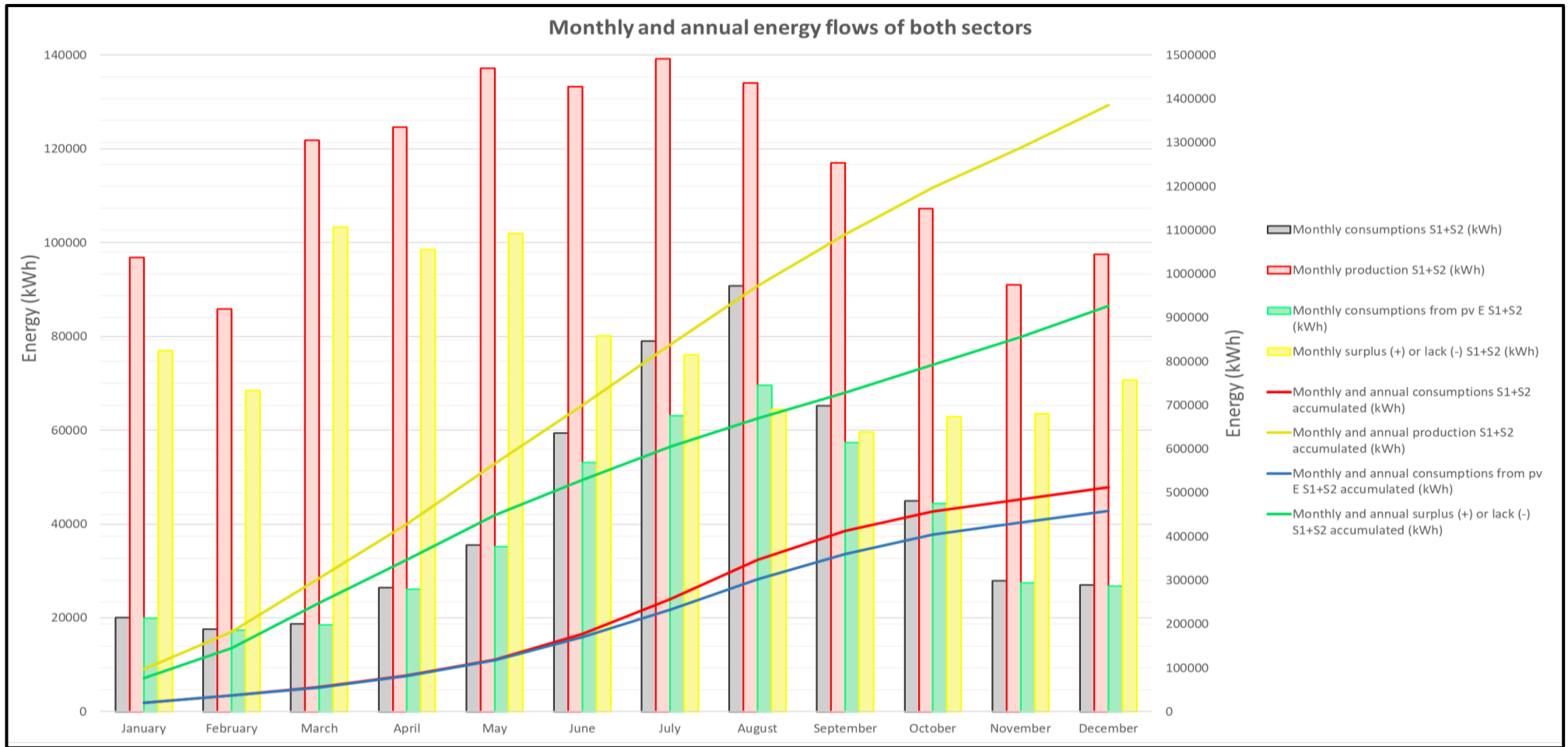


Figure 3.1- Energy flows of both sectors



Figure 3.2- Expected savings and benefits of both sectors in the first year

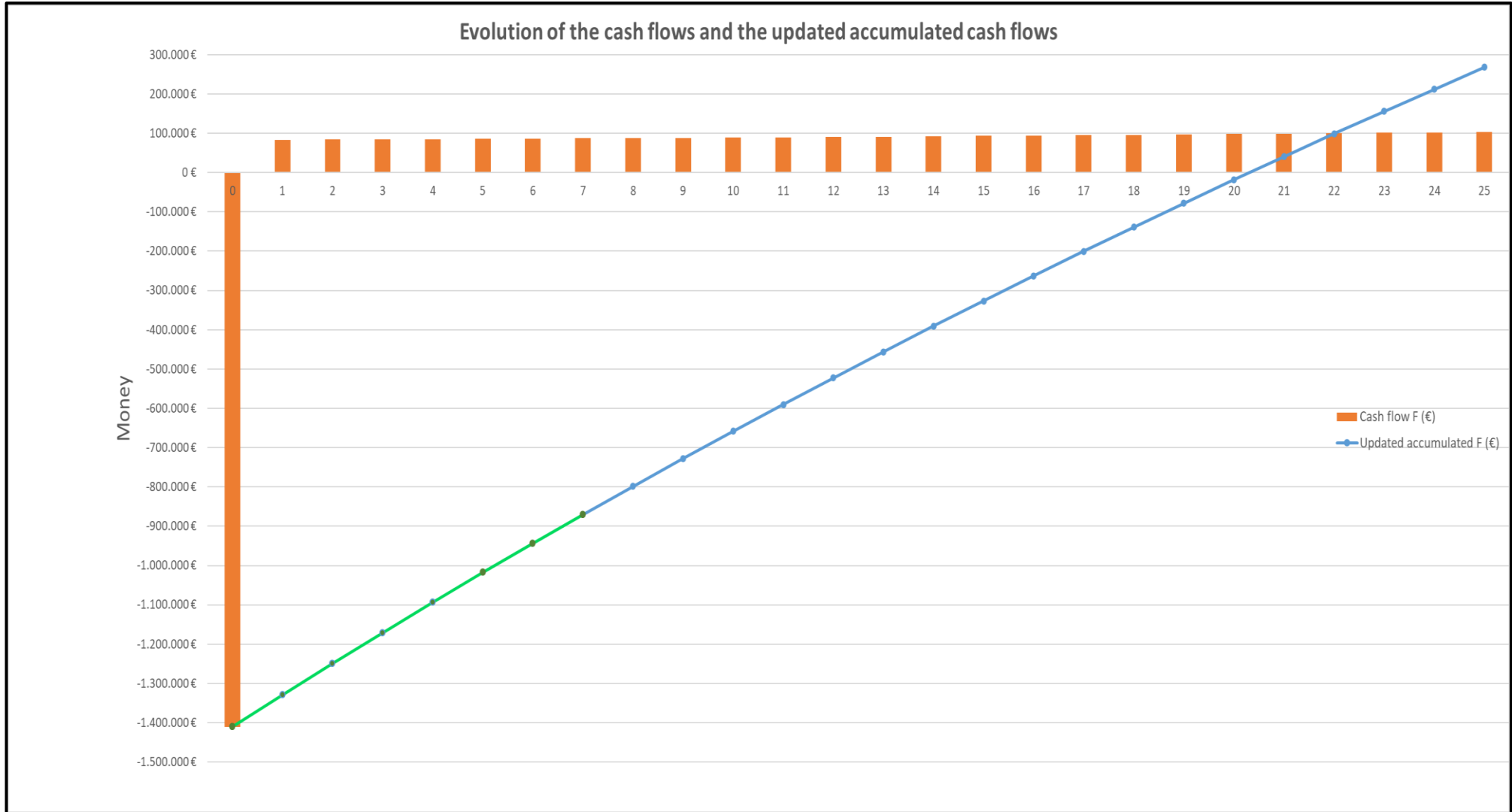


Figure 3.3- Cash flows and updated accumulated cash flows

On the other hand, the following conclusions can be drawn from the three previous graphs:

- In the first of them (Figure 3.1), it is observed how in every month the energy produced by the photovoltaic installation is higher than the consumption needs, which means that in all of them there is a surplus of energy that can be sold in the network and, therefore, from which benefits can be obtained. In turn, it is observed how in the months in which the water and energy needs are higher (June-October), despite the fact that the energy production of the installation is notably higher, as the energy needs increase to a much greater extent, the energy surpluses are lower. On the contrary, in those months in which less radiation is received, but the needs of the irrigation sectors are much lower (November-May), despite the fact that energy production is lower, greater surpluses of energy are obtained that can be sold in the net. The self-consumption level is, in the first year, presented by the eq. (3.3):

$$S.C_{level} = \frac{\text{Annual consumptions from pv E}}{\text{Annual consumption needs}} = \frac{459.062,91}{512.558,85} \rightarrow S.C_{level} \approx 0,8956 = 89,56\% \quad (3.3)$$

- The second graph (Figure 3.2) is closely related to the first, since it reflects, in monetary terms, the different energy flows existing in the installation. In this way, it can be seen how in the months that were previously indicated as having higher energy production, but even higher energy demand (June-October), the benefits from savings are higher than the benefits from the sale of surplus energy, while that in the other months (November-May) a higher profit is obtained from the sale of surpluses than from savings due to the decrease in energy demand from the network.
- Finally, the last graph (Figure 3.3) reflects two facts: the first, that the cash flows are somewhat higher each year, going from about 83.360 € to 102.799 €, since although an annual power loss of the photovoltaic generator has been considered, and therefore a decrease in the energy that is obtained both for self-consumption and for sale and an increase in the demand for energy from the network, the established CPI allows the benefits to increase slightly each year (about 800 € per year); the second, that the cumulative updated cash flow becomes positive at the beginning of year 20, as previously indicated by the PP.

As a last conclusion in the economic aspect, to emphasize that the financial parameters obtained would change taking into account the annual interest derived from the bank loan required for the partial or total financing of the investment (it should be remembered that the budget is closely of a million and a half euros, and that the Promoter is an irrigation society with about 20-25 members). In addition, accounting for the investment at once in year 0 instead of the annual payment corresponding to the entity that lends the money distorts the results obtained to some extent. Therefore, just as an example, and without going into greater detail, two possible scenarios are proposed:

Case 1 (Pessimistic): Financing of 100% of the initial investment through a bank loan, with an annual interest of 2,5% and a repayment term of 18 years.

Table 3.5- Financial parameters considered (Case 1)

Initial capital C (€)	1.410.752,56
Annual interest i (%)	2,5
Years of payment t (y)	18
Periods per year (-)	1
Number of payments (-)	18
Payment per period (€)	98.287,24
Annual payment (€)	98.287,24
Payment of interests (€)	358.417,84
Total payment (€)	1.769.170,39

Table 3.6- Annual payment of the loan amortization and the interests generated (Case 1)

Period	Initial balance	Share	Interests	Amortization	Final balance
1	1.410.752,56 €	98.287,24 €	35.268,81 €	63.018,43 €	1.347.734,12 €
2	1.347.734,12 €	98.287,24 €	33.693,35 €	64.593,89 €	1.283.140,23 €
3	1.283.140,23 €	98.287,24 €	32.078,51 €	66.208,74 €	1.216.931,50 €
4	1.216.931,50 €	98.287,24 €	30.423,29 €	67.863,96 €	1.149.067,54 €
5	1.149.067,54 €	98.287,24 €	28.726,69 €	69.560,56 €	1.079.506,98 €
6	1.079.506,98 €	98.287,24 €	26.987,67 €	71.299,57 €	1.008.207,41 €
7	1.008.207,41 €	98.287,24 €	25.205,19 €	73.082,06 €	935.125,35 €
8	935.125,35 €	98.287,24 €	23.378,13 €	74.909,11 €	860.216,24 €
9	860.216,24 €	98.287,24 €	21.505,41 €	76.781,84 €	783.434,41 €
10	783.434,41 €	98.287,24 €	19.585,86 €	78.701,38 €	704.733,02 €
11	704.733,02 €	98.287,24 €	17.618,33 €	80.668,92 €	624.064,10 €
12	624.064,10 €	98.287,24 €	15.601,60 €	82.685,64 €	541.378,46 €
13	541.378,46 €	98.287,24 €	13.534,46 €	84.752,78 €	456.625,68 €
14	456.625,68 €	98.287,24 €	11.415,64 €	86.871,60 €	369.754,08 €
15	369.754,08 €	98.287,24 €	9.243,85 €	89.043,39 €	280.710,69 €
16	280.710,69 €	98.287,24 €	7.017,77 €	91.269,48 €	189.441,21 €
17	189.441,21 €	98.287,24 €	4.736,03 €	93.551,21 €	95.889,99 €
18	95.889,99 €	98.287,24 €	2.397,25 €	95.889,99 €	0,00 €

Table 3.7- Results of the financial indicators of the economic analysis (Case 1)

Parameter	Value
NPV (€)	-36.339,98 €
IRR (%)	2,3020%
PP	>25

Therefore, in this case, the project would not be profitable (although narrowly), since the NPV is negative, the IRR is lower than both the discount rate k and the interest on the bank loan (EAR) and the PP is longer than the estimated duration of the installation (25 years).

Table 3.8- Results of income, expenses and evolution of annual updated accumulated cash flows (Case 1)

Year (y)	Incomes from the sale of surpluses and the save of cons. from grid (€)	Expenses due to the payment of the interests(€)	Expenses per purchase of energy (€)	Expenses per maintenance (€)	Cash flow F (€)	Updated F (€)	Updated accumulated F (€)
0					-1.410.752,56 €		-1.410.752,56 €
1	92.407,13 €	-35.268,81 €	-5.046,49 €	-4.000,00 €	48.091,83 €	46.918,86 €	-1.363.833,70 €
2	93.263,44 €	-33.693,35 €	-5.198,38 €	-4.080,00 €	50.291,70 €	47.868,37 €	-1.315.965,33 €
3	94.118,68 €	-32.078,51 €	-5.354,33 €	-4.161,60 €	52.524,24 €	48.773,98 €	-1.267.191,35 €
4	94.972,46 €	-30.423,29 €	-5.514,44 €	-4.244,83 €	54.789,90 €	49.636,94 €	-1.217.554,41 €
5	95.824,39 €	-28.726,69 €	-5.678,82 €	-4.329,73 €	57.089,15 €	50.458,49 €	-1.167.095,92 €
6	96.674,04 €	-26.987,67 €	-5.847,56 €	-4.416,32 €	59.422,49 €	51.239,82 €	-1.115.856,09 €
7	97.520,99 €	-25.205,19 €	-6.020,78 €	-4.504,65 €	61.790,38 €	51.982,10 €	-1.063.874,00 €
8	98.364,79 €	-23.378,13 €	-6.198,59 €	-4.594,74 €	64.193,33 €	52.686,45 €	-1.011.187,54 €
9	99.204,97 €	-21.505,41 €	-6.381,10 €	-4.686,64 €	66.631,83 €	53.354,00 €	-957.833,55 €
10	100.041,06 €	-19.585,86 €	-6.568,44 €	-4.780,37 €	69.106,39 €	53.985,80 €	-903.847,74 €
11	101.234,99 €	-17.618,33 €	-6.740,41 €	-4.875,98 €	72.000,28 €	54.874,64 €	-848.973,11 €
12	102.438,30 €	-15.601,60 €	-6.916,63 €	-4.973,50 €	74.946,57 €	55.726,96 €	-793.246,15 €
13	103.650,89 €	-13.534,46 €	-7.097,21 €	-5.072,97 €	77.946,25 €	56.543,80 €	-736.702,35 €
14	104.872,65 €	-11.415,64 €	-7.282,25 €	-5.174,43 €	81.000,33 €	57.326,14 €	-679.376,21 €
15	106.103,45 €	-9.243,85 €	-7.471,84 €	-5.277,92 €	84.109,84 €	58.074,95 €	-621.301,27 €
16	107.343,18 €	-7.017,77 €	-7.666,11 €	-5.383,47 €	87.275,83 €	58.791,18 €	-562.510,09 €
17	108.591,70 €	-4.736,03 €	-7.865,16 €	-5.491,14 €	90.499,37 €	59.475,74 €	-503.034,35 €
18	109.848,86 €	-2.397,25 €	-8.069,11 €	-5.600,97 €	93.781,54 €	60.129,53 €	-442.904,83 €
19	111.114,52 €		-8.278,06 €	-5.712,98 €	97.123,47 €	60.753,42 €	-382.151,41 €
20	112.388,50 €		-8.492,15 €	-5.827,24 €	98.069,10 €	59.848,72 €	-322.302,68 €
21	113.670,63 €		-8.711,49 €	-5.943,79 €	99.015,35 €	58.952,38 €	-263.350,31 €
22	114.960,73 €		-8.936,21 €	-6.062,67 €	99.961,85 €	58.064,31 €	-205.286,00 €
23	116.258,61 €		-9.166,43 €	-6.183,92 €	100.908,26 €	57.184,43 €	-148.101,57 €
24	117.564,06 €		-9.402,29 €	-6.307,60 €	101.854,17 €	56.312,66 €	-91.788,90 €
25	118.876,86 €		-9.643,91 €	-6.433,75 €	102.799,20 €	55.448,92 €	-36.339,98 €

Case 2 (Optimistic): Financing of ≈92% of the initial investment through a bank loan, with an annual interest of 2% and a repayment term of 8 years.

In this case, 115.000€ will be directly paid by the Sociedad de Riego as part of the initial investment of year 0.

Table 3.9- Financial parameters considered (Case 2)

Initial capital C (€)	1.295.752,56
Annual interest i (%)	2
Years of payment t (y)	8
Periods per year (-)	1
Number of payments (-)	8
Payment per period (€)	176.882,92
Annual payment (€)	176.882,92
Payment of interests (€)	119.310,81
Total payment (€)	1.415.063,37

Table 3.10- Annual payment of the loan amortization and the interest generated (Case 2)

Period	Inicial balance	Share	Interests	Amortization	Final balance
1	1.295.752,56 €	176.882,92 €	25.915,05 €	150.967,87 €	1.144.784,69 €
2	1.144.784,69 €	176.882,92 €	22.895,69 €	153.987,23 €	990.797,46 €
3	990.797,46 €	176.882,92 €	19.815,95 €	157.066,97 €	833.730,49 €
4	833.730,49 €	176.882,92 €	16.674,61 €	160.208,31 €	673.522,17 €
5	673.522,17 €	176.882,92 €	13.470,44 €	163.412,48 €	510.109,70 €
6	510.109,70 €	176.882,92 €	10.202,19 €	166.680,73 €	343.428,97 €
7	343.428,97 €	176.882,92 €	6.868,58 €	170.014,34 €	173.414,63 €
8	173.414,63 €	176.882,92 €	3.468,29 €	173.414,63 €	0,00 €

Table 3.11- Results of the financial indicators of the economic analysis (Case 2)

Parameter	Value
NPV (€)	272.836,46 €
IRR (%)	4,0885%
PP	20,223

Since there are now more favourable conditions, with a smaller bank interest and a shorter loan repayment period, as well as a smaller loan considering that a small part of the initial investment can be made with own funds, all indicators are favourable for the execution of the project, being even slightly better than those obtained initially, when the annual expenses derived from the repayment of the loan were not considered.

Table 3.12- Results of income, expenses and evolution of annual updated accumulated cash flows (Case 2)

Year (y)	Incomes from the sale of surpluses and the save of cons. from grid (€)	Expenses due to the payment of the interests(€)	Expenses per purchase of energy (€)	Expenses per maintenance (€)	Cash flow F (€)	Updated F (€)	Updated accumulated F (€)
0					-1.295.752,56 €		-1.295.752,56 €
1	92.407,13 €	-25.915,05 €	-5.046,49 €	-4.000,00 €	57.445,59 €	56.044,48 €	-1.239.708,08 €
2	93.263,44 €	-22.895,69 €	-5.198,38 €	-4.080,00 €	61.089,36 €	58.145,74 €	-1.181.562,34 €
3	94.118,68 €	-19.815,95 €	-5.354,33 €	-4.161,60 €	64.786,80 €	60.160,98 €	-1.121.401,36 €
4	94.972,46 €	-16.674,61 €	-5.514,44 €	-4.244,83 €	68.538,58 €	62.092,57 €	-1.059.308,79 €
5	95.824,39 €	-13.470,44 €	-5.678,82 €	-4.329,73 €	72.345,40 €	63.942,79 €	-995.366,00 €
6	96.674,04 €	-10.202,19 €	-5.847,56 €	-4.416,32 €	76.207,97 €	65.713,89 €	-929.652,11 €
7	97.520,99 €	-6.868,58 €	-6.020,78 €	-4.504,65 €	80.126,99 €	67.408,05 €	-862.244,06 €
8	98.364,79 €	-3.468,29 €	-6.198,59 €	-4.594,74 €	84.103,17 €	69.027,39 €	-793.216,68 €
9	99.204,97 €		-6.381,10 €	-4.686,64 €	88.137,24 €	70.573,98 €	-722.642,69 €
10	100.041,06 €		-6.568,44 €	-4.780,37 €	88.692,25 €	69.286,25 €	-653.356,45 €
11	101.234,99 €		-6.740,41 €	-4.875,98 €	89.618,60 €	68.302,35 €	-585.054,10 €
12	102.438,30 €		-6.916,63 €	-4.973,50 €	90.548,17 €	67.327,62 €	-517.726,47 €
13	103.650,89 €		-7.097,21 €	-5.072,97 €	91.480,71 €	66.361,97 €	-451.364,50 €
14	104.872,65 €		-7.282,25 €	-5.174,43 €	92.415,97 €	65.405,30 €	-385.959,21 €
15	106.103,45 €		-7.471,84 €	-5.277,92 €	93.353,69 €	64.457,51 €	-321.501,70 €
16	107.343,18 €		-7.666,11 €	-5.383,47 €	94.293,60 €	63.518,52 €	-257.983,18 €
17	108.591,70 €		-7.865,16 €	-5.491,14 €	95.235,40 €	62.588,23 €	-195.394,94 €
18	109.848,86 €		-8.069,11 €	-5.600,97 €	96.178,79 €	61.666,56 €	-133.728,38 €
19	111.114,52 €		-8.278,06 €	-5.712,98 €	97.123,47 €	60.753,42 €	-72.974,96 €
20	112.388,50 €		-8.492,15 €	-5.827,24 €	98.069,10 €	59.848,72 €	-13.126,24 €
21	113.670,63 €		-8.711,49 €	-5.943,79 €	99.015,35 €	58.952,38 €	45.826,14 €
22	114.960,73 €		-8.936,21 €	-6.062,67 €	99.961,85 €	58.064,31 €	103.890,45 €
23	116.258,61 €		-9.166,43 €	-6.183,92 €	100.908,26 €	57.184,43 €	161.074,88 €
24	117.564,06 €		-9.402,29 €	-6.307,60 €	101.854,17 €	56.312,66 €	217.387,54 €
25	118.876,86 €		-9.643,91 €	-6.433,75 €	102.799,20 €	55.448,92 €	272.836,46 €

Chapter 4.

Conclusions

Photovoltaic energy has gained great weight in recent years, and its growth is expected to continue at a high rate, becoming the main (or second) renewable energy worldwide in the coming decades. Its applications are numerous, as already mentioned above.

In the project that illustrates this master's thesis, the aim was to achieve the highest level of self-consumption by installing a photovoltaic generator that would supply the energy demand of two pumping groups. Finally, due to the available space and establishing a reasonable budget, it was decided to install a total of 2320 panels, which with a peak power in STC of 400 Wp gives rise to a photovoltaic installation of 928 kWp, so it is of a considerable size. This means that in the first year almost 90% of self-sufficiency is reached, which is progressively decreasing due to the loss of efficiency of the panels due to their degradation. At the same time, this quantity of panels means that great benefits are obtained, not only due to the savings in the purchase of energy from the network, but also due to the sale of surpluses in those moments when it is not necessary to pump water (or a part of the energy can be injected into the network). However, due to the large outlay that must be made in year 0, the benefits, although important, are not reached until the last five years of the installation's useful life. Based on the last mentioned, it is necessary to take into account several assumptions that have been considered (although trying to be as strict and objective as possible) in this project:

- The water and energy needs have been assumed to be constant throughout the useful life of the projected installation. In the future, the needs may increase, due to greater cultivation area or due to the substitution of rainfed crops for irrigated crops, they may be reduced or they may be practically the same.
- The irradiance levels used for the calculations of the power deliverable by the panels have also been considered constant. This is also perfectly variable in successive years, not only due to the weather itself but also due to the evolution of solar activity.
- A multitude of parameters have been assumed in this project, such as the percentages of industrial profit and general expenses, the discount rate, the interest rate of the bank loan, the own funds that can be counted on to make the investment, the prices of purchase and sale of energy or the evolution of both the associated emissions of various pollutants when consuming energy from the network and the CPI of energy. On the other hand, to say that it has been tried to choose conservative values in many cases to obtain fewer misleading results.

It would be interesting to study other alternatives in which the percentage of self-consumption is lower, or also the possibility of increasing the capacity of the reservoirs to allow a greater volume of water to be stored and, perhaps with this, to be able to allocate a greater percentage of photovoltaic energy its sale in the electrical network.

On the other hand, although it is true that, in principle, the profitability of the project would be assured and that the reduction in pollutant emissions in successive years is undeniable (although it would be necessary to analyse the emissions during the life cycle of the components used), Threats that may arise in the field of energy generation must also be taken into account. For example, it could be the case that the price of energy in the network is reduced, or increased less than expected, reducing savings, due to the improvement of the efficiency in the production of existing technologies or even the penetration of new energy sources, such as nuclear fusion, which could make the facility's profitability lower than expected.

Annex I.

Plans



Scale 1:2.500.000



Scale 1:36.000



Scale 1:110.000

Legend	
	Railroad network
	Railroad network
	Dual carriageway A-35
	Autonomous road of Com. Val CV-649

MASTER'S FINAL PROJECT IN INDUSTRIAL ENGINEERING,
SPECIALIZATION IN ENERGY GENERATION



Project: **DESIGN OF A PHOTOVOLTAIC SOLAR INSTALLATION FOR THE IRRIGATION OF THE VALLADACULTIVATION AREA (VALENCIA)**

Plan: **Situation and location**

Author: **Victor Felip Plaza**

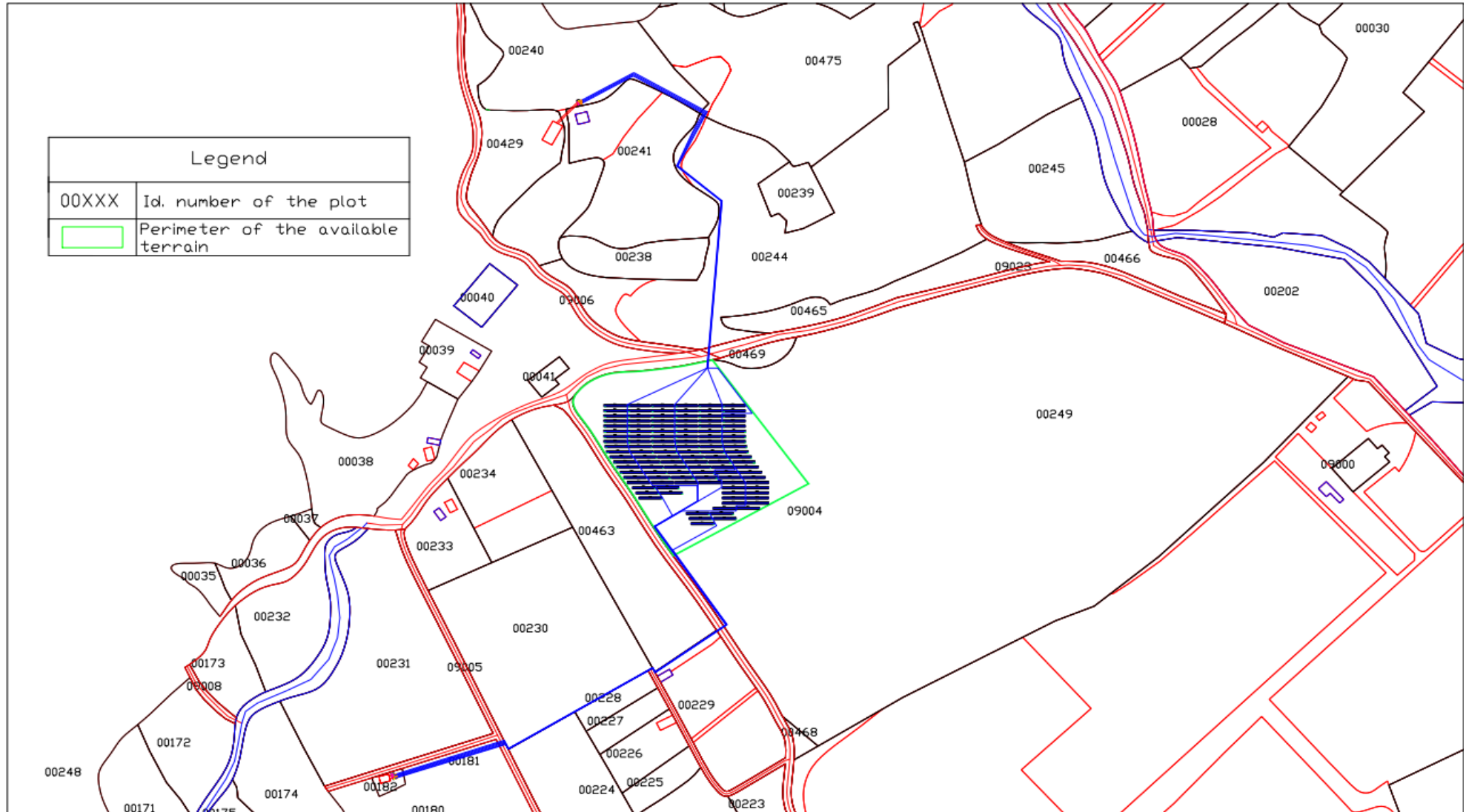
Signature:


Date: **March 2021**

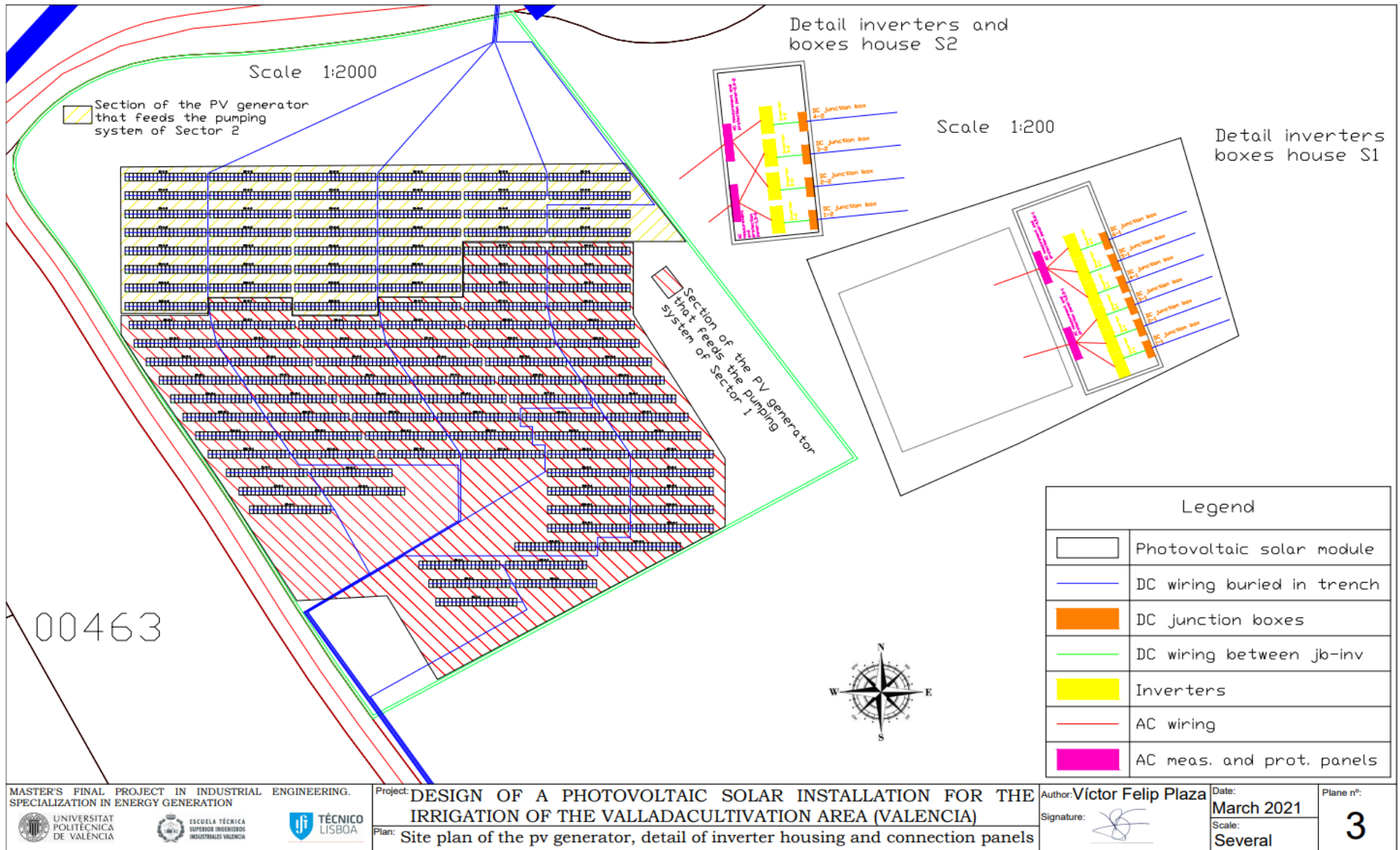
Scale: **Several**

Plane n°:

1



MASTER'S FINAL PROJECT IN INDUSTRIAL ENGINEERING. SPECIALIZATION IN ENERGY GENERATION	Project: DESIGN OF A PHOTOVOLTAIC SOLAR INSTALLATION FOR THE IRRIGATION OF THE VALLADACULTIVATION AREA (VALENCIA) Plan: Site plan of the photovoltaic generator	Author: Victor Felip Plaza Signature: 	Date: March 2021 Scale: 1:10000	Plane n°: 2
--	--	---	--	--------------------



MASTER'S FINAL PROJECT IN INDUSTRIAL ENGINEERING.
SPECIALIZATION IN ENERGY GENERATION



Project: **DESIGN OF A PHOTOVOLTAIC SOLAR INSTALLATION FOR THE IRRIGATION OF THE VALLADACULTIVATION AREA (VALENCIA)**

Plan: **Site plan of the pv generator, detail of inverter housing and connection panels**

Author: **Victor Felip Plaza**

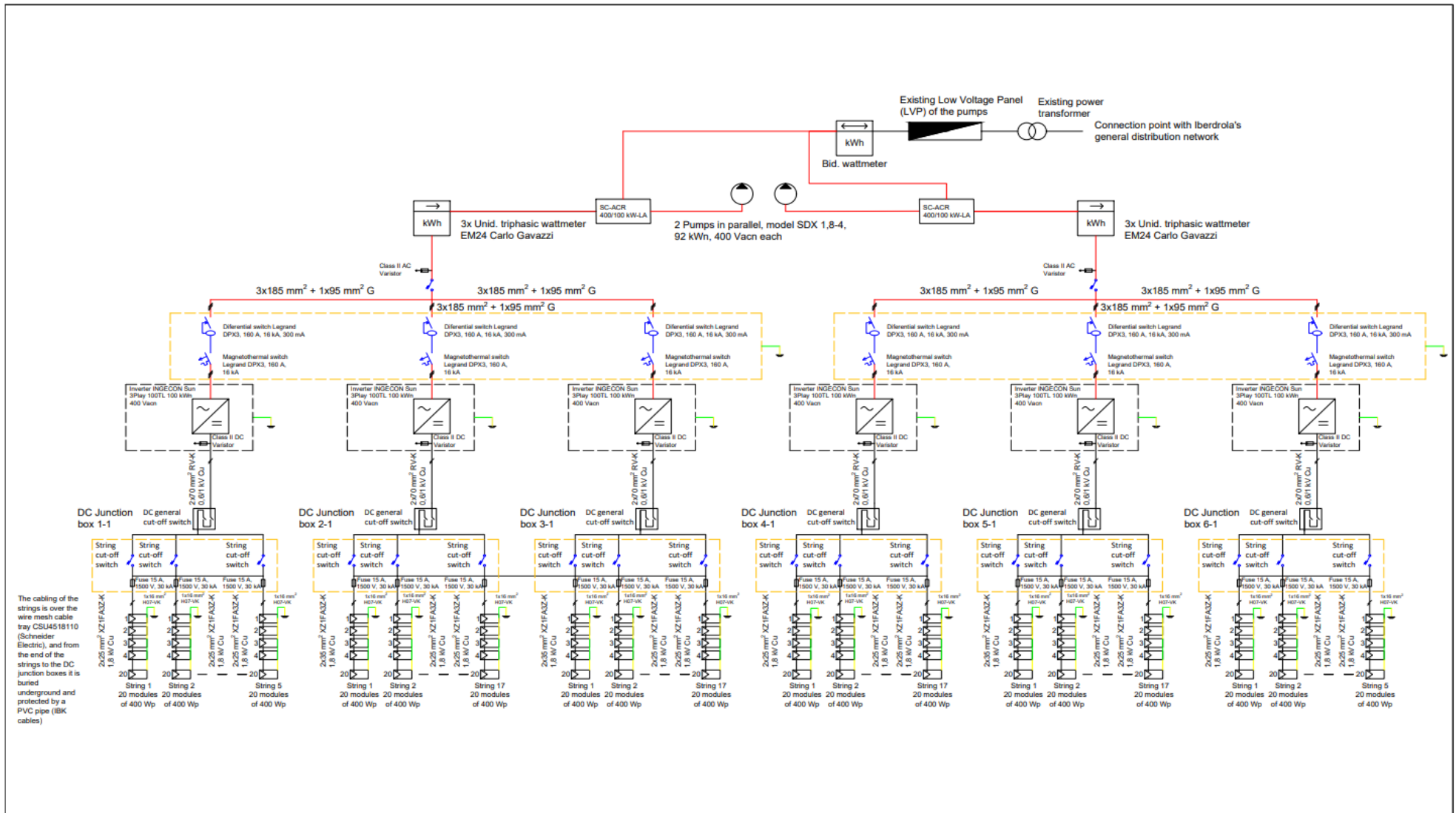
Signature:

Date: **March 2021**





Scale: **Several**

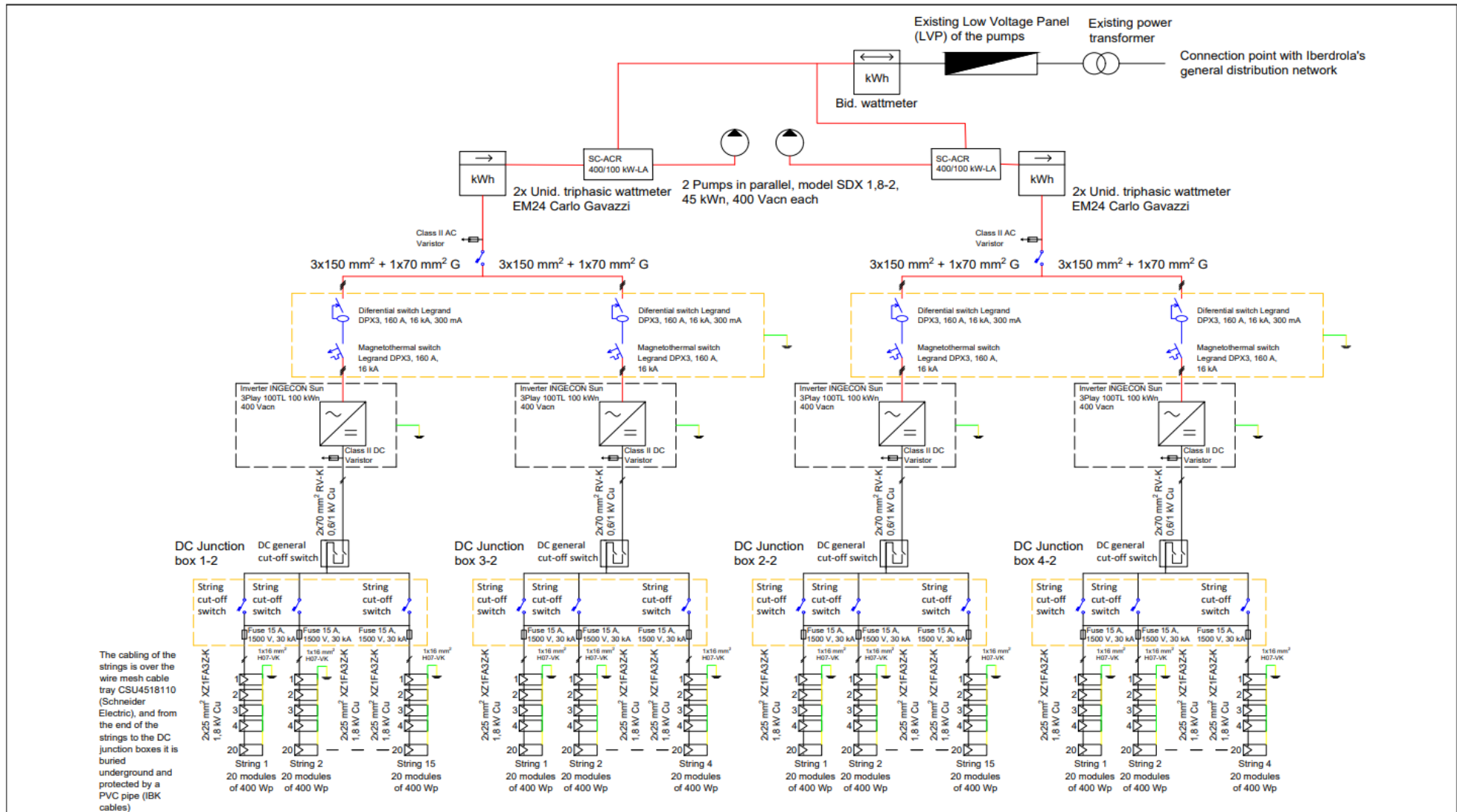
Plane nº:

3



The cabling of the strings is over the wire mesh cable tray CSU4518110 (Schneider Electric), and from the end of the strings to the DC junction boxes it is buried underground and protected by a PVC pipe (IBK cables)

MASTER'S FINAL PROJECT IN INDUSTRIAL ENGINEERING. SPECIALIZATION IN ENERGY GENERATION   	Project: DESIGN OF A PHOTOVOLTAIC SOLAR INSTALLATION FOR THE IRRIGATION OF THE VALLADACULTIVATION AREA (VALENCIA)	Author: Víctor Felip Plaza	Date: March 2021	Plane nº: 4
	Plan: Single-line diagram of the installation of Sector 2	Signature: 	Scale: N/S	



MASTER'S FINAL PROJECT IN INDUSTRIAL ENGINEERING. SPECIALIZATION IN ENERGY GENERATION



Project: DESIGN OF A PHOTOVOLTAIC SOLAR INSTALLATION FOR THE IRRIGATION OF THE VALLADACULTIVATION AREA (VALENCIA)

Plan: Single-line diagram of the installation of Sector 2

Author: Víctor Felip Plaza

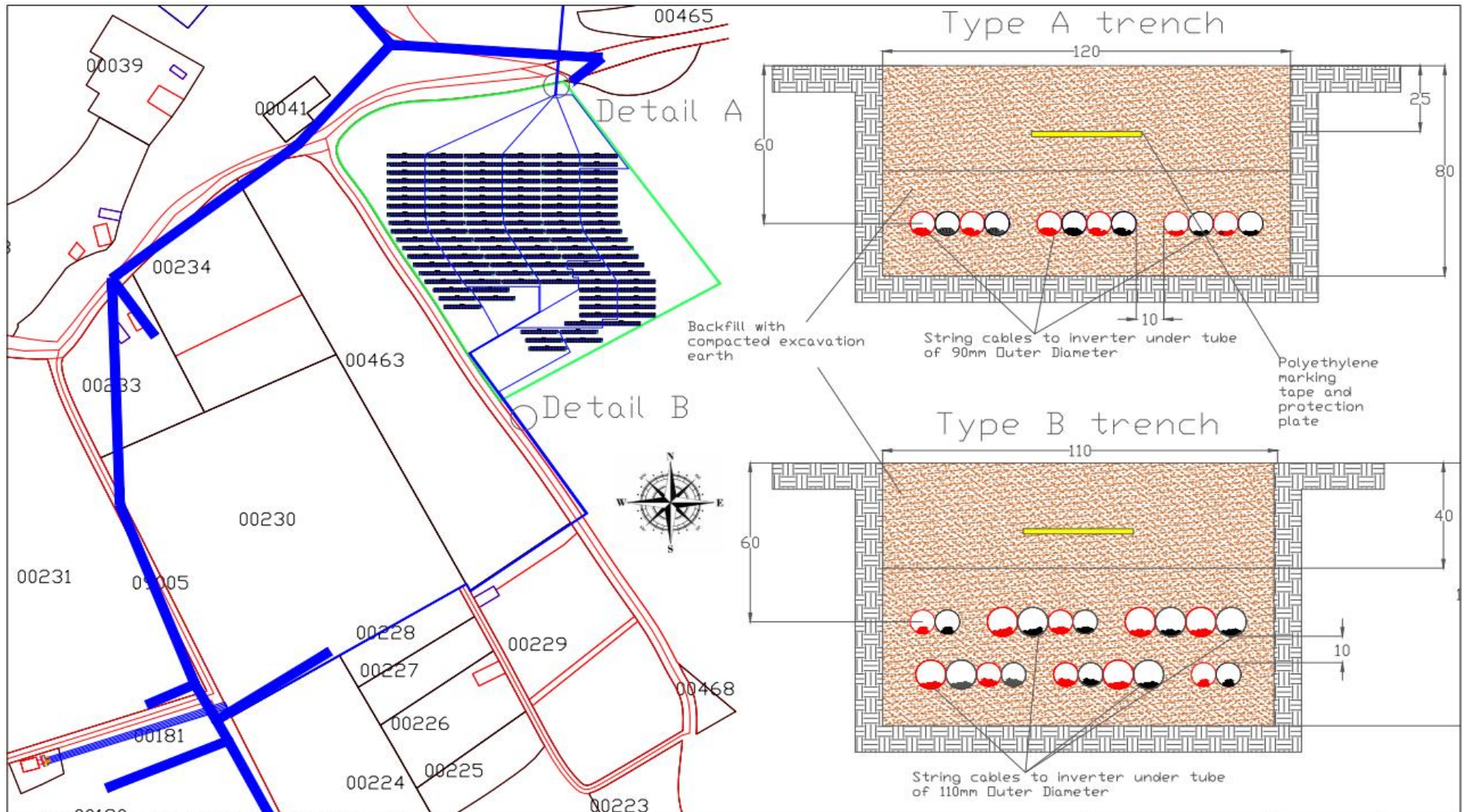
Signature:

Date: March 2021

Scale: N/S

Plane nº:

5



MASTER'S FINAL PROJECT IN INDUSTRIAL ENGINEERING. SPECIALIZATION IN ENERGY GENERATION 	Project: DESIGN OF A PHOTOVOLTAIC SOLAR INSTALLATION FOR THE IRRIGATION OF THE VALLADACULTIVATION AREA (VALENCIA)	Author: Victor Felip Plaza Signature:	Date: March 2021 Scale: N/S	Plane n°: 6
	Plan: Detail plan of the trenches			

Annex II.

Environmental analysis of the project

II.1 Introduction

This chapter aims to collect the impacts, both positive and negative, that the execution of the installation projected in this document could have on the natural environment in which it is developed, as well as the possible measures to be adopted to mitigate, at least partially, the consequences of said effects if they were harmful.

In this way it is intended, on the other hand, to show the compliance of this project with Law 21/2013, dated on December 9th, of Environmental Assessment, which "establishes the bases that must govern the Environmental Assessment of plans, programs and projects that may have significant effects on the environment, guaranteeing a high level of environmental protection throughout the State territory, in order to promote sustainable development".

II.2 Project peculiarities

In accordance with the provisions of Article 5 of Title I, the Environmental Assessment, in the case of a project, is understood as an Environmental Impact Assessment. In turn, it concludes:

- Through the "Environmental Impact Statement", with respect to those submitted to the Ordinary Environmental Impact Assessment procedure, in accordance with the provisions of Section 1 of Chapter II of Title II.
- Through the "Environmental Impact Report", with respect to those submitted to the Simplified Environmental Impact Assessment procedure, in accordance with the provisions of Section 2 of Chapter II of Title II.

At the same time, it is convenient to indicate that those projects that are in Annex I of this Law are adapted to the provisions of Section 1, while those numbered in the Annex II do so to the provisions of Section 2.

This project is not included in the group of projects included in Annex I (see Group 3. Energy industry, and Group 9. Other projects), nor in that of Annex II (see Group 4. Energy industry and Group 9 . Other projects). For this reason, it should not be submitted to either the Ordinary or the Simplified Environmental Impact Assessment, respectively.

The reason for this is that, in this case, a modification of a pre-existing project takes place. If carried out from 0, this project would be included in "Group 8. Hydraulic engineering and water management projects", specifically section a) **Extraction of groundwater** or recharge of aquifers (not included in Annex I) when the **annual volume of water extracted or supplied is greater than 1 cubic hectometre and less than 10 cubic hectometres per year** "of Annex II, so a Simplified Environmental Impact Assessment would be necessary. This is because the extraction of the 1.57 hectometres cubic meters ($1,570,661.28 \text{ m}^3$) would be projected from 0, and not only, as is done in this thesis, the photovoltaic part that must, at least to a large extent, supply the energy needs for said extraction.

II.3 Actions carried out in the natural environment

The most relevant actions carried out in the natural environment as a result of the development of the works to build the designed project are those mentioned below:

- Emission of polluting gases due to the circulation of the vehicles in charge of transporting the materials and removing the waste.
- Alteration of the terrain due to land movement and excavation of trenches.
- Removal of a certain cultivation area, as well as other plants that may exist in the area finally destined for the installation of the components of the photovoltaic installation.
- Laying of cabling in the subsoil.
- Noise generation.
- Residues generation.

II.4 Impacts on the environment

The aforementioned actions can produce a series of potential impacts in the area where they take place. Some of the most notable are the following:

- **Impacts on fauna:** In the project development zone there is no evidence of the existence of nests of protected bird species, since it is land destined to the cultivation of fruits and vegetables. On the other hand, there is no evidence of the existence of burrows of moles or rabbits in the vicinity. These works could only affect insects and minor animals, such as ants or worms.
- **Impacts on the flora:** There are also no species of protected trees affected, since the land destined for the photovoltaic installation corresponds to a plot previously destined for cultivation, and the occupied area is of a few thousand m^2 .
- **Impacts on the ground:** The earthworks carried out for the excavation of trenches and the installation of the photovoltaic panels is of little relevance, since they are not large earthworks nor at great depth. The erosivity of the land could increase a little but it would not be relevant because it would not be used again for the cultivation or growth of any plant species. Nor would there be contamination of the water, since these works, in addition to being small, are located far from the extraction point of the same in the two existing wells.
- **Impacts on people or populations:** There is no negative impact on people or nearby populations.
- **Impacts on existing infrastructures:** There is no infrastructure that could be negatively affected in the vicinity of the land on which the executed project would be located, be it industrial, road, energy generation or historical heritage.

II.5 Environmental benefits

Therefore, the execution of this project would not only entail a reduced environmental impact, but also the environmental benefits that this would entail due to the reduction of polluting emissions associated with the generation of part of the electrical energy supplied by the network, and that of another form would be the only source of energy supply of the pumping groups, would be appreciable throughout the useful life of the project.

However, for its optimization, it is necessary to try to generate the least amount of waste possible, both in the construction stage and throughout the useful life of the project, carrying out a correct maintenance of the components to avoid their unnecessary substitution and a later end of life suitable for them, since solar panels have components that are harmful to the environment.

In this sense, it is possible to carry out an estimation of the amount of annual and total emissions and waste in the useful life of the project, which has been set at 25 years (hence the feasibility analyses have been carried out with this time horizon), that can be avoided by installing the photovoltaic plant designed in this document. For this, the following Table II.1, extracted from the latest report developed by the “[Observatorio de la Electricidad](#)”, published in 2016, and which relates the electricity consumption of the network with the corresponding generation of different pollutants, is used:

Table II.1- Environmental impact of the electricity consumption. Source: Observatorio de la Electricidad [41]

__ kWh	x 0,174=	_____ kg CO ₂
__ kWh	x 0,366 =	_____ gramos SO ₂
__ kWh	x 0,261 =	_____ gramos NO _x
__ kWh	x 0,293 =	_____ mg RAA
__ kWh	x 0,00240 =	_____ cm ³ RBMA

Where:

- CO₂: Carbon dioxide.
- SO₂: Sulphur dioxide.
- NO_x: Nitrogen oxides.
- HARW: High Activity Radioactive Waste.
- LMARW: Low and Medium Activity Radioactive Waste.

On the other hand, it is relevant to indicate that the value of each of the indices that relate the electricity consumption from the network with the emission of a specific pollutant has been reduced by 1% from the second year to the last. This has been done because, in anticipation that renewable energies continue to gain weight in the generation and injection of current in the network and that traditional energies will be able to slightly reduce the emissions associated with their electricity production, the energy consumption from the network will be associated with decreasing levels of polluting emissions.

At the same time, a relevant assumption has been taken into account: the water needs are assumed to be constant, that is, the variation in the environmental impact of electricity consumption is not being analysed if it varies for any reason, such as higher irrigation needs either by increasing the cultivated area or by substituting part of the area devoted to rainfed crops by crops that require greater water needs.

Therefore, knowing the electricity consumption that theoretically it is possible to save annually through electricity generation through the photovoltaic installation and with the above factors, the following results are obtained (Figure II.1 and Figure II.2):

Estimated annual emissions and waste of different pollutants

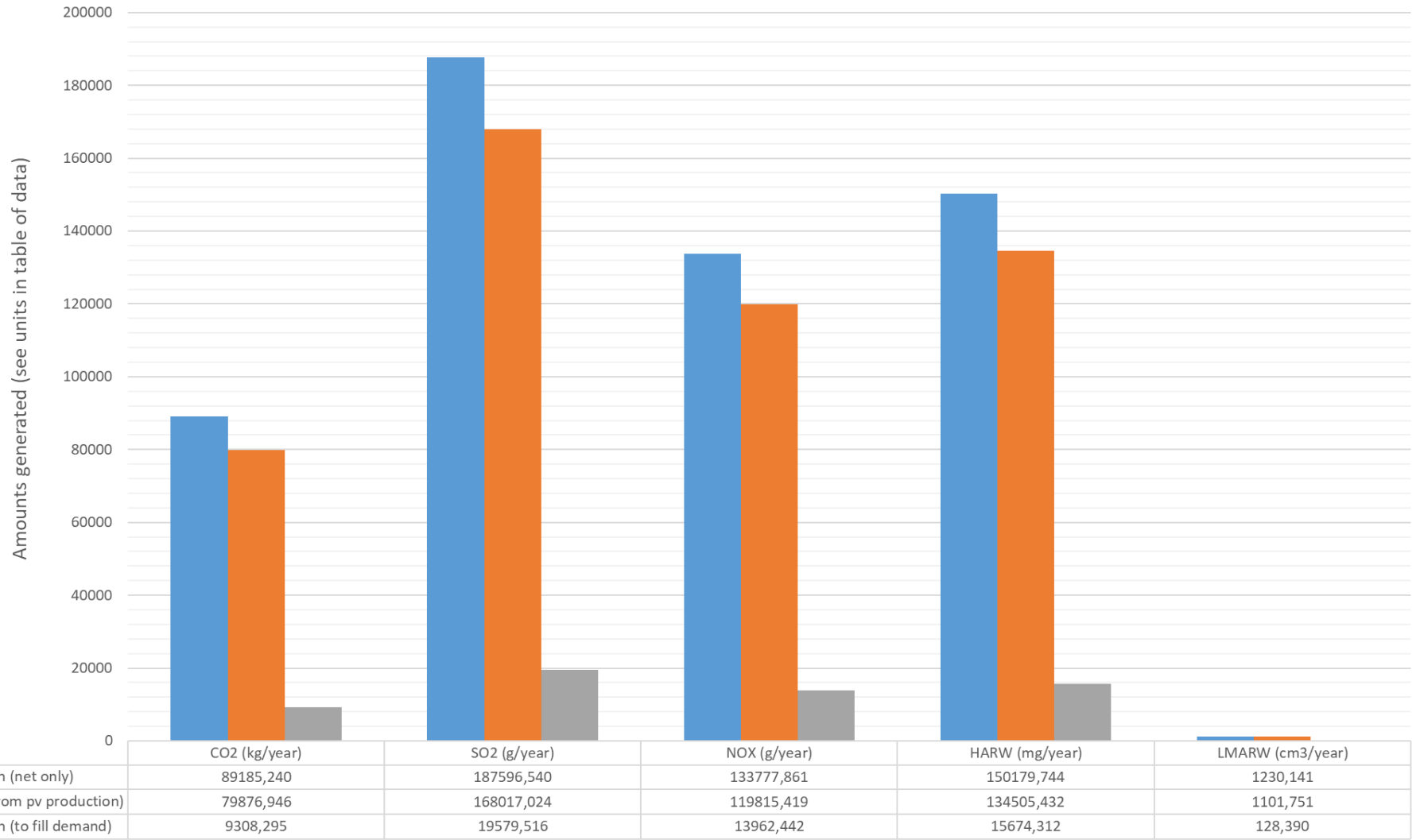


Figure II.1 Estimated annual emissions of different pollutants, without and with the pv installation

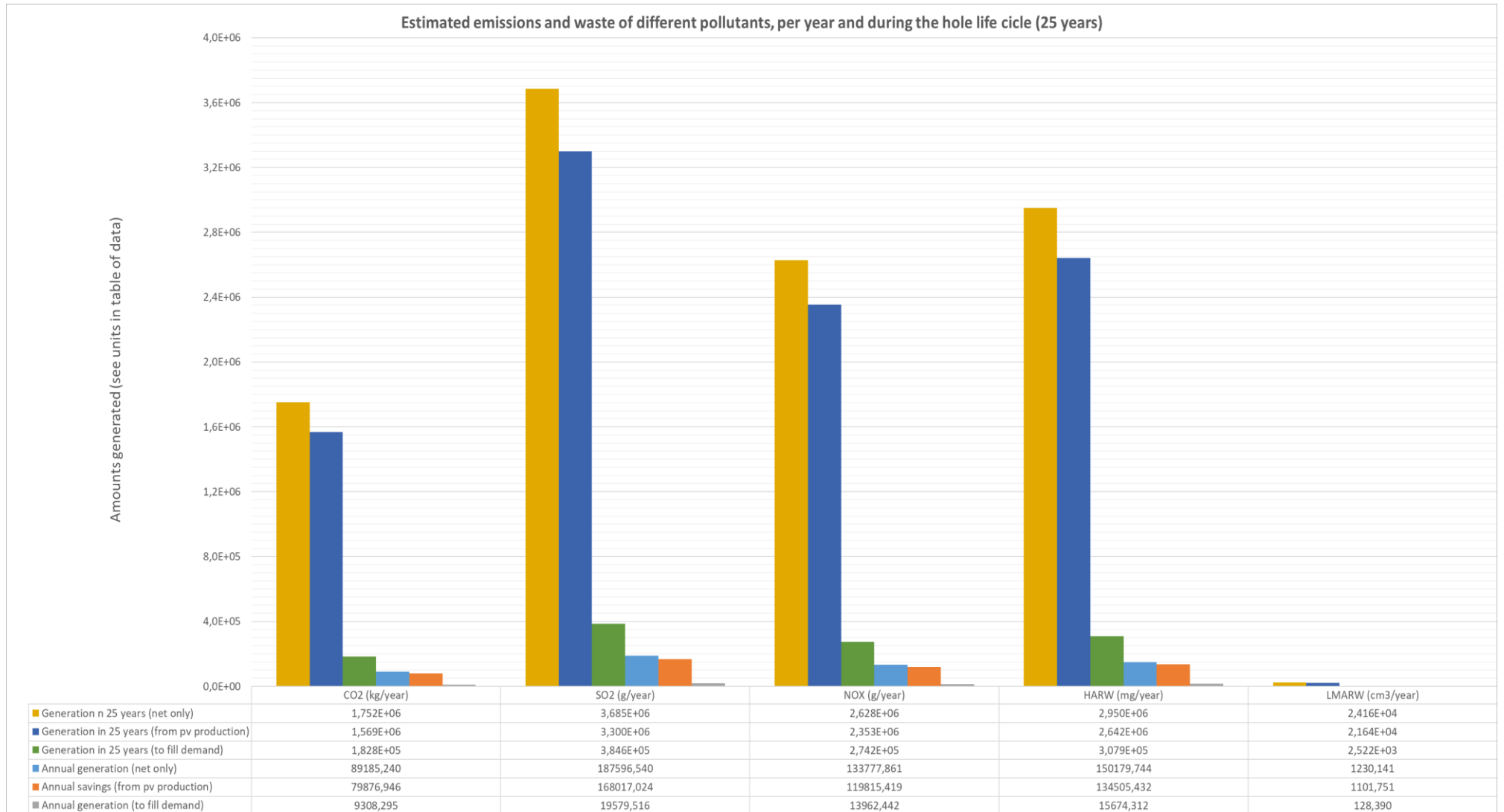


Figure II.2- Estimated emissions of different pollutants during the next 25 years, without and with the pv installation

Annex III.

Planning of the
temporal evolution of
the execution of the
works

III.1 Introduction

This Annex presents the result of the execution schedule obtained with the MS Project software. In this way, by configuring the achievement and estimated duration of the tasks involved in the works of this electricity supply project by means of this software, it is possible to know the evolution of their development, the critical path of the project and the estimated final duration of its execution in a fast and intuitive way. In this sense, the so-called Gantt Chart has been used for its representation.

The start day of the work is taken into account once the necessary administrative authorizations and prior building licenses have been obtained. Therefore, the entire duration of the project could be one or several weeks longer, if the period of time necessary to obtain said authorizations and licenses were taken into account.

A representation of the Gantt diagram can be found in [Figure III.1](#).

III.2 Gantt Chart

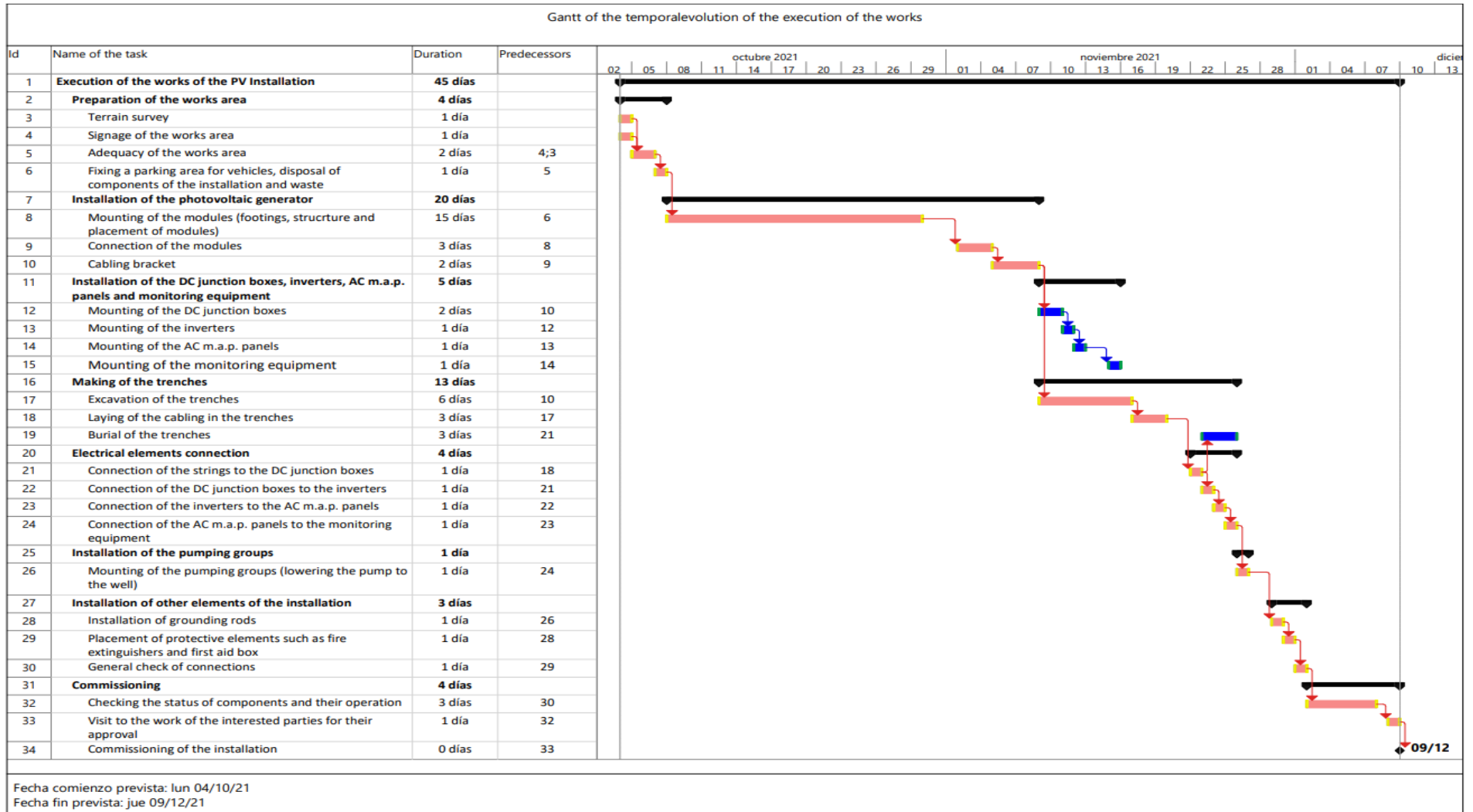


Figure III.1- Gantt diagram

Annex IV.

Bibliographic references

- [1] **World Economic Forum (13th June 2018)**. *La tecnología está impulsando una cuarta ola de ambientalismo*. Obtenido de <https://es.weforum.org/agenda/2018/06/la-tecnologia-esta-impulsando-una-cuarta-ola-de-ambientalismo/>
- [2] **Castilla-La Mancha media (2nd December 2019)**. *Las fechas clave en la lucha contra el cambio climático* <https://www.cmmedia.es/noticias/mundo/las-fechas-clave-en-la-lucha-contra-el-cambio-climatico/>
- [3] **British Petroleum (16th June 2020)**. *Statistical Review of World Energy 2020 | 69th edition*. <https://www.bp.com/content/dam/bp/business-sites/en/global/corporate/pdfs/energy-economics/statistical-review/bp-stats-review-2020-full-report.pdf>
- [4] **Ren21. (18th June 2019)** (*Global Status Report. A Comprehensive Annual Overview of the State of Renewable Energy*). https://www.ren21.net/gsr-2019/chapters/chapter_01/chapter_01/
- [5] **Ren21. (16th June 2020)** (*Global Status Report. A Comprehensive Annual Overview of the State of Renewable Energy*). https://www.ren21.net/gsr-2020/chapters/chapter_01/chapter_01/
- [6] **International Renewable Energy Agency (29th September 2020)**. *Renewable Energy and Jobs – Annual Review 2020*. <https://www.irena.org/publications/2020/Sep/Renewable-Energy-and-Jobs-Annual-Review-2020>
- [7] **Hogarsense (21th February 2019)**. *Historia de la energía solar*. <https://www.hogarsense.es/energia-solar/historia-energia-solar>
- [8] **PV Education (16th August 2016)**. *Absorption coefficient*. <https://www.pveducation.org/pvcdrom/pn-junctions/absorption-coefficient>
- [9] **National Renewable Energy Laboratory (NREL) (12th February 2019)**. *Best research-cell efficiency chart*. <https://www.nrel.gov/pv/cell-efficiency.html>
- [10] **SolarPower Europe (1st December 2019)**. *EU Market Outlook For Solar Power / 2019 - 2023*. https://www.solarpowereurope.org/wp-content/uploads/2019/12/SolarPower-Europe_EU-Market-Outlook-for-Solar-Power-2019-2023_.pdf?cf_id=5387
- [11] **El periódico de la Energía (16th January 2020)**. *Historia de la fotovoltaica en España: desde sus inicios en 1984 a sus objetivos para 2030*. <https://elperiodicodelaenergia.com/historia-de-la-fotovoltaica-en-espana-desde-sus-inicios-en-1984-a-sus-objetivos-para-2030/>
- [12] **Red Eléctrica de España (REE) (30th June 2020)**. *Las energías renovables en el sistema eléctrico español 2019*. <https://www.ree.es/es/datos/publicaciones/informe-de-energias-renovables/informe-2019>
- [13] **Det Norske Veritas (DNV) (11th September 2019)**. *Energy Transition Outlook 2019*. https://www.euractiv.com/wp-content/uploads/sites/2/2019/09/DNV-GL-ETO-2019-%E2%80%93-Power-Supply-and-Use_single_LR_under-embargo.pdf
- [14] **AutoSolar (19th April 2015)**. *¿Que es un sistema de bombeo de agua solar?*. <https://autosolar.es/blog/aspectos-tecnicos/que-es-un-sistema-de-bombeo-de-agua-solar>
- [15] **Montero Ortiz, H. (2018)**. *Análisis de recuperación energética en sistemas de redes de riego a presión con bombas funcionando como turbinas. Aplicación a la red de Canyoles VI (Vallada, Valencia)*. <https://riunet.upv.es/handle/10251/109116>

- [16] Instituto de Ingeniería del Agua y Medio Ambiente (IIAMA) (30th October 2002). *Manual del usuario de EPANET 2.0*.
https://www.iiama.upv.es/iiama/src/elementos/Software/2/epanet/EN2Manual_esp_v20012_ext.pdf
- [17] ResearchGate (11th December 2018). *Equivalencia de coeficientes de rugosidad de Hazen-Williams, Chezy-Manning y Darcy-Weisbach para modelos de redes a presión en Epanet*.
https://www.researchgate.net/publication/329567002_Equivalencia_de_coeficientes_de_rugosidad_de_Hazen-Williams_Chezy-Manning_y_Darcy-Weisbach_para_modelos_de_redes_a_presion_en_Epanet
- [18] Blog TECNOSOL (5th December 2016). *Distancia entre filas de paneles solares para evitar el sombreado*. <https://tecnosolab.com/noticias/distancia-entre-filas-de-paneles-solares/>
- [19] ITC-BT-08. *Guía técnica de aplicación. Protecciones* (14th December 2016). *Sistemas de conexión del neutro y de las masas en redes de distribución de energía eléctrica*.
<https://www.plcmadrid.es/rebt/itc-bt-08/>
- [20] ITC-BT-17. *Guía técnica de aplicación. Instalaciones de enlace* (3rd September 2017). *Dispositivos generales e individuales de mando y protección. Interruptor de control de potencia*.
http://www.f2i2.net/documentos/IsiF2I2/rbt/guias/guia_bt_17_sep03R1.pdf
- [21] ITC-BT-18. *Guía técnica de aplicación. Protecciones* (5th October 2018). *Instalaciones de puesta a tierra*. http://www.f2i2.net/documentos/IsiF2I2/rbt/guias/guia_bt_18_oct05R1.pdf
- [22] ITC-BT-21. *Guía técnica de aplicación. Instalaciones interiores o receptoras* (18th December 2020). *Tubos y canales protectores*.
http://www.f2i2.net/documentos/IsiF2I2/rbt/guias/guia_bt_21_sep03R1.pdf
- [23] ITC-BT-22. *Guía técnica de aplicación. Instalaciones interiores o receptoras* (12th December 2018). *Protección contra sobreintensidades*. <https://www.plcmadrid.es/rebt/itc-bt-22-proteccion-contra-sobreintensidades/>
- [24] ITC-BT-24. *Guía técnica de aplicación. Instalaciones interiores o receptoras* (12th December 2018). *Protección contra los contactos directos e indirectos*. <https://www.plcmadrid.es/rebt/itc-bt-24-proteccion-contra-los-contactos-directos-e-indirectos/>
- [25] ITC-BT-40. *Guía técnica de aplicación* (18th September 2017). *Instalaciones generadoras de baja tensión*. <https://www.plcmadrid.es/wp-content/uploads/rebt/itc40/ITC-BT-40.pdf>
- [26] Prysmian club (9th January 2019). *Cálculos de caídas de tensión. Valores oficiales de conductividad para Cu y Al*. <https://www.prysmianclub.es/calculos-de-caidas-de-tension-valores-oficiales-de-conductividad-para-cu-y-al/>
- [27] AutoSolar (31st October 2019). *Panel Solar 400W PERC Monocristalino ERA*.
<https://autosolar.es/panel-solar-24-voltios/panel-solar-400w-perc-monocristalino-era>
- [28] Saclima (27th March 2017). *Ingeteam trifasico Ingecon Sun 3Play 100 TL*.
<http://www.saclimafotovoltaica.com/wp-content/uploads/2017/03/Ficha-T%C3%A9cnica-Inversores-Ingeteam-Sun-3Play-100-TL.pdf>
- [29] DocPlayer. *Cables para instalaciones de energía solar fotovoltaica*.
<https://docplayer.es/57317216-Cables-para-instalaciones-de-energia-solar-fotovoltaica.html>

- [30] **General Cable (25th January 2015)**. *Cable de Baja Tensión ENERGY RV-K FOC, Cobre, 0.6/1 kV, XLPE, Cubierta de PVC Flexible*.
<https://cdn.generalcable.com/assets/documents/LATAM%20Documents/Mexico%20Site/Productos%20y%20Soluciones/Baja%20Tensi%C3%B3n/ENERGY-RV-K-FOC-CU-XLPE-CUBIERTA-PVC-FT-2015-0125.pdf>
- [31] **IBK Cables**. *CATALOGO MATERIAL ELECTRICO-C3*.
<https://www.ibkcables.es/archivos/Cat%C3%A1logoMaterialEI%C3%A9ctrico-IBKCables.pdf>
- [32] **DF Electric (12th May 2019)**. *Catálogo FOTOVOLTAICOS - DF Electric*.
<https://dfelectric.es/documentacion/documentos-fotovoltaicos/fusibles-y-bases-fotovoltaicos.pdf>
- [33] **DEHNguard (20th June 2019)**. *DEHNguard modular YPV ... FM - DEHN IBÉRICA*.
<https://www.dehn.es/store/p/es-DE/F1600268/dehnguard-modular-ypv-fm>
- [34] **Bombas Ideal (1st August 2018)**. *Serie S - Bombas Ideal*. <https://www.bombasideal.com/wp-content/uploads/2018/11/800-CAT-SD-50-60-Hz-D-081018-compressed.pdf>
- [35] **Merkasol (6th October 2020)**. *Estructura Paneles Solares SUNFER CVA915XL Suelo o Cubierta Plana*. <https://merkasol.com/Estructura-Paneles-Solares-Sunfer-CVA915XL-Suelo-o-Cubierta-Plana>
- [36] **Grupo Sinelec (10th September 2019)**. *Barras de conexión para instaladores (Pletina)*.
<https://gruposinelec.com/barras-de-conexion-para-instaladores-pletina/>
- [37] **TEX C.A.(1st February 2001)**. *Prensaestopas para Cables*.
<http://www.texca.com/publicaciones/tdcables.htm>
- [38] **Sofamel (15th October 2020)**. *Tarifa Octubre 2020*.
https://sofamel.com/data/eshop/sofamel/uploads/docs/mailings/Tarifa_Octubre2020.pdf
- [39] **Legrand (20th June 2013)**. *Catálogo DX³ / TX³ - Legrand*.
<https://www.legrand.es/documentos/Catalogo-Proteccion-DX3-TX3-Legrand.pdf>
- [40] **Banco de España (4th December 2020)**. *Estadísticas – Tipos de interés y tipos de cambio*.
<https://www.bde.es/webbde/es/estadis/infoest/a1906.pdf>
- [41] **World Wildlife Fund (WWF) (4th May 2016)**. *Observatorio de la Electricidad mayo 2016*.
https://wwfes.awsassets.panda.org/downloads/oe_mayo_2016.pdf?39680/Observatorio-de-la-electricidad-mayo-2016